ABSTRACT

Title of Dissertation: SIMPLIFIED NUCLEIC ACID ISOLATION AND DETECTION TECHNIQUES FOR POINT-OF-CARE APPLICATIONS

Imaly A. Nanayakkara
Doctor of Philosophy, 2019

Dissertation directed by: Professor Ian M. White
Department of Bioengineering

The first step towards the treatment of any disease is diagnosis; however, a major hindrance towards monitoring diseases remains the availability of rapid diagnostic tests to detect DNA and RNA biomarkers. Unfortunately, traditional assays to test for these analytes are limited to centralized laboratories. For example, the gold-standard sample preparation methods to isolate and purify nucleic acid analytes require multiple hands-on steps, numerous chemicals, and specialized equipment. Recent research endeavors have made incremental progress to simplify these procedures by miniaturizing these steps, but still require the numerous chemicals and bulky peripheral instrumentation for operation. Similarly, gold-standard detection methods, namely quantitative PCR (qPCR), rapidly cycle between near-boiling

temperatures, thus mandating the use of sophisticated instrumentation with high power demands. These methods for sample preparation and target detection are overall laborious, time-consuming, and require technical expertise thereby imposing large time, and financial costs for diagnoses. To address these challenges, this dissertation aims to shift the paradigm of how we approach sample preparation for nucleic acid isolation, and to design novel assays for rapid, specific, and multiplexed detection in a single reaction.

First, a new sample preparation method is presented that simultaneously accomplishes three time-consuming sample preparation steps (cell lysis, DNA capture, and purification) in less than ten minutes. This platform enables DNA isolation from whole blood droplets, with subsequent amplification and detection of both genomic and pathogenic DNA bound to the microparticle surface. Second, we explore optimizations of a popular isothermal DNA amplification technique that previously demonstrated multiplex detection of bacterial genomes. By developing a triplex assay towards the identification of drug resistant bacteria, we address inhibition that is normally observed with this technique, and present strategies towards achieving amplification within 30 minutes. Lastly, we outline design consideration towards the development of a novel amplification scheme specifically for microRNA targets. This system leverages both DNA and RNA polymerases to achieve positive feedback and thus, requires evaluation of enzymes, sequence design, and buffers to inform assay design. Together, this work advances the development of NAATs towards a simplified, specific and multiplexed system.

SIMPLIFIED NUCLEIC ACID ISOLATION AND DETECTION
TECHNIQUES FOR POINT-OF-CARE APPLICATIONS

by

Imaly Anoshka Nanayakkara

Dissertation submitted to the Faculty of the Graduate School of the
University of Maryland, College Park, in partial fulfillment
of the requirements for the degree of
Doctor of Philosophy
2019

Advisory Committee:
 Associate Professor Ian M. White, Chair
 Associate Professor Jason D. Kahn
 Professor Don L. DeVoe
 Professor Gregory F. Payne
 Professor Keith E. Herold

Dedication

To Ammi, Apuchi, and Malli, for your unconditional love and support, and for always believing in me. The values of hard work and perseverance you have instilled in me have led me here, and your kindness, empathy, and helping hand to others have given me the drive to advocate and help those less fortunate than myself.

To my UMD family, Anjana, Josh, Charlotte, Leo, George and Ryan. I would not have made it to the end without your support and encouragement. Thanks for all the academic discussions, vent sessions, and endless laughter. I can't put into words how much your support has meant to me.

To my friends who have long supported me throughout my academic career, Bonnie, Nancy, Angie, Sarah, Anissa, Michelle and Christine. Thanks for always motivating me to the finish line.

Acknowledgements

I could not have completed the work presented in this dissertation without the support from a number of people.

I would like to thank both past and current graduate students of the White lab. Drs. Kunal Pandit, Stephen Restaino and John Goertz first welcomed me to the group, and helped me get started in the lab. Thanks to Kunal and Stephen, who have laid the foundation for the work presented here and were the best of mentors, even after leaving UMD. Thanks to John for fostering and pushing my intellectual curiosity; your feedback and fresh perspectives throughout my doctoral work has greatly motivated me. I have learned so much for you all, and am thankful for your continued encouragement and friendship. Current lab members, Hieu Nguyen, Alessandra Zimmermann, and Micaela Everitt, have provided input during group meetings, and provided camaraderie, support, and laughter, especially during this last year.

My advisor and mentor, Dr. Ian White, provided guidance, thoughts, and ideas for each step that culminated to this dissertation. I am so grateful for your dedication and patience, and for allowing me to pursue endless possibilities to achieve my goals. Your guidance has not only fortified my abilities as a researcher, but has encouraged my confidence and growth.

The former and current undergraduates of the White lab have provided thoughts, ideas, and experimental support. You all have taught me how to teach others, which has been invaluable. This includes Divya Jain and Sumouni

iii

Table of Contents

List of Tables

List of Figures

List of Abbreviations

3SR: self-sustained sequence replication
Bst 2.0: Bst 2.0 DNA polymerase
Bst 3.0: Bst 3.0 DNA polymerase
Bst Full: Bst DNA polymerase, Full Length
Bst LF: Bst DNA polymerase, Large Fragment
cDNA: complementary DNA
DARQ LAMP: detection of amplification by release of quenching loop-mediated
   isothermal amplification
DNA: deoxyribonucleic acid
DNAP: DNA polymerase
EXPAR: exponential amplification reaction
FBD: fluorogenic bidirectional displacement
FRET: Förster resonance energy transfer
HCR: hybridization chain reaction
hgDNA: human genomic DNA
HIV: human immunodeficiency virus
LAMP: loop-mediated isothermal amplification
LOC: lab-on-a-chip
Mg^{2+}: magnesium cation
miRNA: microRNA
mRNA: messenger RNA
MRSA: methicillin-resistant *Staphylococcus aureus*
NAAT: nucleic acid amplification test
NASBA: nucleic acid sequence-based amplification
NTC: no target control
PCR: polymerase chain reaction
POC: point-of-care
qPCR: quantitative or real-time polymerase chain reaction
QPD: quencher probe duplex
RCA: rolling circle amplification
RDT: rapid diagnostic test
RNA: ribonucleic acid
RNAP: RNA polymerase
rRNA: ribosomal RNA
RT: reverse transcriptase
SP6: SP6 RNA polymerase
T7: T7 RNA polymerase
TCA: transcription cycling amplification
TMAC: tetramethylammonium chloride
tmRNA: transfer-messenger RNA
TTP: time to positive

Chapter 1. Introduction

Currently, gold standard approaches to nucleic acid amplification tests (NAATs) are limited to central laboratory facilities due to the necessary instrumentation, the infrastructure required to support the instrumentation, and the need for trained technicians to perform these assays. However, this model imposes large financial and time burdens, and creates a significant window between sample collection and diagnostic result (sample-to-answer time). In environments such as rural clinics or emergency care, where a rapid result is required to inform immediate treatment, the central laboratory model hinders informed clinical decisions and thus patient care. As a result, a large focus within the diagnostic community is the development of near-patient or point-of-care (POC) testing with the goals of testing immediately upon sample collection and achieving rapid assay and analysis results for quicker sample-to-answer times. Advancements in this area would allow clinicians to not only perform these tests quickly and cheaply, but also facilitate a more dynamic and informed approach towards targeted treatment for patients.

Rapid diagnostic tests (RDTs) such as glucose meters and pregnancy tests have already been employed within the healthcare system. Given their success and prevalence in the healthcare system, the development of RDTs has been expanded for the detection of infectious diseases, such as human immunodeficiency virus (HIV), tuberculosis, and malaria.[1] Of the commercial

assays for infectious disease detection, most typically leverage a variation of a binding assay specifically for protein, commonly agglutination assays, enzyme-linked immunosorbent assays, or lateral flow immunochromatographic tests.[2] However, these methods of detection are often inferior in both sensitivity and specificity compared to the molecular diagnostics that would normally be performed in the central lab setting.[3] These deficiencies motivate further development of diagnostic assays, for both protein and nucleic acids that are on par with their molecular diagnostic counterparts with regard to performance, while addressing the challenges of cost and time.

Several commercial POC NAATs have already been developed, where the model comprises a reader that contains the necessary hardware and detection instrumentation, and separate cartridge consumables that are specific to the target of interest. The most popular of these platforms has been the Cepheid XPert®. This fully integrated system centers on a cartridge that enables testing of nucleic acid targets directly from a complex matrix such as blood. The cartridge couples with the reader to perform cell lysis and DNA isolation, and DNA amplification.[4,5] While these systems and other commercial platforms have successfully integrated sample preparation, amplification, and detection into one automated platform with a sample-to-answer readout, their impact at the POC has yet to be realized due to their cost, energy consumption, the need for a power source and a specialist for maintenance and repair.

To remedy the aforementioned challenges associated with NAATs, there are three large foci within the diagnostic community: developing novel

amplification methods, devising more specific detection methods, and redesigning sample preparation methods. The first focus aims to devise alternative methods and technologies to replace the temperature cycling-driven method of amplification, with a variety of amplification schemes that operate at a single temperature. These techniques, known as isothermal amplification schemes, lead to less sophisticated and bulky instrumentation, which translates to a more affordable system for POC applications. Detection from isothermal methods can be quantified by using the same intercalating dyes that are traditionally used, and thus can be easily integrated with developed fluorescence detectors amenable to POC environments. To further drive down costs, lateral flow approaches have been employed in which immobilized oligonucleotides hybridize to the amplicons produced during the amplification reaction and are detected with nanoparticles.[6–8] However, this increases the sample-to-answer time with the requirement of a post-amplification detection method. Overall, isothermal methods offer promise towards the development of a POC NAAT, but often suffer from nonspecific amplification due to the constant enzyme activity at these single operating temperatures.

The second challenge involves addressing the need for specific target detection, particularly with isothermal amplification schemes. As mentioned previously, fluorescence is often achieved with an intercalating dye, a nonspecific DNA binding dye. Therefore, distinguishing the results of on-target versus off-target amplification is impossible without post-amplification analyses. To address this concern, dual-labeled probes that leverage Förster

resonance energy transfer (FRET) have been designed to hybridize directly to the target of interest. The main challenge with employing this type of readout with isothermal amplifications is that not all of these techniques enable FRET probe degradation for signal generation. As a result, many groups have used a molecular beacon approach. Similar to the FRET probes, molecular beacons also leverage two labels; however, here, binding of a reaction product to the molecular beacon drives signal generation. These molecular beacons are complex in their design, primarily to ensure that nonspecific hybridization does not occur. For applications where multiple nucleic acid targets are assayed in a single tube, minimizing nonspecific interactions becomes increasingly difficult.

Lastly, despite the advances made towards simplifying amplification methods, sample preparation remains a major hindrance in realizing a truly integrated and low-cost system for NAATs. This is primarily because most efforts focus on miniaturizing the gold standard methods of sample preparation, namely cell lysis and DNA isolation, and DNA purification. Cell lysis has been integrated into devices with the incorporation of microparticles, thermal heaters, and chemical agents. However, the arduous process of DNA purification remains a bottleneck in this process. Purification methods often require multiple precise buffer exchanges, and as a result, a complex fluid handling system needs to be incorporated within the system in order to perform these steps without compromising downstream amplification. Convenient

solutions that move away from this model of sample preparation are critical to realizing a POC NAAT, but have yet to be developed.

Towards the goal of streamlining methods required for NAATs, this work develops novel technologies to shift the paradigm of how we approach sample preparation, and to present strategies for the design of multiplex isothermal amplification schemes for a variety of nucleic acid targets. Specifically, Chapter 3 details the development of a microparticle-based platform that enables cell lysis and DNA extraction in less than 10 minutes. This platform enables amplification directly off of the solid phase, and is amenable to future automation of the platform. Chapter 4 assesses a FRET-based approach for loop-mediated isothermal amplification, a popular isothermal amplification method, and presents strategies to better inform assay design for multiplex detection towards the detection of methicillin-resistant *Staphylocuccus aureus* (MRSA). Lastly, Chapter 5 presents a novel amplification technique for the direct detection of microRNA, a growing target of interest in biomarker discovery. Here, I outline the steps one should consider when designing a dual-enzyme system to achieve rapid, specific, multiplex detection of microRNA.

Chapter 2. Molecular diagnostics for nucleic acid biomarkers

Currently, most molecular diagnostics are performed exclusively in centralized laboratories due to the need for sophisticated instrumentation, and the technical expertise required to handle these assays. With medical care now shifting to provide a patient-centric approach, there is an increased need for sensitive and specific tests that can be performed in near-patient settings (i.e. doctors' offices, rural clinics, at-home testing, etc.), also termed point-of-care (POC) testing. The two major challenges towards an integrated device for nucleic acid amplification tests are sample preparation, and amplification that allows for specific, multiplexed detection. This chapter will detail the strategies and recent advancements to devise novel solutions and approaches for both these modules.

2.1   Nucleic acid amplification tests

NAATs are a powerful tool used every day for diagnosing and monitoring various diseases. These tests take advantage of the gene-specific sequences of DNA that can be directly detected, and achieve greater sensitivity than other protein detection methods[9] (i.e. immunoassays). As a result, NAATs are a commonly-used diagnostic for antimicrobial resistance,[10] infections caused by immunovariant viruses and early detection of viral infections.[11] Due to the required training and the sophisticated instrumentation, NAATs are most routinely used in centralized laboratories, and not in near-patient settings or

6

low resource-settings where the technical support for these facilities is lacking or absent.

NAATs are comprised of three main modules: sample preparation, amplification, and detection.[12] Sample preparation often involves a multi-reagent procedure that involves three major steps. First, DNA-containing cells within a complex matrix, such as blood, are lysed using chaotropic salts to disrupt hydrogen bonding and effectively denature proteins. The DNA is then extracted from the lysate, either by separation using solvents or spin columns. Lastly, the DNA is purified for downstream analysis. The most common amplification method is polymerase chain reaction (PCR) and requires thermocycling to facilitate DNA melting, primer annealing and extension to produce PCR products, or amplicons, at an exponentially increasing rate. Finally, real-time detection is most commonly realized using fluorescence with the use of nucleic acid stains or oligonucleotide probes that are cleaved during extension. Overall, sample preparation and amplification are the two modules that are the foci of current diagnostics research, as they remain to be the most time- and resource-consuming aspects.

2.2   Sample preparation

For most NAATs, a sample taken directly from the patient must be processed to yield a pure DNA sample prior to analysis as proteins and cellular debris present can inhibit the assay. Standard clean-up protocols require either chemical lysis with a solid-phase support to purify and immobilize the released DNA with high yield, or mechanical lysis with the use of glass beads. However,

the chemicals used to lyse cells and the solvents used to purify DNA can inhibit downstream amplification, and multiple buffer exchanges are required to bind, wash, and elute the DNA. These protocols are unrealistic for POC applications given that they are difficult to integrate with lab-on-a-chip (LOC) platforms without external equipment and technical expertise. This section details the gold-standard methods, outlines why they are unsuitable for POC applications, and reviews current research endeavors aiming to address the challenges associated with implementation of sample preparation in an integrated device.

2.2.1 Conventional methods for sample preparation

In order to perform any molecular diagnostic in a central laboratory setting, a patient sample must be purified to isolate the given target. There are many different methods for nucleic acid purification of a cell lysate, such as phenol-chloroform extraction and ethanol precipitation,[13,14] however these methods rely on sophisticated instrumentation (i.e. centrifuges), and various buffers, consisting of high and low ionic conditions or toxic chemicals, as well as technical expertise to conduct these procedures.

These methods have been simplified by using a solid phase extraction[15] in a spin-column by reducing DNA extraction and purification to 30 minutes (Figure 2.1); however this method presents the same disadvantages as the aforementioned methods. Given the multiple steps and the need for centrifugation involved in all preparation methods, there is a high level of expertise required. Additionally these methods do not facilitate a

high-throughput method for purifying and extracting multiple samples, due to the cumbersome hands-on steps required.
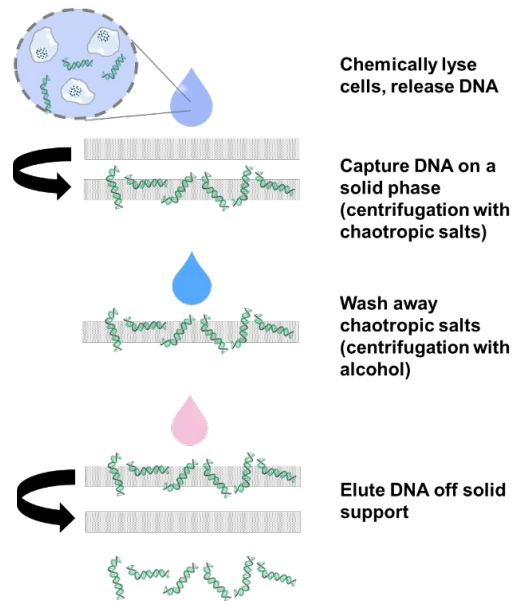
Figure 2.1. Schematic detailing solid-phase extraction. A cell suspension is first lysed with chaotropic salts prior to DNA extraction. The lysate is then added to a spin column with a silica membrane so that the DNA will bind to the solid phase upon centrifugation. The chaotropic salts present in the lysate facilitate this by forming salt bridges between the silica membrane and the DNA backbone (both are negatively charged). Washes with ethanol are added to remove protein aggregates and debris, and finally, a low-ionic strength buffer or deionized water is added to elute the DNA off the silica membrane.

In an effort to make NAATs more accessible to POC, research has been focused on miniaturizing these methods using microfluidic platforms. At the micron scale, the advantages of these systems involve smaller sample volumes, and faster assay times.[16–18] However, many of these systems perform sample preparation off chip. While cell lysis can be integrated into a microfluidic format easily, either by microfabrication to achieve mechanical lysis for bacteria,[19–22] integration of heaters for thermal lysis,[23–26] or addition of chemicals for chemical lysis,[27–29] integration of DNA extraction from a lysate is not as straightforward. The most obvious solution is to integrate the macroscale

solid phase extraction techniques within a microfluidic device, however the challenges with this method involve fabricating the valves necessary to pass the different buffer across the silica membrane. Additionally, this method still requires multiple reagent exchanges, so these systems require fluid handling control that adds to the complexity of the overall system. The ideal system would allow a one-step method of extracting DNA from a cell lysate.

2.2.2 Microparticle- and polymer-based methods

2.2.2.1   Microparticle-based sample preparation

Historically, bead-based approaches have offered a one-sided solution towards achieving a stream-lined cell lysis and DNA extraction method. For example, glass beads have historically been used to mechanically rupture cells,[30] however it still requires the later steps of DNA purification for downstream analyses. Similarly, surface-modified magnetic particles[14] have been shown to effectively isolate DNA but only from a lysed cell suspension as beads begin to disintegrate under cell lysis conditions. However, magnetic microparticle platforms have pushed the diagnostics field towards a simplified approach to sample preparation as they minimize the instrumentation demands as well as the consumables required when compared to gold-standard DNA extraction methods. Because magnetic particles enable easy separation when the DNA is complexed onto the bead surface, the most resource intensive aspect involves the multiple buffer exchanges. Briefly, microparticles are traditionally functionalized with a silica or an amine coating for cell lysis and

affinity-based DNA binding. Particles functionalized with silica have the same reagent-exchange requirements[31–33] to its macroscale counterpart, but no longer require centrifugation or additional consumables. For amine-coated magnetic microparticles, DNA is bound onto the surface of these microparticles by taking advantage of the electrostatic charges present on both the particles and the DNA. However, instead of using buffers of different ionic conditions, buffers of different pH are employed instead,[34] thereby removing the concerns of salts and alcohol that inhibit PCR downstream. At low pH, the amines present of the microparticle surface become protonated and electrostatically bind to the negatively-charged DNA. With a high pH buffer, these amines become neutrally charged, resulting in the elution of DNA from the microparticle surface. The elution step done at room temperature results in roughly 40% of the DNA being released, most likely due only a fraction of the amines becoming neutral; to ensure complete elution of the bound DNA, the elution step is done at 80 °C to melt the DNA off the bead surface, resulting in 100% release. As a result, the use of aminated beads also have the same reagent-exchanges characteristic of gold-standard methods, and thus both aminated and silica coated particles provide an incremental improvement towards a one-step cell lysis and DNA extraction platform.

To address the need for simplified sample preparation, commercial products that leverage magnetic particles have targeted the need for streamlined DNA capture and purification. One such product are DYNABeads DNA Direct, where the introduction of their magnetic particles in a single, rapid

11

pipetting motion efficiently lyses a cell suspension and allows for the released DNA to complex the DYNABeads. After a series of washes, either the DNA can be eluted off the DYNABead surface, or the DNA/DYNABead complexes can be added directly into a PCR reaction without significant inhibition.[35] However, this protocol does require separate buffers for binding and washing steps, therefore reagent-exchange is still necessary for this platform.

2.2.2.2   Membrane-based sample preparation

While microparticle-based approaches present a facile method for cell lysis and DNA extraction, they do not address the issues of sample collection or sample transfer. Microparticle-based methods still rely on a skilled technician to pipet the sample and the microparticles for sample preparation and then transfer the suspension for amplification and analysis. As a result, membranes have become an increasingly popular avenue[36,37] in developing a low-cost lysis and DNA extraction technology. Overall, membrane substrates offer the advantages of wicking to transport fluids, having a porous or fibrous network to allow for filtration and storage, and allowing for flexible modification methods (either during fabrication, or after with the use of chemicals) that further enhance the substrate's storage abilities. For sample collection and transfer, having a membrane-based system greatly simplifies the amount of user handling as a sample could be directly spotted onto the substrate. Depending on the overall scheme, the flexibility of paper could facilitate sample transfer through wicking, separation, and folding of the substrate to another functionalized region.

The two most popular and well-known paper-based platforms are developed by Whatman: the 903 protein saver platform and the FTA platform. Whatman advertises these two platforms specifically for sample collection, transport and storage. The 903 protein saver platform was first developed for dried blood spot collection for screening purposes. However, this platform does not offer an integrated method for cell lysis or DNA extraction, leaving the user to perform standard purification procedures[38] mentioned previously. The FTA platform is advertised as a substrate that lyses cells, denatures proteins and protects nucleic acids from nucleases and UV damage. However, the key limitation in using the FTA platform is that proprietary reagents must be used in order to either remove protein aggregates or to elute the DNA from the substrate for downstream analysis.[38] While the Whatman platforms do achieve membrane-based cell lysis specifically for sample collection, this is an incremental step and does not address the key issues of the high number of hands-on steps and sample transfer.

Given the aforementioned benefits of using a paper substrate for a diagnostic, research groups have developed numerous lateral flow assays for DNA detection. As a module within the assay, groups have incorporated a DNA capture or DNA concentration step, either with the use of glycogen working in conjunction with chaotropic salts,[39,40] or using chitosan.[41] However, because these platforms require the transport of DNA across the substrate via wicking, only small DNA targets can be tested using this format. If bacterial genomes or larger were to be tested, the size of these genomes would not allow them to

wick along the length of the substrate; if genomic DNA was assayed on this platform, the DNA would have to be sheared prior to running the assay, adding hands-on steps and user handling.

2.2.2.3   Chitosan-based sample preparation methods

Chitosan is a biopolymer that has historically been leveraged for gene delivery given that it is a naturally derived polymer, allowing for a biocompatible, non-immunogenic and biodegradable vehicle.[42] Molecular weight has been thoroughly investigated to determine optimal conditions for polyplex formation between the chitosan and the DNA material used for transfection.[43] Molecular weight has been shown to impact not only the particle size of the polyplexes, but also the binding affinity between the chitosan and the nucleic acid, and DNA dissociation from the polyplex. Specifically, chitosan of molecular weight 150 kDa and higher has exhibited higher DNA binding with limited release of the DNA cargo whereas chitosan of lower molecular weight has been shown to be less stable in forming polyplexes,[44] resulting in poor DNA binding and high release of DNA from the polyplex when formed.

Leveraging knowledge from these gene delivery studies, chitosan has since been employed for DNA extraction, as the amines present along the polysaccharide can also be employed for charge-based binding. Chitosan consists of two main subunits: ß-D-glucosamine and ß-N-acetyl-D-glucosamine. The presence of the deacetylated glucosamine unit contributes a charge to the overall polymer, giving it a pK_a of 6.4,[45] where the polymer is

14

protonated at pH lower than its pK_a. At pH lower that chitosan's pK_a, the protonated amine groups allow for strong electrostatic interactions between the chitosan and DNA backbone. When the pH is greater than chitosan's pK_a, these amine groups become neutrally-charged and the diminished electrostatic interactions allow for the bound DNA to then elute off of the chitosan. Cao, et al.,[46] demonstrated charge-switching for DNA extraction using chitosan-coated silica particles, where 90% of λ-phage DNA in pH 5 buffer was captured onto the surface of chitosan-coated particles. When chitosan-coated particles were incubated with a pH 9 buffer, roughly 87.5% was extracted, thereby exhibiting the first chitosan platform for DNA extraction for low volume samples.

Since this initial demonstration, chitosan has been leveraged in microfluidic biosensors to improve upon DNA-based assays. Byrnes, et al., demonstrated this charge-switching behavior for the purification and concentration of DNA by loading chitosan into nitrocellulose and glass fiber membranes towards the development of lateral flow test.[41] The inclusion of chitosan into the lateral flow strips allowed for purification and concentration from matrices with interfering agents such as excess protein and non-target DNA. For large sample volumes, this platform is extremely flexible for its applications for urine testing or environmental water testing, without compromising DNA recovery. Similarly, Kendall, et al., leveraged chitosan by functionalizing it onto a porous monolith within a thermoplastic, microfluidic chip to better facilitate in-line DNA clean-up methods.[47] Both of these approaches

provide systems that provide high yield, but are limited to applications where target DNA is already in solution.

2.2.2.4 Outlook for NAAT sample preparation

Gold-standard sample preparation methods have remained tethered to the central laboratory due to the need for sophisticated instrumentation, and multiple hands-on steps that require technical expertise. However, by leveraging different form factors such as microparticles and paper, and employing materials commonly employed for DNA binding, DNA extraction methods have improved by removing the requirement for centrifugation. These methods still require multiple buffer exchanges that can be cumbersome to implement within a microfluidic device or integrated system. The ideal sample preparation platform would facilitate simultaneous cell lysis and DNA extraction with a single-buffer system, all occurring within a single tube. In doing so, this would eliminate the many hands-on steps that typically require user intervention, as well as the complicated fabrication required for multiple buffer exchanges. Shifting the sample preparation paradigm to a single-tube format would enable a platform that can be easily automated, and facilitate downstream amplification with minimal inhibitory effects. The subsequent section will discuss work that has been done in our lab to address the challenges discussed above, and Chapter 3 will outline the improvements to our platform to enable simultaneous cell lysis and DNA extraction towards direct PCR amplification.

2.2.2.5 Chitosan microparticles for DNA isolation and amplification

Previously, our group has leveraged whole magnetic microparticles made of chitosan to characterize DNA capture and amplification directly from the microparticle surface.[48] Whole chitosan microparticles were fabricated by crosslinking the outer layer of chitosan emulsions (Figure 2.2A, B). Due to the dense matrix of chitosan, we observed an alkaline shift in pK_a, resulting in strong electrostatic between the chitosan and DNA that prevented the DNA from eluting off the surface (Figure 2.2C). This is similar to what groups in the drug delivery field have previously observed, and enables direct amplification of the bound genomes from the microparticle surface, eliminating the need for elution and its required hands-on steps. By leveraging this shift in pK_a, we have devised a simplified approach to sample preparation by using chitosan whole
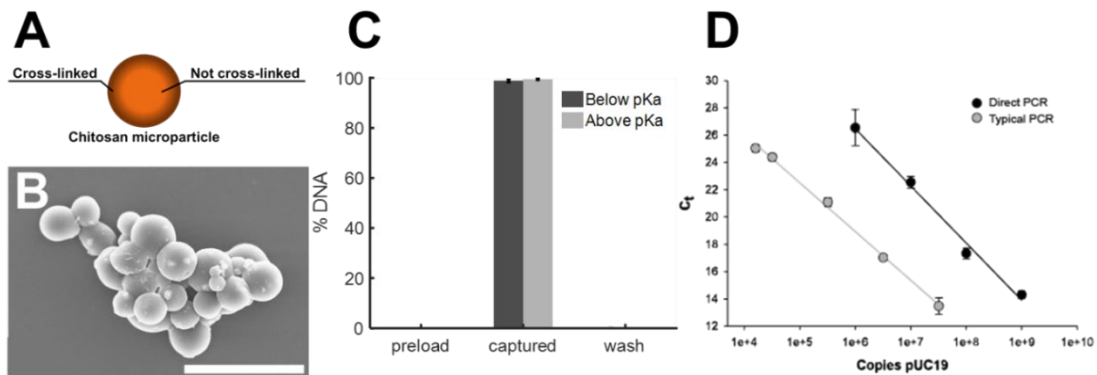
Figure 2.2. Characterization of whole chitosan microparticles. (A) Schematic of an individual microparticle where outer layer of chitosan in crosslinked and inner layers remain uncrosslinked. (B) SEM image of chitosan microparticle clusters. Individual particles are roughly 0.5 to 8 μm in diameter, and aggregate into clusters that are roughly 20 μm in diameter. Scale bar is 10 μm. (C) Capture efficiency of chitosan microparticles using plasmid DNA (pUC19) at pH lower and higher than the pKa of chitosan (6.5) (D) Calibration curves for DNA amplified in solution (termed Typical PCR, in gray) and DNA amplified directly off microparticle surface (termed Direct PCR, in black). Figures adapted and modified from KR Pandit, **IA Nanayakkara** et al.,[27] with permission.

microparticles for direct DNA extraction and amplification by performing PCR directly at the surface of the microparticles.

The main drawback from whole chitosan microparticles is the poor PCR efficiency when compared to typical, solution-based PCR; for a given concentration of DNA, there is roughly a 6-7 cycle delay between the typical PCR control and microparticle-based amplification (termed direct PCR, Figure 2.2D). We hypothesize that this arises from how the whole chitosan microparticles are fabricated, where chitosan is crosslinked together using glutaraldehyde. When the DNA is bound to the microparticle, it is deeply embedded within the matrix, preventing access of the polymerase to certain regions of template. Additionally, whole chitosan microparticles cannot be leveraged towards a one-step cell lysis and DNA extraction approach; these microparticles lack a solid core, and therefore, they rupture even during gentle agitation when binding with DNA in solution and lack the robustness required for cell lysis. Between the lower limit of detection due to the cycle delay and the fragility of the microparticles, the chitosan microparticle platform must be restructured and redesigned for improved direct PCR performance and robustness. The continuation of this work will be discussed in Chapter 3.

2.3   Nucleic acid sequence amplification and detection

The earliest examples of nucleic acid amplification can be dated to the early 1960s[49] with the use of in situ DNA hybridization assays. The Southern blot is one of the most popular of these methods. First conceived in 1975,[50] the Southern blot involves first fragmenting DNA with the use of restriction

endonucleases, separating the fragments with gel electrophoresis, transferring the products to a cellulose nitrate strip, and lastly labeling with radioactive RNA downstream for direct visualization of the fragments. Since then, hybridization assays have evolved into dot blot assays – involving the direct deposition of target DNA and thus, eliminating the need for fragmentation and separation[51] – and then into the modern-day DNA microarrays, which leverages direct labeling of target DNAs or RNAs with a fluorophore (Figure 2.3).
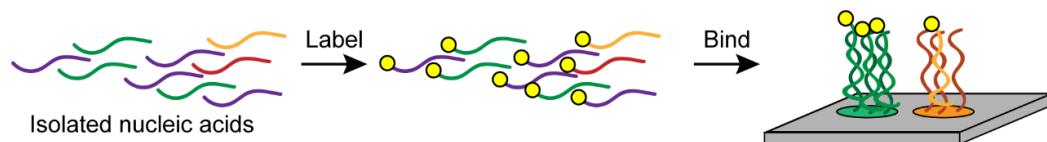
Figure 2.3. DNA microarrays. Following isolation of target nucleic acids, a labeling kit is used to conjugate a fluorophore to the end of the target. This enables visualization following hybridization with complementary probes that are immobilized onto a solid phase.

These assays involve multiple steps that require technical expertise, such as blocking the substrate to minimize nonspecific adsorption, adding reagents such that concentration gradients are minimized, and washing of excess target sequences. Additionally, the sensitivity and limits of detection are largely dependent on the complementarity of the target DNA to the capture oligonucleotides, the thermodynamic stability of these probes,[52] as well as the labeling mechanism for detection.[49]   Detection has been previously demonstrated with radiolabeling,[50,53,54] chemiluminescence,[55–57] and fluorescence.[58,59] However, all of these methods of detection are measures of single binding event, where one binding event leads to a proportional number of detection events. For POC applications where low copy detection is necessary, often hybridization assays are limited in their sensitivity and limit of

detection thresholds. As a result, diagnostic technologies have looked to increase the number of DNA molecules produced from a single binding event, such that when coupled to detection methods, like fluorescence, we can achieve much lower sensitivities than traditional hybridization assays. The following sections highlight the evolution of gold-standard methods for nucleic acid amplification, the limitations of these methods, and existing alternatives that address the needs for POC NAATs.

2.3.1 Polymerase chain reaction (PCR)

Polymerase chain reaction, or PCR, is a sensitive assay where single-copy limits of detection can be realized. First realized in 1985,[60] PCR first involved using Klenow polymerase, a thermolabile polymerase from *E. coli*, to amplify short gene-specific sequences of DNA by cycling between temperatures repeatedly. Because of the repeated melt step required to denature DNA, enzyme needed to be added to the reaction every cycle. However, shortly thereafter, DNA polymerase from *T. aquaticus* (Taq polymerase) was discovered to be a thermostable alternative[61] and can survive extended incubation at 95 °C. This led to the standard PCR reaction that is still in use today: these reactions require having an excess of primers, DNA sequences that are complimentary to an 18 – 25 base-pair region of the target that are extended by the polymerase to create copies of the template, or amplicons. With multiple cycles of heating and cooling – duplex melting and primer extension – the DNA region of interest is amplified exponentially. This is

especially useful for applications requiring low-copy detection,[62,63] which would otherwise be impossible using a hybridization assay.
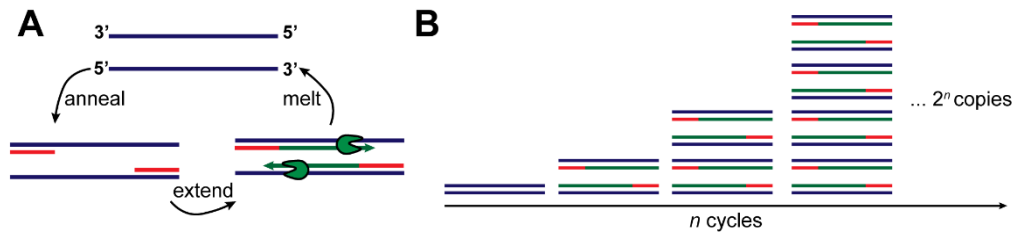
Figure 2.4. Polymerase Chain Reaction (PCR). (A) PCR consists of cycling among three steps: melt to denature the DNA, anneal for primer binding, and extend to polymerize the primers to create copies of the sequence of interest. (B) With each cycle, the amount of products double so that at the end of n cycles, there are 2^n copies more than the starting amount of DNA.

PCR is only suitable for DNA templates, as they do not degrade at high temperatures. For RNA targets, an additional step is required, involving the use of a reverse transcriptase (RT). Originating from retroviruses,[64,65] reverse transcriptase historically converts the viral RNA genome into a complementary DNA (cDNA) to enable integration into the host genome. By using this enzyme in conjunction with PCR for RNA analyses, the RNA sequences of interest can serve as a template with a universal set of primers to create cDNA, which can be later quantified with the approaches outlined in the next section. This remains to be the most popular method of low copy RNA quantification for gene expression studies, and has since been extended to other RNA targets, such as circulating RNA,[66–68] RNA viruses,[69–71] and microRNA (miRNA).[72–74] Because the RT step for RNA quantification involves an enzyme with differing operating conditions than the Taq polymerase and a different set of primers, historically this step has been done separately prior to PCR and therefore increases the technical expertise and assay time for these tests. As diagnostic

assays have modernized, one-step RT⁻PCR have been developed to leverage the use of gene-specific primers, and thus enable a one-pot reaction for both steps of the assay; however this also increases the likelihood of primer-dimers and nonspecific product formation,[75] and compromises sensitivity and limit of detection.

2.3.1.1 Quantitative PCR (qPCR) and Taqman PCR

With the development of quantitative or real-time PCR (qPCR), PCR technology quickly became a more powerful tool as it was no longer hindered by post-processing for the detection of amplicons (i.e. gel electrophoresis). Because qPCR allows for simultaneous product synthesis and measurement, it is attractive for diagnostic applications. The first approach used the DNA binding dye, ethidium bromide, where in the absence of double-stranded DNA, there is no fluorescent signal but in its presence, the dye binds between the DNA grooves or bases and produces a fluorescent signal.[76] As more product is synthesized, the fluorescent signal increases; by defining a fluorescence threshold, the amount of DNA in the original sample can be quantified based on the time taken to reach the given intensity. However, because DNA binding dyes target all DNA present, this method does not lend to specificity in detection. Often, nonspecific amplification can occur for two main reasons: the first being the amplification of dimerized primers, and the second being the result of primers binding to other sequences in the target, known as off-target amplification. As a result, the amplification of either primer-dimers or off-target annealing will contribute to the amount of DNA being generated. DNA binding

dyes, as a result, will also fluoresce with these nonspecific products, and provide inaccurate quantification. For applications where multiplexed detection is necessary, DNA binding dyes do not provide specific quantification information as it measures the total DNA being produced. As a result, DNA binding dyes are often not used for multiplexing, unless spatial multiplexing is incorporated. Since the original publication, other DNA binding dyes have been developed specifically for PCR applications, such as the SYBR dyes[77,78] and other cyanine dyes,[79,80] to address assay inhibition that is characteristic of older DNA binding dyes.

A more specific approach can be employed with Taqman PCR (also referred to as a nuclease assay), in which a "probe" sequence is introduced to the reaction that hybridizes with the target downstream of a primer region. This probe leverages Förster resonance energy transfer, or FRET, as one end is conjugated to a fluorophore – the donor molecule – and the other end is conjugated to a fluorescence-quenching molecule – the acceptor molecule. In its intact form, no fluorescent signal is generated from the donor due to the proximity of the two molecules. However, as the polymerase synthesizes new DNA, the nuclease activity of the polymerase degrades the probe, separating the fluorophore and the quenching molecule and thereby resulting in the emission of the donor fluorophore.[81] Because this signal is generated only if the exact target sequence is replicated, rather than if any sequence is replicated, Taqman PCR adds specificity and multiplexing to the assay that can be leveraged for one-pot, multi-analyte detection. Taqman PCR remains to be

23

the most attractive method for applications requiring high specificity. Examples of developed Taqman PCR assays for diagnostics include the quantification of fetal DNA from maternal plasma for noninvasive prenatal diagnostics,[82] and implementation in Cepheid's XPert®, a Taqman PCR system developed specifically for low-resource settings, towards the identification of the Ebola viral strains.[83]

2.3.1.2   Limitations of PCR for POC diagnostics

Given the prevalence of PCR for laboratory testing, it has naturally become one of the first molecular amplification systems translated for near-patient settings. Microfluidic systems have demonstrated significant strides in miniaturizing PCR systems, effectively reducing the sample volume required by discretizing the sample into droplets and decreasing assay times by improving the thermal kinetics. However, these systems require bulky peripheral instrumentation, such as syringe pumps required for sample discretization, and user intervention. As a result, commercial PCR systems for POC settings still test larger volumes. Another important aspect to note is the cost and speed limitations of these integrated systems. The Cepheid XPert is one of the most widely-used systems for PCR NAATs, integrating sample preparation, amplification, and detection. However, because of the complex hardware and valve integration required for buffer exchanges and fluid transport, these systems can be too expensive for near-patient settings (the overall system being roughly $17,000 with each test-specific cartridge at roughly $10 as reported in 2012).[84] In additional to the financial burdens, these

systems have high power demands in order to cycle between temperatures. While cost and power constraints are not limiting factors for POC environments like doctors' offices, integrated platforms like the Cephied XPert still have assay times close to an hour. In these environments, the need for faster assays is the driving factor for POC NAAT development. For environments such as resource-limited settings, a POC NAAT needs to be cost-effective, cheap, and robust. To truly bring NAATs closer to the bedside, novel amplification methods that can address speed, while also moving away from thermocycling-driven amplification, would make these tests more accessible in a variety of near-patient environments. The following sections outline several developed isothermal amplification schemes, and how they compare to PCR for POC settings.

2.3.2 Developed isothermal amplification schemes

As mentioned previously, the sophisticated instrumentation required to cycle between 2 – 3 temperatures requires complex design and power constraints for any POC device. To minimize the footprint of these devices, significant efforts have been focused on assays that operate at a single temperature, known as isothermal amplification schemes, to eliminate the need for temperature-dependent melting and annealing of nucleic acids. This section aims to illustrate these novel polymerase-driven amplification schemes, and to discuss their advantages and limitations towards applying these methodologies for POC NAATs.

2.3.2.1　　　Non-polymerase driven isothermal amplification schemes

One of the main limitations for any enzyme-based amplification is to ensure the activity of the polymerase. As a result, there is often an incorporated "hot start" step,[85] to melt off either aptamers,[86] proteins,[87] or wax[88] that prevents activity of the enzyme during reaction preparation, or it requires cold transport or lyophilization of reaction components to ensure the enzyme's function. Another consideration for any enzyme-driven amplification scheme is its robustness against inhibitors that are normally present in crude samples. Often, these enzymes are highly sensitive to these inhibitors, and require that the sample be purified in order to maintain optimal function. Therefore, these assays require rigorous sample preparation to ensure that inhibitors such as heme from blood,[89] urea from urine,[90] etc. are not introduced into the assay. Because of these limitations, there are some amplification schemes that aim to eliminate enzymes all together, and rely on using synthetic nucleic acid sequences to achieve transduction.

Hybridization chain reaction (HCR) is a popular enzyme-free amplification scheme that leverages single stranded DNA sequences designed to self-assemble into more complex structures at room temperature. The assembly of these structures is driven by the free energy of base pairs, and are designed such that the synthetic sequences do not hybridize – and thereby start the amplification reaction – until the addition of the target DNA. As a result, HCR presents an attractive alternative, as no external instrumentation (i.e.

heaters, thermocyclers) is required and can be easily implemented in most POC settings.

HCR involves the design of two hairpins with small loops, which act as a kinetic trap given the stability of the structure.[91] The addition of the target sequence triggers strand displacement in the hairpins, and allows them to bind together to form a larger complex, analogous to polymerization in an enzyme-based amplification scheme. This continuous hybridization occurs until the two hairpins are entirely incorporated into these "polymerized" structures (Figure 2.5). Because HCR is a linear amplification scheme, in which there is a proportional amount of signal produced in relation to the amount of target added, the reaction times needed for low concentrations are on the scale of hours. As a result, several nonlinear HCR methods have been developed; examples of this involve triggering the self-assembly of dendritic DNA super structures,[92] and increasing the amount of hairpins to produce concatenated structures – termed hyperbranched HCR.[93] Both of these HCR methods result in quadratic, if not exponential, signal amplification, and therefore achieve high sensitivity with high specificity.[94] However the design of these additional hairpin monomers for both dendritic and hyperbranched HCR are equally complex, and present another barrier towards wide use of HCR systems.

Because HCR is very dependent on strand displacement via toe hold exchange, and the stability of the stems that form the hairpin, these are critical parameters in designing the assay. Any small variation in the hairpins can cause failure of the HCR process, most often due to the "leakage" of the
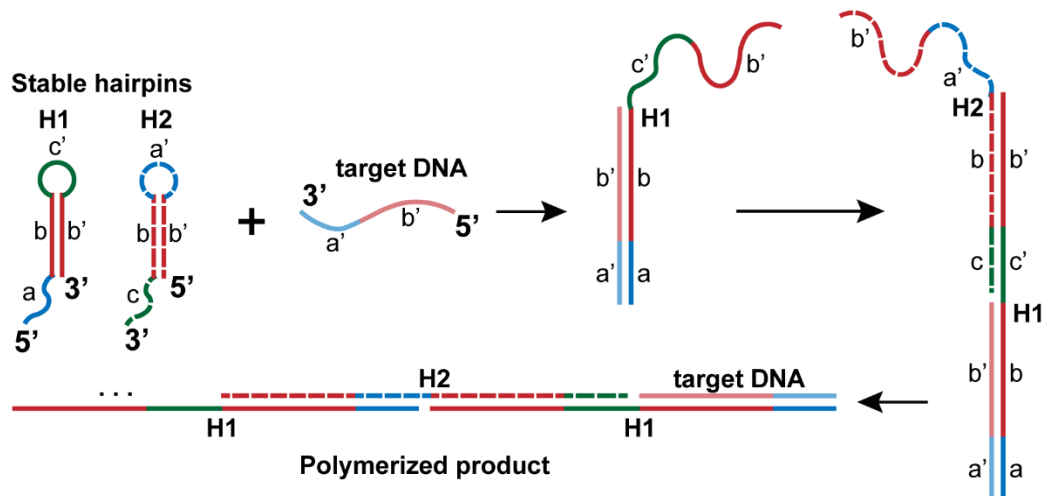
Figure 2.5. Hybridization chain reaction (HCR). Hairpins H1 and H2 contain stems that act as kinetic traps, and do not interact with one another. Only upon addition of the target DNA does toe-hold exchange begin, first opening H1 and linearizing the hairpin. Because H2 contains an overhang that is complementary to newly linearized H1, toe-hold exchange will occur again allow H2 to hybridize to H1. These structures continue to participate in toe-hold exchange and hybridization to form a polymerized product that can be detected downstream.

hairpins where the hairpins begin to nonspecifically hybridize and start amplification. Despite design constraints placed on GC content, toe-hold length, and stem lengths, any variation in temperature can cause shifts in the thermodynamic equilibrium and also negatively impact the assay. Between these design constraints and the poor sensitivity of HCR, this enzyme-free method is limited to laboratory use, or is coupled with other linear enzymatic amplification schemes[95,96] in order to achieve the desired limit of detection.

2.3.2.2 Polymerase-driven isothermal amplification schemes

2.3.2.2.1 Loop-mediated isothermal amplification (LAMP)

To address the issue of thermocycling, one isothermal method that has been developed is loop-mediated isothermal amplification, or LAMP, where DNA is amplified continuously with high specificity at a constant 65 °C in under an hour. Briefly, LAMP leverages 4 – 6 primers that are specific to 6 – 8 regions

of the target, respectively. These primers either serve to create loops, which can act as primer binding sites downstream, or to act as bump primers, that facilitate strand displacement to produce amplicons. The first round of amplification produces a dumbbell-like structure with two loops on either end as the starting material (Figure 2.6A, orange structure). These loops contain primer binding and extension sites that continue amplicon generation with increasing loop structures to feedback into the amplification scheme (Figure 2.6B). The final products range in size as a result of the various primer annealing combinations, and consequently, this method of DNA amplification allows for low limits of detection. The first publication of this method was shown
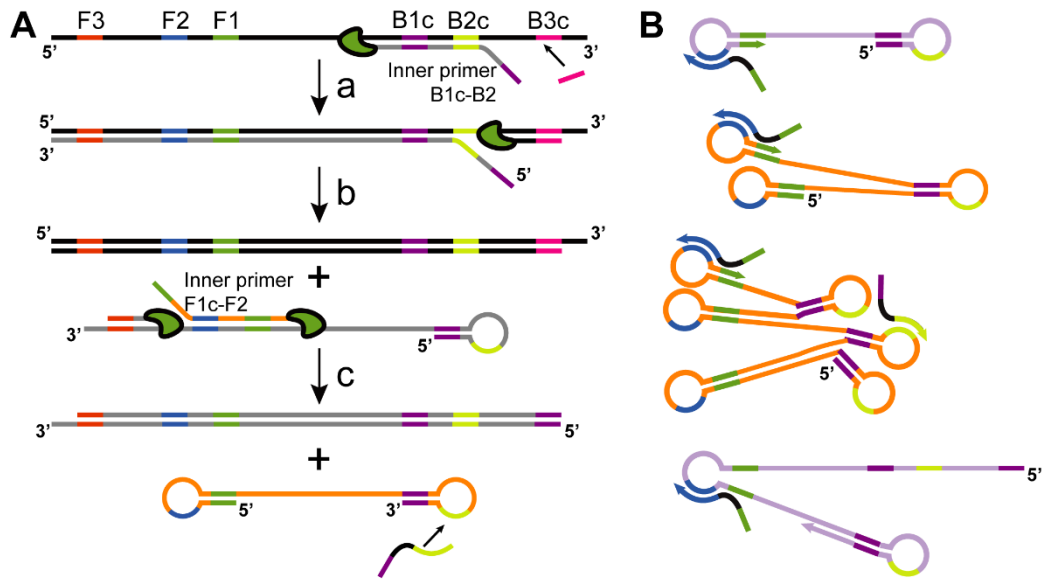
Figure 2.6. Loop-mediated isothermal amplification (LAMP). (A) Four core primers, termed bump primers and inner primers, target six regions of the template. The inner primers consist of a sequence that hybridizes to either B2 or F2, and contains an overhang with B1c or F1c. Upon extension of the primer, the newly formed DNA will create either B1 or F1, thereby allowing the overhang to hybridize and form a loop. Because this scheme employs strand-displacing enzymes, bump primers targeting B3 or F3 serve to push the amplicon off the template to allow for additional primers to anneal and extend. This results in the formation of a dumbbell structure (orange structure, A, or purple dumbbell, B) that yields further concatenations to produce higher molecular weight products for detection (B) with either fluorescence, colorimetry, or turbidimetry.

to be able to detect as few as six copies of hepatitis B viral DNA.[97] By eliminating the need for themocycling by having a single operating temperature, and leveraging four to six primers with a high amount of polymerase, LAMP assays can enable single copy detection within 30 minutes,[98,99] significantly reducing assay times that are characteristic of PCR.

LAMP has since become a widely recognized amplification scheme specifically for POC applications due to the simpler instrumentation required for detection. With LAMP, thermocyclers are no longer required and detection methods can extend beyond using intercalating dyes, through methods such as calcein fluorescence in the presence of by-products of nucleic acid polymerization or turbidity of the reaction volume due to the high concentration of generated DNA.[100] Additionally, LAMP has been used in microfluidic devices, in conjunction with a reverse transcriptase step, for the detection of HIV RNA and achieved a detection limit of fewer than 10 copies of RNA with a run time of one hour.[101] Despite the advantages of LAMP, this amplification scheme requires a constant temperature of 65 °C, and therefore requires more power than isothermal amplification systems which operate at 37 °C. Some reports have utilized chemical heating (inspired by hand warmers) along with engineered phase-changing materials to maintain a constant 65 °C for the duration of the reaction without consuming electricity.[102–104] Additionally, the assay is entirely dependent on the complex design and specificity of the four primers involved and therefore, any mismatch will significantly impact the efficiency of the reaction.[105] Another reported disadvantage includes the high

rate of false positives[106] as the four to six primers involved can form secondary structures and consequently, nonspecific extension sites; researchers have been able to address this with the use of molecular beacons for additional specificity, however for a POC application, this would also increase the cost of a device.

2.3.2.2.2   Exponential Amplification Reaction (EXPAR)

Another isothermal method that has leveraged strand-displacing polymerases is the exponential amplification reaction or EXPAR. EXPAR produces exponential signal generation by leveraging the instability of short duplexed DNA at higher operating temperatures.[107] Briefly, a target will bind to a template and be extended. Upon extension, a nicking enzyme will recognize the newly-formed duplexed DNA and create a cut on the produced amplicon. Due to the thermal instability, the short DNA will melt off of the template, and facilitate the cycle of extension, nicking, and melting to exponentially produce amplicons. Because of the simple template design, exponential amplification can be achieved either by direct EXPAR or copy EXPAR. Direct EXPAR involves a symmetric template where complementary target sequences flank the recognition site of the nicking enzyme. Upon extension of the target, a target analog is created and released upon nicking. This newly released analog can then bind to another template and continue the amplification reaction (Figure 2.7A). However, with copy EXPAR, two templates are designed: the target binding to the first template will create a secondary trigger sequence that will melt off the template upon nicking. This trigger will then bind to the second

template, where two complements to the trigger flank the nicking enzyme's recognition sequence. Once the trigger binds, exponential amplification will occur as it does with direct EXPAR, but is driven by the products of the first amplification reaction (Figure 2.7B).
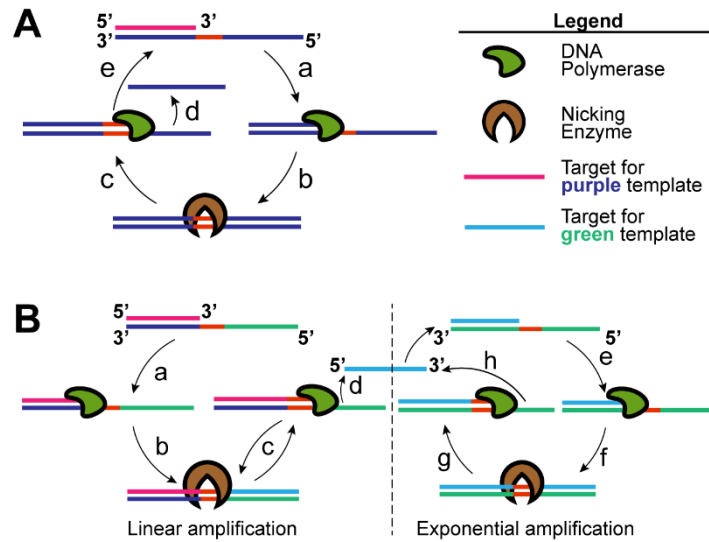
Figure 2.7. Exponential amplification reaction (EXPAR). (A) Direct EXPAR employs a symmetric template that contains the reverse complement sequence of the target DNA flanking either side of nicking enzyme recognition sequence. Upon binding of the target (a), the polymerase (green) extends the target to form a duplex (b). The nicking enzyme (brown) then recognizes the double-stranded duplex and its recognition sequence, and cuts the upper strand (c). Due to thermostability, the short DNA melts off the duplex (d), which leads to it binding to a new template (e) and continuing the process of extension and nicking (c). (B) Similar to direct EXPAR, copy EXPAR is a two template system, where the first template only contains one copy of the reverse complement to the target (a). Extension and nicking of enzyme (b, c) leads to the creation of a new amplicon that participates in direct EXPAR with the second template (d). Here, the new amplicon produces analogous products via extension and nicking (e-h) to feedback into the system, along with the amplicons produced from a-c.

Because EXPAR is highly sequence-dependent and is well suited for short oligonucleotides, it has been utilized heavily in miRNA detection given the many mutations present in a family of miRNA, and the advantage of direct amplification instead of a two-step amplification scheme (RT-PCR). Since the original publication, the simple design of EXPAR has been leveraged and redesigned for miRNA to discriminate let7a variants,[108] where variants that had

mutations towards the 3' end of sequence (where extension of the miRNA would occur) amplified significantly later than the perfect complement. Given its robust amplification efficiency for miRNA, FRET-based hairpin probes, quantum-dot conjugates,[109] and gold nanoparticles with surface-enhanced Raman spectroscopy[110] have been leveraged to achieve multiplexed detection with EXPAR. Across the various types of detection and reporter methods for EXPAR, detection limits ranging from sub-femtomolar to 100 fM can be achieved.[111]

The main challenge in realizing a POC NAAT that utilizes EXPAR is the high nonspecific background signals when multiplex detection is involved. In traditional amplification schemes such as PCR, the target acts as the template where primers recognize the template to begin extension; however with EXPAR, the target instead acts as the primer upon binding to the template to begin the amplification reaction. As a result, for low target concentrations, there is a higher chance of DNA synthesis in the absence of primers,[112,113] which is exacerbated in the presence of a nicking enzyme,[114] and thus contributes to both a high background signal and nonspecific amplification. In addition, when designing multiple templates for multiplex detection, there is a higher chance of nonspecific interactions between the different templates which would result in additional extensions to generate nonspecific products. There are several ways to mitigate the nonspecific background signal, such as using a WarmStart polymerase,[115] using copy EXPAR instead of direct EXPAR,[116] minimizing the GA-rich regions in the template,[116] or the inclusion of additives such as

tetramethylammonium chloride (TMAC) or trehalose;[117] however some of these approaches simply delay the onset of nonspecific amplification by five to ten minutes, without eliminating it entirely.[117] As a result, limits of detection, sensitivity and specificity can be severely hindered in a multiplexed reaction, and would rely on spatial multiplexing for detection.

2.3.2.2.3   Rolling Circle Amplification (RCA)

Rolling circle amplification (RCA) provides a simple and efficient isothermal method of amplification that is amenable to both DNA and RNA targets. Building on the work of Nilsson et al., the target acts as a primer that binds with a padlock probe, a DNA sequence that has two complementary sites to the target (Figure 2.8A). Upon hybridization, a ligase acts on the probe and joins to the two ends, effectively circularizing the probe and creating a template. By having two complementary sites to the target, this adds specificity to the reaction, especially for targets that may have single nucleotide variations as mismatched ends of the probe are poor candidates for efficient ligation.[118] However, this early work relied on gel electrophoresis to differentiate ligated probes from unligated probes. Additionally, due to the single conversion ratio of the padlock to the circularized form, this ligation method was only suitable for targets that are in high concentration. RCA addresses the need for lower sensitivity with the incorporation of a polymerase in addition to the padlock probe and ligation. Inspired by rolling circle replication, the method that bacteria use to replicate plasmids, the polymerase acts on the primer following ligation and replicates the circular template to produce single-stranded DNA amplicons

of high molecular weight (Figure 2.8B).[119] Each amplicon will contain repeats of the template's complementary sequence, which can be leveraged for downstream product verification either with restriction enzymes that are sequence-specific, or with the use of molecular beacons.

Because RCA, as outlined above, requires assay times on the order of hours due to its linear nature, augmented methods of RCA have been developed to address the need for nonlinear amplification to achieve higher sensitivities and lower limits of detection. One such method, multiprimed RCA, involves having multiple primer binding sites on the circularized template (Figure 2.8C). As a result, multiple amplification products can be generated upon binding to a single circle. Another variation of exponential RCA is hyperbranched RCA, where multiple primers are designed to be complementary to the generated RCA product (Figure 2.8D). Similarly, the same exponential signal generation can be achieve with designing multiple circles that recognize the generated RCA product (Figure 2.8E). With the incorporation of the nicking enzyme recognition sequence, the amplicon can be nicked and then become a primer for these secondary circles, further driving amplification.
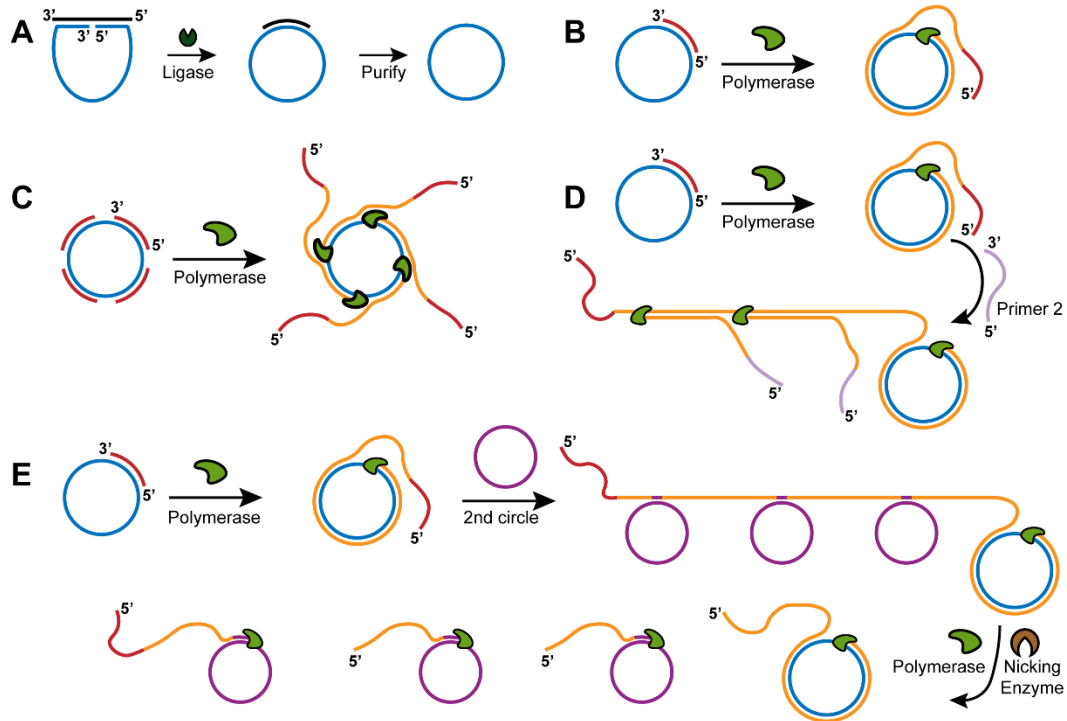
Figure 2.8. Rolling Circle Amplification (RCA). (A) depicts the creating of circular templates, where a ligation template (black) recognizes to the two complementary arms of the padlock probe. Upon hybridization, ligase joins the ends of the padlock, circularizing the probe. (B) RCA takes place once a primer (red) hybridizes the probe. The polymerase recognizes the free 3' end and begins templating along the circle. Once it has made a full turn, it'll displace the polymerized amplicon and continue synthesizing DNA. (C) Multiprimed RCA. Multiple primers hybridize to the circularized template, providing more extension sites for exponential amplification. (D) Hyperbranched RCA: Secondary primers are designed to hybridize to the generated amplicon, providing another avenue for exponential amplification. (E) Hyperbranched RCA: Secondary circular templates hybridize to the generated amplicon. Upon nicking, the amplicon then serves as a second primer to further drive exponential amplification.

Because of the facile sequence design, low operating temperature of 37 °C, and easy implementation, RCA is a popular isothermal method for a variety of applications, one of which is miRNA detection. The small lengths of miRNA again make it an ideal candidate for both a ligation template, and a primer for polymerization. Many groups have presented augmented RCA methods to achieve the sensitivities required for miRNA. While the early reports for miRNA detection involved traditional RCA[120] and hyperbranched RCA,[121] these methods succumb to the challenges of realizing RCA for practical

36

biosensing purposes; specifically, the ligation reaction required for circularization often leads to linear multimeric secondary products[122] and consequently require purification, or requires strict optimizations for the enzymes involved in the reaction[121] to minimize nonspecific amplification. To circumvent these issues, more recent RCA strategies have utilized pre-circularized templates, where in the absence of the target, are a dumbbell structure. These specialized dumbbell templates only become circularized when bound to the perfect miRNA complement,[123] or once ligated, still maintain their dumbbell structure in order to produce secondary double-stranded structures in the amplicon, thus enabling real-time detection with the use of DNA binding dyes.[124] With these specialized dumbbell templates, limits of detection range from subfemtomolar to single femtomolar concentrations.

Despite these advances, there are few published reports that leverage exponential RCA for multiplexed detection. Possible limitations of RCA for applications requiring multiplexing involve the design of multiple templates or multiple primers for each target of interest. In a single-tube reaction, it is imperative that none of the templates or primers nonspecifically hybridize to create extension sites for the polymerase to act. Additionally, multiplex detection would rely on the use of molecular beacons, which come with their own design burdens. As a result, exponential RCA would be limited to spatial multiplexing for a POC application.

2.3.2.2.4   Nucleic acid sequence-based amplification (NASBA)

The last amplification scheme that will be discussed involves the sequence-dependent nature of RNA polymerase transcription. Nucleic acid sequence-based amplification (NASBA), also known as self-sustained sequence replication (3SR), was specifically developed to allow for the direct detection of RNA sequences, as an alternative to multistep RT-qPCR methods. NASBA mimics the *in vivo* retroviral replication of an RNA template, by using three enzymes and two primers to achieve exponential product generation.[125] Here, the RNA target acts as the template and primer binding site to begin the reaction (Figure 2.9A). Upon binding of the first primer, which contains the sense sequence of the RNA polymerase promoter, reverse transcriptase will act on the 3' end of the primer and begin extending it. Following extension, the RNA is removed with the use of RNase H, freeing the newly synthesized DNA to acts a template to continue the reaction. A second primer then hybridizes and is extended of the synthesized DNA, now creating a duplexed promoter. The double-stranded promoter then initiates transcription with the RNA polymerase, a sequence-specific enzyme that only acts upon a duplexed promoter. Transcription of the duplexed DNA creates RNA that can feed back into the reaction, leading to exponential generation of RNA (Figure 2.9B). This RNA can be quantified with traditional methods such as gel electrophoresis, or more commonly, with molecular beacons[126] specific to the generated RNA amplicons to enable real-time detection.
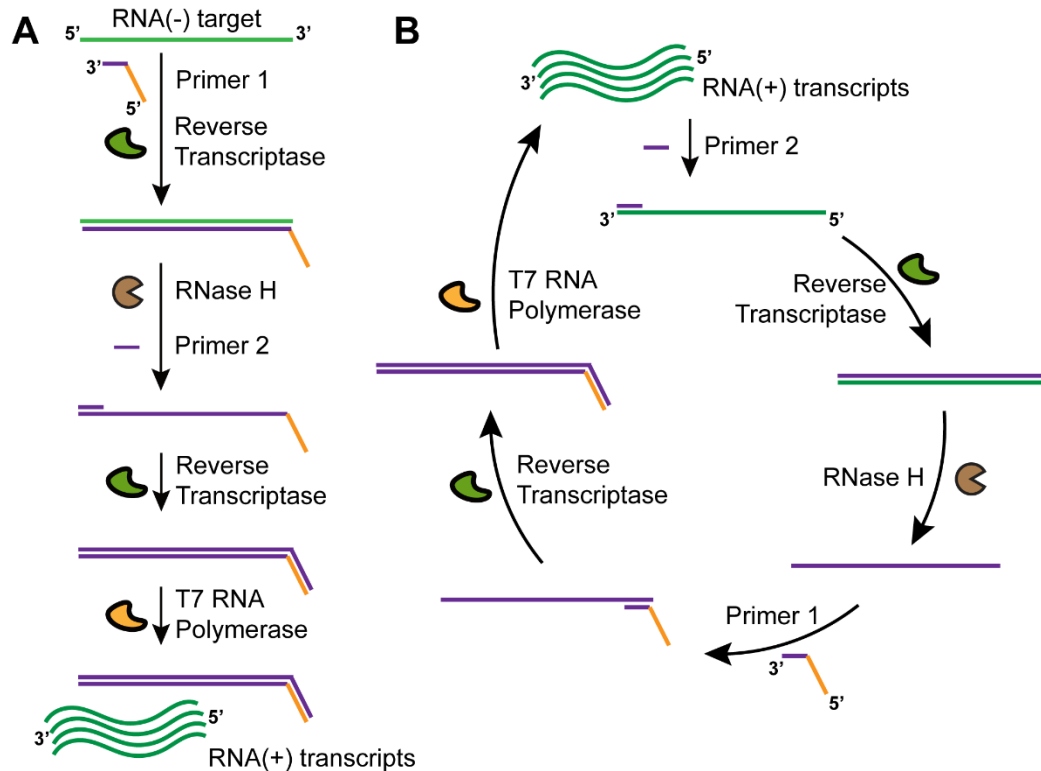
Figure 2.9. Nucleic acid sequence-based amplification (NASBA). (A) Linear phase: An RNA target first hybridizes with Primer 1. Primer 1 consists of an overhang that encodes for the T7 promoter. Reverse transcriptase recognizes the free 3' end and extends Primer 1. RNase H, an enzyme that selectively degrades RNA, proceeds to remove the target to then allow Primer 2 to hybridize the remaining DNA strand. Reverse transcriptase extends Primer 2, thus producing a full duplex containing the double-stranded promoter. T7 RNA polymerase then recognizes the double-stranded promoter, and produces antisense (RNA (+)) analogs of the initial RNA target. (B) Exponential phase: RNA (+) strands feedback into the system as they can first hybridize with Primer 2. Similar to the linear phase, the primer is extended and RNase H acts on the RNA transcript by degrading it. Primer 1 then binds to the remaining DNA. Because there are now two free 3' ends, polymerization by the reverse transcriptase leads to the full duplex, and again the double-stranded promoter. This further produces RNA transcripts and facilitates exponential amplification.

Because NASBA enables the real-time detection of RNA within a single-tube reaction operated a single temperature, it has been employed since the 1990's for the quantification of viral[127–131] and bacterial[132–134] RNA targets. Since then, the RNA targets tested have expanded to include genomic, messenger (mRNA), ribosomal (rRNA) and transfer-messenger RNA (tmRNA) targets. Since its creation in the early 1990s, it has been commercialized by Organon Teknika (now owned by Biomerieux), where all buffer and enzyme

components are available as part of the NucliSENS Basic Kit, and primers and molecular beacon probes specific to the intended target are purchased separately.[135] Targets range from rRNA targets for bacterial identification, mRNA specific to the translation of proteins (such as gp105 mRNA for identification of human herpes virus 6), and non-coding regions[135] or group-specific antigen genes[136] of viral genomes. With the partnering sample preparation and DNA extraction platforms as well as the custom amplification and detection instrumentation, this NucliSENS kits have demonstrated sample-to-answer times of roughly 4 hours when assaying 24 samples.[137] Additionally, several studies have shown that NASBA performs similarly to existing commercial Taqman PCR assays, enabling the adoption of this platform in central labs where specific diseases of interest are highly prevalent.[138] Again, because the modules of sample preparation and DNA amplification are highly dependent on the availability of refrigeration and access to a power source, the NucliSENS platforms are again tethered to the central lab. Previously, CorisBioConcept leveraged NASBA for the identification of *Leishmania* and *T. Cruzi* using lateral flow tests for detection.[139] These assays normally took roughly 90 minutes to run, and cost about $26 per test. However, this company now focuses solely on dipstick-based assays that no longer require amplification beforehand and thus, no longer provides these products. Despite this, it does demonstrate that NASBA is a suitable technology for POC applications.

Overall, NASBA provides a sensitive and robust method for direct detection of RNA targets. By leveraging the target as the hybridization template for primers downstream, it reduces the chance of off-target amplification and transcription. However, there have been several reports suggesting that for certain disease targets, NASBA does not provide the necessary specificity as compared to traditional PCR tests.[140] This is in part due to early stage amplification that occurs due to the nonspecific transcription of dimerized primers, specifically those where the T7 RNA polymerase promoter region is included.[141] As a result, extra care must be taken when designing primers and molecular beacons for these assays, as any nonspecific hybridization will inevitably lead to a high background signal, or worse a false-positive result.

2.3.3 Outlook for DNA amplification methods

With the directed evolution Taq polymerase and the specificity brought by sequence-specific binding of targets, PCR and its derivatives for other nucleic acid targets have offered sensitive detection, often with a wide dynamic range and low limits of detection. However, as the diagnostic community aims to bring these assays outside of the central laboratory, the temperature-driven model of amplification falls short due to the instrumentation constraints of these near-patient settings. Significant progress has been made towards the development of isothermal amplification schemes for both RNA and DNA targets alike. While PCR is often criticized for its instrumentation burdens, PCR offers the advantages of having specific activity with the use of hot-start mechanisms and temperature-cycling to drive the specific binding and

extension of primers and the activity of Taq polymerase. While the aforementioned isothermal schemes that are presented as improved alternatives to PCR, often they present new design challenges due to the constant activity of these enzymes at a single temperature. As a result, most of these schemes suffer from some form of nonspecific amplification, either caused by the robust activity of the polymerases involved, or unintended hybridization that leads to additional extensions sites on which the polymerase recognize. Additionally, these schemes are heavily reliant on DNA binding dyes, which do not differentiate on-target versus off-target amplification. Therefore, novel detection methods to achieve multiplex detection, as well as insights towards achieving specific amplification in an assay need to be expanded to better inform assay design and translation towards an integrated device. Chapters 4 and 5 aim to address these issues where we assess a previously reported probe-based method towards multiplex detection of three MRSA genes, and we evaluate different design considerations towards the development of a novel amplification scheme specific to microRNA targets, respectively.

Chapter 3. Simplifying nucleic acid amplification from whole blood with direct PCR on chitosan microparticles[1]

3.1   Introduction

NAATs, in particular PCR, are commonly used in diagnostics as discussed in Chapter 2, including inherited diseases, cancer, and infectious diseases.   In recent years, an extraordinary amount of research and development has been directed at the transition from central lab PCR tests to near-patient NAATs. The first demonstrations of microfluidic PCR date back nearly 25 years;[142,143] recent review articles report numerous demonstrations of miniaturized PCR[144,145] and isothermal NAATs[146] that target near-patient applications.

While PCR and other NAATs have been successfully miniaturized, the amplification reaction and signal measurement are not the most challenging components to implement in a near-patient or low-resource setting. In reality, the sample processing steps present the steepest challenges, especially for diagnostic assays aiming to achieve the cost targets and the regulatory clearance for near-patient use. Traditionally, nucleic acid purification is carried out using a solid phase extraction technique.[147] The most commonly used commercially available format is a spin column with a silica membrane

---

[1] This work was published in Analytical Chemistry, 89(6) 2017, 3773-3779

designed for use with a centrifuge. First, DNA is liberated from cells using a lysis buffer. Then, binding, washing, and elution solutions are driven through the column in series by centrifugal force. Chaotropic salts in the lysis buffer drive adsorption to the silica. Alcohol is then used to wash away the salts and cellular debris, which would otherwise inhibit PCR. Finally, purified nucleic acids are eluted into a moderate salt buffer.

The high number of hands-on precise steps in this approach prevent it from being carried out in a near-patient setting. Using magnetic silica microparticles for lysis and solid phase extraction limits the reliance on a centrifuge, thus enabling the opportunity for automation. With this approach, one can utilize a robotics-assisted system to perform some sample preparation steps, but this is still not appropriate for near-patient applications. Over the last decade, several reports have demonstrated integrated sample preparation with PCR in microsystems by mimicking the solid phase extraction and elution steps in a microfluidic format;[148–156] however, because of the number of steps required, the microsystems tend to be somewhat complicated and require external equipment to run, thus making them too costly and in some cases too cumbersome for near-patient use. This is true for commercial point-of-care platforms as well, such as the Cepheid XPert®, the Roche cobas® LIAT system, and the Atlas *io*™. While these are integrated systems that allow for sample-to-analysis detection, they rely on conventional lysis methods (i.e., chaotropic salts[157–159]or sonication[160,161]) and multi-step solid phase extraction to capture target DNA following a separate lysis step. The multiple sequential

reagent additions required in these systems to facilitate binding and elution of DNA necessitate sophisticated fluid handling and instrumentation. More promising may be the development of foldable paper systems that mimic the many steps of conventional solid phase extraction, though these techniques could also benefit from a reduced number of steps to speed the assay, and to meet regulatory standards for use outside of a central lab. Ultimately, a new methodology that minimizes the number of steps in sample preparation is necessary for practical near-patient NAATs, whether they are performed in conventional assay tubes/plates, in microsystems, or other novel formats.

In our previous work we introduced a streamlined approach that we termed direct PCR in which nucleic acid sequences are amplified directly off of the capture and purification surface, thus avoiding most of the steps in the conventional protocol. Chitosan microparticles were utilized to capture DNA and to retain the template during the PCR reaction. While chitosan has been used for DNA purification in a charge-switching approach,[162] we showed that, in high density, chitosan can capture and retain DNA even well above the pK_a of the amine groups on the chitosan. This effect with chitosan has been reported previously when designing chitosan systems for drug delivery[163,164] and for microparticle synthesis.[165] Upon showing that we could permanently capture nucleic acids at a PCR-optimal pH, we showed that the captured DNA can be amplified directly from the microparticle surface when the microparticles are added directly to a PCR reaction.

In this work we extend the direct PCR concept to whole blood samples (Figure 3.1). Chitosan-coated magnetic silica microspheres are used to lyse cells and to capture the released DNA in a single step. The microparticles are then added to a PCR reaction to amplify the DNA directly from the surface. We show efficient lysis and amplification using an optimized vortexing method; the cycle threshold for our approach is only shifted by a few cycles compared to typical solution-based PCR. We also show that avoiding washes entirely (which can lead to the simplest near-patient implementation) does not inhibit PCR. Finally, we demonstrate amplification of DNA sequences from whole blood samples using our direct PCR approach. First we show the amplification of human genomic DNA released by the cells in a droplet of blood, and then we demonstrate the amplification of plasmid DNA (representing circulating DNA, e.g., from viruses) spiked into blood droplets.
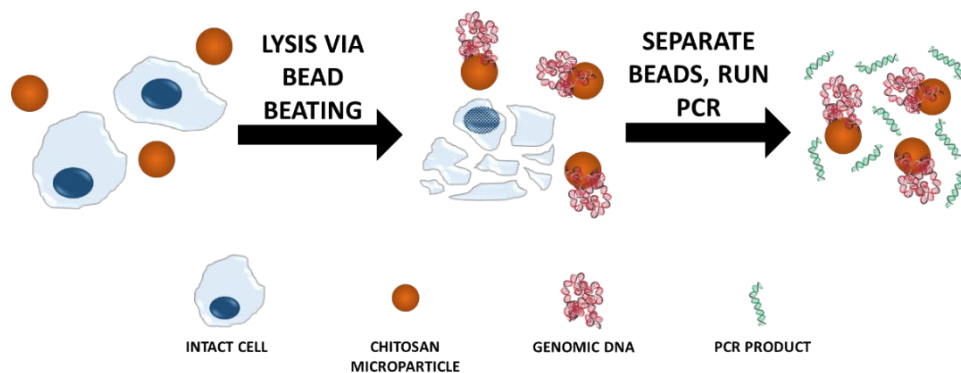
Figure 3.1. Direct PCR. Chitosan-coated silica microparticles lyse cells under vortex and capture DNA in the same step. The microparticles are then added to a PCR reaction where the DNA is amplified directly from the microparticle surface.

3.2   Materials and Methods

3.2.1   Chitosan-coated microparticle fabrication

Chitosan-coated microparticles were fabricated by reacting epoxides present on the surface of modified silica microparticles with the amine groups on the chitosan (Figure 3.2A). A stock solution of 1% (w/v) low molecular weight chitosan (Sigma) was prepared in a 1% (v/v) acetic acid solution (pH = 3.73). Prior to the attachment of chitosan to the microparticle, the stock solution was diluted to 0.1% (w/w) low molecular weight chitosan in de-ionized (DI) water and brought to pH 9 using 1 M NaOH (Macron). The moderately high pH is necessary for the amine-epoxide reaction; because of the higher pH, the chitosan solution must be dilute due to its poor solubility above a pH of about 6.5. Epoxide-coated magnetic silica microparticles (600 µL, 10 mg/mL), 3 µm in diameter (Amsbio), were washed three times in 0.1% (w/w) Triton X-100 (Sigma) in DI water. The 0.1% chitosan solution (500 µL) was then added to the magnetic microparticles and vortexed overnight. Following functionalization, the chitosan-coated microparticles were washed three times using 0.1% (w/w) Triton X-100 in DI water and then stored in 10 mM Tris, 0.1% (w/w) Triton X-100 (pH 8.5) at a concentration of 50 mg/mL at room temperature. Following functionalization, large aggregates of chitosan microparticles were present, which were later broken apart during the subsequent washing steps. While the individual microparticles have a diameter of 3 µm, the majority of the microparticles appear in clusters that range between 15 to 25 µm (Figures 3.2B-C). The chitosan microparticles used in this work

47

have shown efficient DNA capture and amplification when stored at room temperature for up to six weeks.
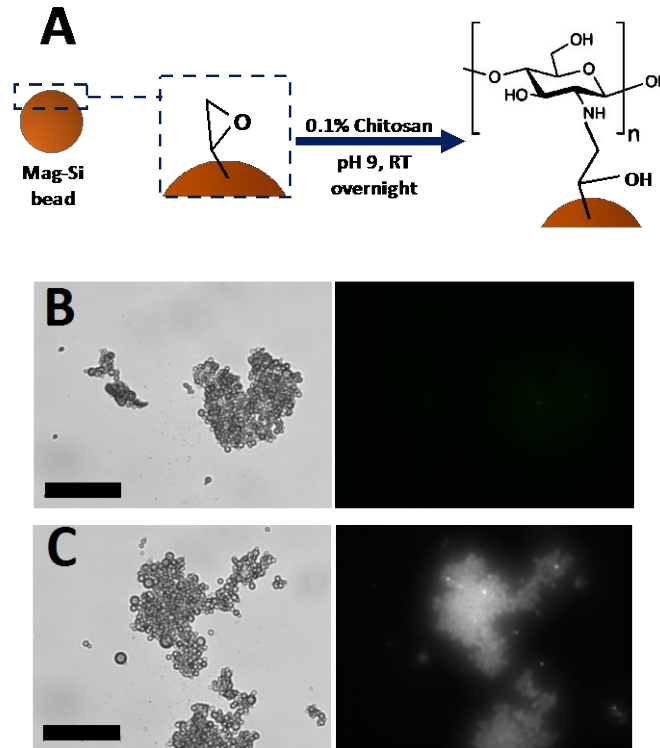
Figure 3.2. Chitosan microparticle fabrication and DNA binding. (A) Magnetic silica microparticles are covalently functionalized with chitosan by reacting the epoxide groups on the particles to the amine groups on chitosan. Chitosan-coated microparticles are capable of capturing DNA upon mild vortexing. Bright field and fluorescence images are shown before (B) and after (C) vortexing the microparticles with DNA.

3.2.2 Direct PCR with purified DNA

Direct PCR was assessed using plasmid (pBR322, New England Biolabs) and human genomic DNA (hgDNA). Purified hgDNA was isolated from MCF7 cells (ATCC) using a DNeasy Blood and Tissue Kit (Qiagen) prior to the experiments according to the manufacturer's recommendations. For DNA capture, 200 µg of chitosan microparticles were added to 95 µL of loading buffer

(10 mM Tris, 0.1% Triton X-100, pH 8.5), after which 1 μL of DNA diluted in DI water was introduced to the solution. The chitosan microparticles were then vortexed at the lowest speed for 3 minutes to facilitate DNA capture and were then washed once in loading buffer. Figure 3.2 shows bright field and fluorescence images of the microparticles before (Figure 3.2B) and after (Figure 3.2C) DNA capture. In this qualitative demonstration, 10^9 copies of plasmid DNA were added to 200 μg of chitosan microparticles and immersed in a solution of 1x SYBR Green I. DNA is clearly visible on the chitosan-coated microparticles after capture (Figure 3.2).

Immediately following DNA capture, the microparticles were added to a PCR reaction. All PCR reactions consisted of 1x iQ SYBR Green Supermix (BioRad), 0.25 μM forward primer, and 0.25 μM reverse primer, unless noted otherwise. Bubbles present in the PCR reaction were removed with centrifugation and qPCR was performed using an MJ MiniOpticon thermal cycler (BioRad). The PCR protocol consisted of a 3-minute hot start, followed by 35 thermal cycles, which included a 95 °C melt for 15 seconds and a combined anneal and extension step (temperatures listed in Table 3.1) for 30 seconds, unless noted otherwise. Magnets were placed alongside the PCR wells during thermocycling to pull the chitosan microparticles to the side to minimize interference with the fluorescence measurements. All reported cycle thresholds (Cts) are those provided by the MiniOpticon software.

49

Table 3.1. Primer sequences and annealing temperatures for various DNA templates (F: forward, R: reverse)

DNA source	Primer Sequences	Anneal Temp.
Plasmid	F: 5' – CAC TAT CGA CTA CGC GAT CA – 3' R: 5' – ATG CGT CCG GCG TAG A – 3'	56 °C
Human	F: 5' – TGA GCG CGG CTA CAG CTT – 3' R: 5' – TCC TTA ATG TCA CGC ACG ATT T – 3' ([166])	60 °C (1 minute)

3.2.3 Human genomic DNA binding capacity

To investigate the DNA loading capacity of the microparticles, increasing amounts of DNA were loaded onto chitosan-coated microparticles as described above to yield ratios of 5, 50 and 500 copies of DNA/µg of microparticles (500 copies/µg is equivalent to approximately 0.04 human genome copies per microparticle). Following DNA capture, microparticles were placed in a PCR reaction for qPCR and the cycle threshold was measured for each DNA concentration. We were unable to load higher copies of DNA/µg because increasing the number of cells by 10x or decreasing the number of microparticles by 10x were both found to be impractical.

3.2.4 Cell preparation

MCF7 breast cancer cells were cultured in T25 flasks in DMEM (Life Technologies) supplemented with 10% fetal bovine serum (Life Technologies) and 1% penicillin-streptomycin (Life Technologies) under standard tissue culture conditions. Cells were subcultured approximately every 5 days. In preparation for DNA extraction, MCF7 cells were harvested with trypsin and re-suspended in PBS at a concentration of 10^3 cells/µL.

3.2.5 Cell lysis

For cell lysis, 10 µL of the cell suspension was added to Tris-Triton buffer and 200 µg of chitosan microparticles; this solution was vortexed at moderate speed for 3 minutes for simultaneous cell lysis and DNA capture. One wash step in loading buffer following DNA capture was performed unless otherwise noted. All heating times and vortexing speeds were carefully optimized based on the parameters that led to the lowest qPCR cycle threshold for the respective techniques.

Live/dead staining was used to qualitatively assess both the lysis and DNA capture efficiency. A stock solution of live/dead stain containing 4 µM ethidium homodimer-2 (Life Technologies) and 5 µM calcein AM (Life Technologies) in PBS was prepared. 10 µL of the cell suspension was used for each respective experimental sample; the cells were first immersed in 40 µL of live/dead stain for 30 minutes and imaged with a fluorescence microscope (Olympus IX-51) as a positive control. For the live/dead negative control, cells were heat lysed at 95 °C for 15 minutes and then immersed in 40 µL of the live/dead stain. The experimental samples were stained and imaged after DNA capture. Following DNA capture, chitosan microparticles were stained and imaged to assess DNA coverage on the surface.

Quantitative PCR was used to assess the lysis and DNA capture efficiency of direct PCR with cell lysis. 10 µL of the suspended cells underwent lysis with 200 µg of chitosan microparticles for DNA capture. Following a wash

step, the chitosan microparticles were immediately added to a PCR reaction, as described earlier. All qPCR samples were supplemented with 0.2x EvaGreen and qPCR was performed for 40 cycles. Two controls were included in all experiments: (i) a solution-based PCR with 10^4 copies of purified MCF7 DNA (no chitosan microparticles present), noted as typical PCR, and (ii) direct PCR with 10^4 copies of purified DNA loaded onto the chitosan microparticles. During preparation, the number of DNA copies was measured using a NanoDrop spectrophotometer.

3.2.6 Direct PCR from a whole blood sample

A 1.5 mm lancet (BD) was used to collect 1 µL of blood from a fingertip and was brought to a 10 µL volume with a 3.2% (w/v) sodium citrate (Sigma) solution. Each sample was added to 200 µg of chitosan microparticles in 90 µL Tris-Triton buffer (10 mM Tris, 0.5% Triton X-100, pH 8.5). After the samples underwent mechanical lysis and one wash in loading buffer, the microparticles were immediately placed into a PCR reaction. All PCR reactions were supplemented with 0.2x EvaGreen for fluorescent signal enhancement. Direct PCR with purified DNA and typical PCR controls were also included.

3.2.7 Direct PCR of pBR322 in a whole blood sample

Whole blood was collected using the same procedures as for direct PCR from whole blood. 10^6 or 10^4 copies of pBR322 DNA were added to the blood sample, which was then added to the Tris-Triton buffer and chitosan microparticles. Samples then underwent microparticle-induced lysis and the

microparticles were then washed once before they were added to a PCR reaction, which was supplemented with 0.2x EvaGreen. Direct and typical PCR controls using equal amounts of pBR322 were included.

3.2.8 PCR product validation

Thermal melt analysis and gel electrophoresis were used to confirm PCR products generated from all PCR reactions. The melt analysis was included in the PCR programmed protocols following thermal cycling, where the fluorescence was measured as the temperature increased from 60 °C to 95 °C by 0.5 °C increments at a rate of 0.1 °C /s. Afterwards, supernatants from all samples were separated on a 2% (w/v) agarose gel containing 1x SYBR Green I (Lonza) at 125 V for 45 minutes.

3.3 Results and Discussion

3.3.1 Characterization of direct PCR with human genomic DNA

In our previous work we utilized only plasmid DNA for the characterization of direct PCR (capture and amplification directly from the chitosan surface). In order to utilize direct PCR for diagnostics, it is necessary to demonstrate that the technique can capture and efficiently amplify relevant genomic DNA. In Figure 3.3 we present the cycle thresholds for direct PCR with plasmid DNA and with human genomic DNA. With both samples, the cycle threshold for direct PCR lags the cycle threshold for solution-phase PCR by about 4 cycles. We expect that this threshold cycle difference results from inaccessibility of some template DNA, either because the packed beads in the

PCR reaction prevent much of the bead surface area from being accessed, and/or because some of the targeted sequences are bound too tightly within the chitosan. Nonetheless, even with these challenges, which can be addressed in future work, this streamlined method enables amplification and detection of trace amounts of DNA.
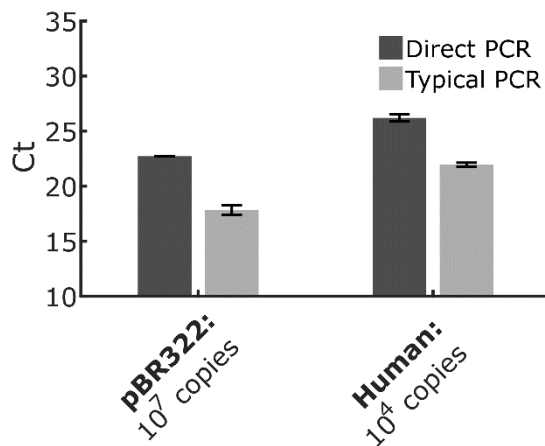
Figure 3.3. Cycle thresholds with direct and typical PCR for plasmid DNA and human genomic DNA (hgDNA).

To assess the binding capacity of the microparticles, increasing amounts of human genomic DNA were loaded onto a fixed mass of microparticles. As the copy number of DNA increased, the cycle threshold observed for direct PCR decreased as expected (Figure 3.4). Interestingly, a negative exponential decay trend can be observed; i.e. the cycle threshold difference between 50 and 5 copies/µg of microparticles is about 2 – 3 cycles while the difference between 500 and 50 is 1 – 2 cycles. Therefore, the upper limit of detection can be approximated to be at least 500 copies of DNA/µg of microparticles. While it would be ideal to confirm this explicitly, higher concentrations of at least 10^6 copies of human genomic DNA would be unrealistic for PCR applications.
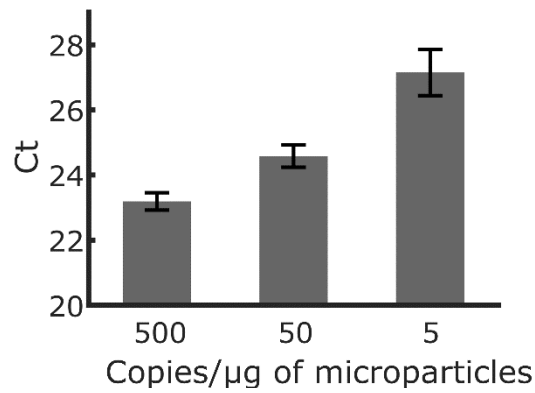
Figure 3.4. Cycle thresholds from direct PCR with 200 µg of chitosan microparticles and an increasing amount of purified human genomic DNA loaded onto the surface. Error bars represent the standard deviation across three samples.

3.3.2 Assessment of direct PCR with integrated lysis

After verifying that the microparticles can capture free DNA from solution under vortex and that the DNA can be amplified directly from the surface after capture, we investigated their capacity to acquire, purify, and amplify genomic DNA directly from complex samples. First, we verified that vortexing the microparticles with intact cells (i.e., bead beating) releases DNA for capture. Figure 3.5 presents the visual results with cultured MCF7 cells. Following lysis, very few intact cells can be observed (Figure 3.5C); additionally, DNA is released into the supernatant, represented by the red fluorescence evident in the supernatant due to the ethidium stain of the released DNA. After the addition and separation of chitosan microparticles, the microparticles become one large aggregate due to the presence of negatively charged DNA on the positively charged microparticle surface (inset of Figure 3.5D).
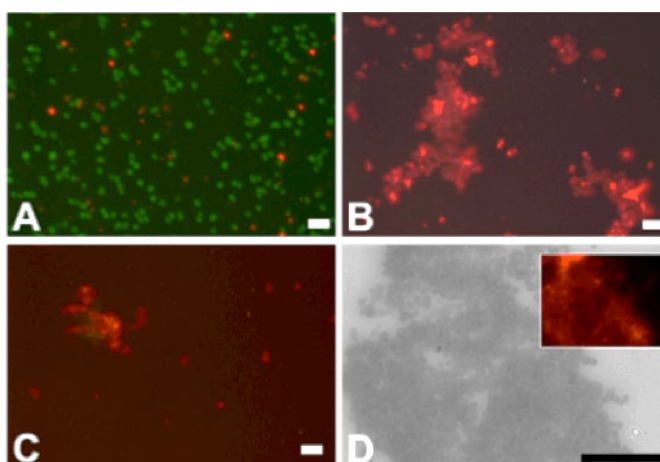
Figure 3.5. Live/dead staining of cells and supernatants after lysis. (A) Live-cell control of MCF7 cells. Green signifies staining with calcein AM (live stain) and red signifies staining with ethidium homodimer-2 (dead stain, i.e., nucleic acid stain). (B) Dead-cell control of MCF7 cells after being heat lysed at 95 °C for 10 minutes. (C) Supernatant following mechanical lysis with chitosan microparticles. (D) Chitosan microparticles from lysed sample following separation of microparticles from the supernatant. Inset shows live/dead staining of the microparticles. Scale bars are 20 μm.

We then assessed the integration of the lysis and direct PCR steps by amplifying the DNA captured by microparticles that had lysed cultured MCF7 cells. Figure 3.6A presents the real-time PCR amplification curves for direct PCR from lysed cells and compares the curves with two controls: direct PCR from purified human genomic DNA and solution-phase PCR with purified human genomic DNA. The results show that direct PCR amplification from a sample of intact cells performs comparably to direct PCR from purified DNA; this demonstrates the potential for simultaneous lysis and immobilization of accessible DNA without the use of PCR-inhibiting lysis reagents. In an attempt to improve lysis and capture efficiency, heat (70 °C) was tested to augment mechanical agitation. No resulting improvement was found in lysis or amplification efficiency (data not shown). As a result, all further experiments were conveniently performed at room temperature.
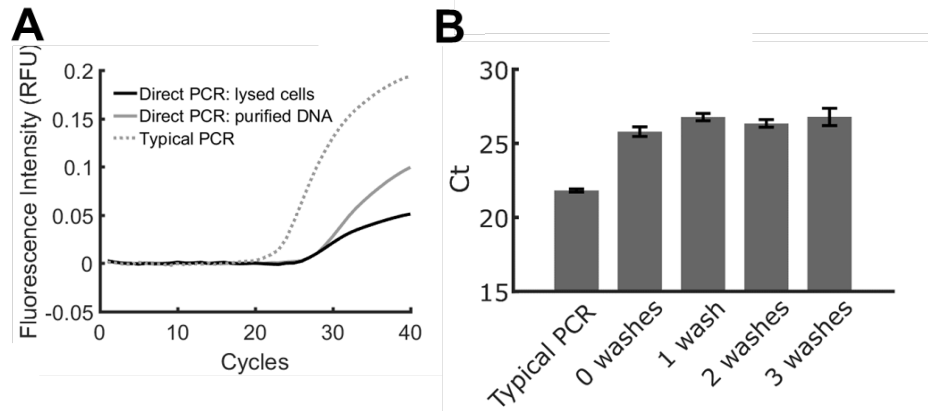
Figure 3.6. Direct PCR characterization of mechanical lysis method. (A) Amplification curves of lysed samples with direct PCR and typical PCR controls with purified DNA of equal copy number to experimental samples. (B) Comparison of cycle threshold with increasing washes following lysis. All experiments used 10^4 cells for lysed samples or 10^4 copies of DNA for direct PCR and typical PCR controls. Real-time curves represent the average of three samples; error bars represent standard deviation across three samples.

After eliminating the need for lysis agents, DNA purification and amplification was simplified to three simple steps: vortex, rinse and amplify. Motivated by the potential to eliminate extraneous manual involvement that can complicate or obviate portable PCR, we sought to eliminate the rinse step between lysis and amplification, as a rinse step may be a labor-intensive intervention that could prohibit near-patient applications. We assessed the impact of rinses by conducting an increasing number of rinses on parallel samples and measuring the difference in cycle threshold. Figure 3.6B shows the cycle threshold for lysis and direct PCR for a range of 0 to 3 rinses. Even with no rinsing, amplification was successful, with a cycle threshold of about four cycles higher than the solution-phase PCR. Further rinsing did not improve the cycle threshold. This demonstrates that in fact the direct PCR approach can truly minimize the number of steps in PCR sample preparation.

3.3.3 Direct PCR from a whole blood sample

The results above demonstrate that the chitosan-coated microparticles can lyse cells to release DNA in a simple bead-beating procedure, that they can capture DNA during the lysis step, and that the bound DNA can be amplified directly from the surface following minimal washing steps. Manual and precise intervention steps are for the most part eliminated as compared to the conventional approach to PCR, suggesting that the direct PCR method may enable near-patient diagnostics, even with complex patient samples. To illustrate this further, we utilized a whole blood droplet as the initial sample. Approximately 1 μL of whole blood was added to the microparticles in buffer and direct PCR (following bead-beating) was performed. The real-time PCR data in Figure 3.7 demonstrate that the amplification curve for a whole blood sample is similar to the curve for direct PCR with pre-purified DNA (10^4 copies), and that both curves lag the typical PCR (10^4 copies) by only 4 cycles. PCR products were confirmed to be the same as those of the typical PCR control using melt curve analysis and gel electrophoresis (Figure 3.8). This suggests similar performance between the whole blood sample and the purified DNA, as we estimate that the whole blood droplet contained approximately 10^4 cells (though the blood droplet volume from the lancet could not be perfectly controlled and the number of white blood cells can vary from 5×10^3 to 10^4 per μL).
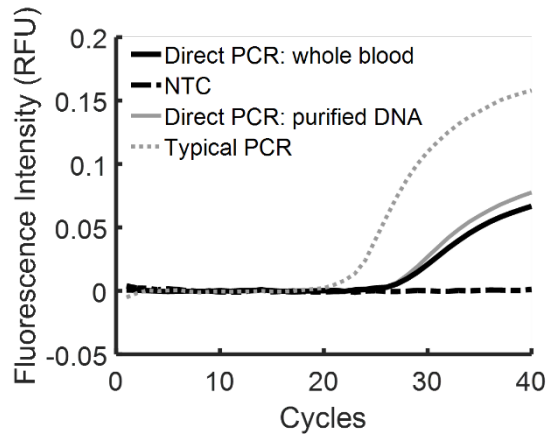
Figure 3.7. Amplification curves of direct PCR from whole blood samples. Direct and typical PCR controls contained 10^4 copies of DNA. Curves represent the average of 3 samples. The cycle threshold for direct PCR in blood is 26.15, which is about 4 cycles higher than the solution phase control (typical PCR).
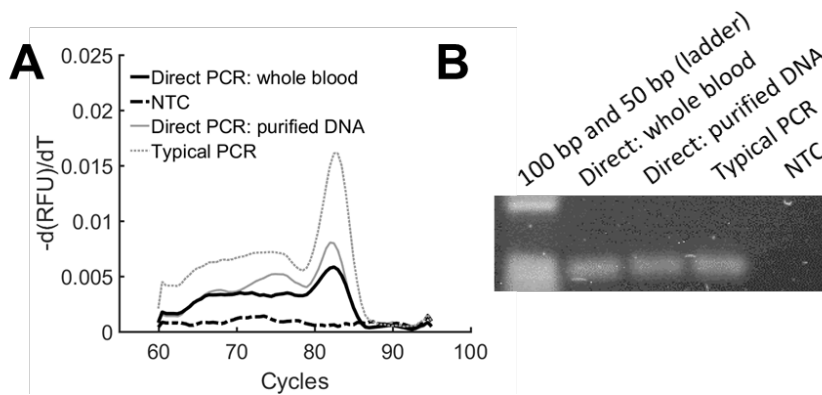
Figure 3.8. Confirmation of PCR products from Figure 3.7. (A) Melt curve analyses show that the melt temperatures, $82.0 \pm 0.5\,°C$, of the amplicons produced by direct PCR from both whole blood and purified DNA match the melt temperature, $82.5\,°C$, of amplicons generated in absence of chitosan microparticles. (B) Direct PCR products run on a 2% agarose gel and stained with SYBR Green I. Lanes are labeled at the top with their respective sample.

While this result illustrates applications of the direct PCR method to genetic disease diagnostics, today there are more immediate needs for near-patient infectious disease diagnostics. Thus we further investigated whether free DNA (e.g., DNA from bloodborne viruses) in blood samples could be captured and amplified with the same methodology. One primary concern

is whether the microparticles would capture viral DNA despite the large mass of human genomic DNA in a blood droplet. To test this, we used pBR322 plasmid DNA spiked into blood samples to represent viral DNA circulating in blood.

Real-time PCR data for the amplification of 10^4 copies of plasmid DNA in blood droplets are presented in Figure 3.8. The amplification data demonstrate that the plasmid DNA in whole blood was amplified, despite the ~10^4 copies of human genomic DNA in the blood sample. For comparison, Figure 3.8 also presents the amplification control for 10^4 copies of pure plasmid DNA using the direct PCR methodology. The data illustrate that the presence of human genomic DNA introduces a notable, but consistent shift of two cycles to reach the threshold for both 10^4 (Figure 3.9) and 10^6 (Figure 3.11) copies when compared to direct PCR controls with pure plasmid DNA. These results suggest that the direct PCR methodology can be applied both to human genetic disease diagnostics and bloodborne infectious disease diagnostics.
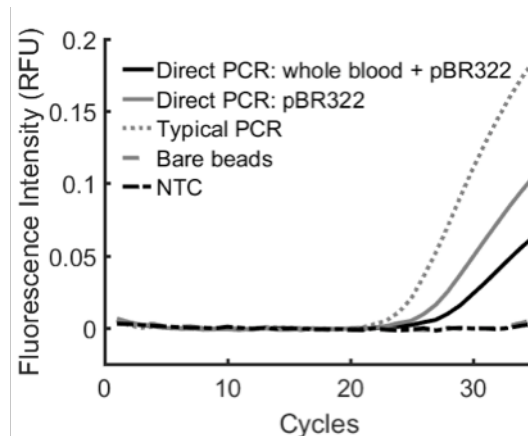
Figure 3.9. Amplification of plasmid DNA (pBR322) in whole blood samples. Direct PCR and typical PCR controls contained 10^4 copies of DNA. Curves represent the average of 3 samples. The cycle threshold for direct PCR of pBR322 in blood is 28.12, which is about 2 cycles higher than the direct PCR control of pBR322 in buffer and 5 cycles higher than the solution phase control (typical PCR).
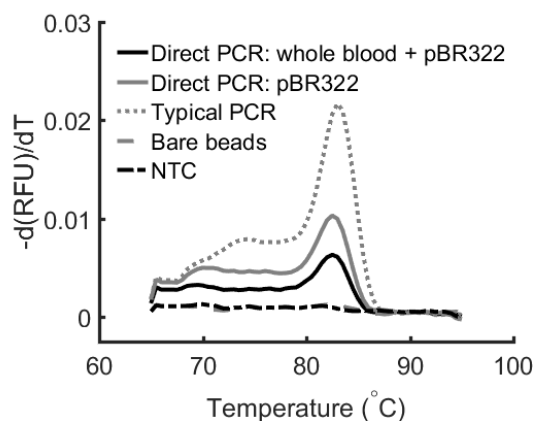
Figure 3.10. Melt curves analysis of PCR products from Figure 3.9. The melt temperatures, 83.0 ± 0.5 °C, of the amplicons produced by direct PCR from both pBR322 alone and pBR322 spiked in whole blood, match the melt temperature, 83.0 °C, of amplicons generated in the absence of chitosan microparticles.
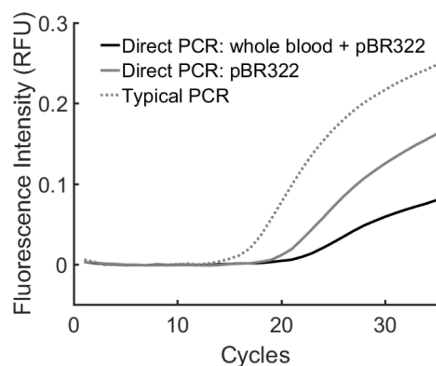
Figure 3.11. Amplification curves of 10^6 copies of pBR322 in whole blood (black line) and without whole blood (gray solid line) in the presence of chitosan microparticles. The dotted gray line is of equal copy number in the absence of chitosan microparticles.

Given the minimal steps required of our direct PCR methodology, chitosan microparticles can be utilized to realize a simple and rapid point-of-care diagnostic. Many research groups have developed microfluidic platforms that are amenable to qPCR with a portable fluorescence analyzer for quantification.[167–169] Since our chitosan microparticles do not require any manipulation during amplification, they can easily be integrated into a

61

microfluidic device or cartridge. Additionally, bead-beating has been implemented in a microfluidic platform either with pneumatic vibration for glass beads[170,171] or by applying a magnetic field to magnetic particles to achieve mixing.[172–174] Given that our chitosan microparticles are magnetic, this can be leveraged as a mechanism for both chaotic mixing and transfer from a DNA capture module to an amplification module, without an additional wash step. In this format, chitosan microparticles can provide a simple, one-step method for sample-to-answer detection of genomic targets.

3.4   Conclusion

In this work we have demonstrated a new streamlined method for PCR-based diagnostics from complex samples. Chitosan-coated microparticles are able to liberate and bind DNA from human cells under simple mechanical agitation; DNA sequences can then be directly amplified from the surface of the microparticles. The required steps for the entire process are (i) to agitate the cells with the chitosan-coated microparticles, and (ii) to transfer the microparticles to a PCR reaction. Minimal washing was shown to be necessary, thus maintaining a low number of steps. Real-time PCR showed that the cycle threshold for direct PCR from whole blood samples is only a few cycles higher than typical solution-based PCR from purified DNA. We believe that this technique has the potential to eliminate all precise intervention steps from PCR diagnostics without the need for sophisticated equipment, and thus may lead to near-patient diagnostics. By demonstrating amplification of human genomic DNA from lysed cells in a blood droplet, we illustrate applications in

genetic disease diagnostics, such as newborn screening, cancer risk assessment, and future applications in personalized medicine. Additionally, by demonstrating the amplification of spiked plasmid DNA in blood droplets, we also highlight applications such as cell-free DNA identification and infectious disease diagnostics. In particular, identification of viral pathogens from a droplet of blood using our simple approach offers new opportunities for infectious disease diagnostics in urgent care clinics and low resource settings.

Chapter 4. Demonstration of a quantitative triplex LAMP assay with an improved probe-based readout for the detection of MRSA[2]

4.1   Introduction

PCR remains at the forefront of molecular diagnostics due to its robustness and familiarity over the past three decades. However, PCR is hindered by its relatively long assay time and instrumentation complexity due to the need to cycle between two to three temperatures. As diagnostic technologies aim to bring assays closer to the patient (POC testing) and to improve sample-to-answer turnaround, nucleic acid amplification tests are slowly moving away from PCR in favor of amplification schemes that operate at a single temperature. Consequently, numerous isothermal methods for nucleic acid amplification have been developed that have reduced the instrumentation demands of precise temperature control, and also achieve faster assay times. Of these methods, loop-mediated isothermal amplification (LAMP) has become the most pervasive.

First developed in 2000 by Notomi, et al.,[97] LAMP leverages a strand-displacing polymerase and four core primers that are specific to six regions of the template. As the reaction progresses, exponential amplification is achieved by the cascading enzymatic generation and subsequent unfolding of synthetic

---

[2] This work was submitted for publication to Analyst.

DNA structures, templated along the target sequence. These structures allow for the generation of different high molecular weight products, thereby facilitating exponential product generation in less than an hour. The multiple structures can participate further in the reaction as they have hybridization sites that allow the core primers to anneal, extend, and produce more amplicons; as a result, LAMP has shown 10-1000 times greater sensitivity as compared to PCR.[175] The increased speed, sensitivity, and specificity[139,176] has made LAMP the premier method for isothermal amplification. Since its original report in 2000, the number of publications related to the development and implementation of LAMP has been increasing at an exponential rate.[177] These publications include diverse applications, including the detection of miRNA targets[178–180] and viral genomes[181–184] with the addition of reverse transcriptase, investigation of enzyme inhibition from sample matrices,[185–187] and the implementation into microfluidic devices for point-of-care applications.[188–190]

As LAMP is often targeted for point-of-care applications, single-reaction multiplexing is important to achieve in order to maintain a small device footprint and to reduce demands on sample volume. The primary hindrance in realizing a LAMP assay for a multiplexed diagnostic remains a robust method for real-time detection. Most reported detection methods for LAMP are end-point techniques, such as leveraging a colorimetric or fluorescence change upon addition of a responsive molecule (i.e. hydroxynaphthol blue[191] or manganese-quenched calcein[192], respectively), using gel electrophoresis to

observe the DNA products generated, or modified primers (i.e. biotinylated or conjugated with a fluorophore[193,194]) for lateral flow detection. These methods can provide a simple readout for a positive or negative result; however, endpoint measurements are not quantitative for exponential amplification assays.

To address the need for quantitative measurements, two main methods have been employed: fluorescence measurements with the addition of an intercalator (i.e. SYBR and SYTO dyes) and turbidity. While these methods generate signals in real time related to the total amount of DNA in the reaction, thus enabling quantification when compared to a standard, they do not provide specific information about the sequence being amplified, thus implying a lack of specificity and an inability to distinguish between multiple targeted sequences amplified simultaneously. As diagnostic technologies progress towards more comprehensive assays that test for more than a single biomarker, nucleic acid amplification tests are moving away from the indirect methods of detection and towards those that are specific to their targets of interest. Examples of this for PCR include Taqman PCR and the use of molecular beacons; analogous approaches would be an ideal solution for multiplexed, quantitative LAMP assays.

To achieve this, FRET-probe-based methods have been developed, including the redesign of the loop primers to act as molecular beacons,[175] fluorogenic bidirectional displacement (FBD) probes,[195] and assimilating probes.[196–198] In all three of these approaches, FRET is utilized at the loop

primer regions such that during amplification, the fluorophore- and quencher-labeled sequences are separated. However, designing and implementing loop primers is often complex and is not always possible, which limits the broad application of these methods. Further, the molecular beacon approach requires 0.8 M betaine, which is also not generalizable across LAMP assays.

One of the first probe-based methods for real-time LAMP detection was developed by Tanner, et al., known as "detection of amplification by release of quenching" (DARQ LAMP, Figure 4.1). Again leveraging the molecular zipper design, this approach utilizes a probe that hybridizes to one quenched inner primer to form a duplex such that once the polymerase encounters the duplex, the probe is displaced and produces a fluorescent signal (Figure 4.1A).[199] Because this duplex targets the inner primer instead of the loop primers, this
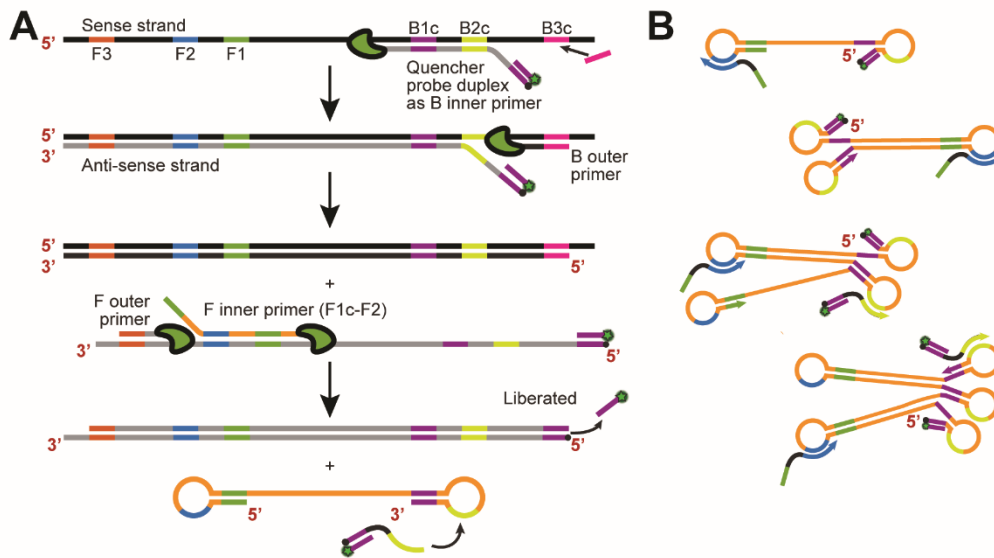
Figure 4.1. Schematic of DARQ LAMP (A) and locations of incorporated QPDs with generated amplicons to continue fluorescent measurements (B). Through a series of polymerization, the QPD becomes incorporated into the produced amplicons. As the reaction proceeds, the strand-displacing activity of the polymerase facilitates the probe's release from the quenched inner primer. Because the QPD can become incorporated in later amplicons, DARQ LAMP enables a real-time and specific readout for LAMP assays.

method can be employed for both four- and six-primer LAMP systems. The authors demonstrated the multiplexing capabilities by interrogating different genomes with individualized primer sets and Bst 2.0. However, since its publication, DARQ LAMP has not been widely employed because the quencher probe duplex (QPD) has been reported to show amplification inhibition.[106,199]

While all of the FRET-based LAMP methods that enabled single-reaction multiplexed detection are problematic, DARQ LAMP is the simplest and most universal to implement. However, it requires further study to elucidate the optimization factors that can reduce the inhibition. Additionally, published work focuses on DARQ LAMP implemented in assays with high magnesium content. Because LAMP assay conditions are highly dependent on the primer set, a more comprehensive understanding of the impacts of DARQ LAMP on reaction efficiency is necessary. Furthermore, the advent of Bst 3.0 DNA Polymerase, which has increased processivity, offers the opportunity to rescue the delayed amplification times of DARQ LAMP, but doing so requires in-depth optimization.

In this study, we investigate for the first time the use of these newer strand-displacing polymerases in LAMP with four- and six- primer systems. We show that DARQ LAMP in previously reported conditions can only operate with high magnesium content, and thus completely inhibit LAMP assays where primer designs require lower magnesium. However, we demonstrate that Bst 3.0 can rescue the amplification for a broader range of assay conditions. We then designed and optimized a DARQ LAMP assay to simultaneously

amplify three genes from the MRSA genome within a single sample. Though the triplex assay had lower amplification performance than optimized singleplex assays, we were able to detect with times-to-positive of less than 30 minutes. The results of this study demonstrate the optimal conditions for a triplex LAMP assay for MRSA detection (a pathogen that requires detection of three genes for confirmation), while also informing the community on approaches for the broader use of DARQ LAMP for multiplexed LAMP.

4.2 Materials and Methods

4.2.1 Preparation of DNA standards

Genomic DNA from methicillin-resistant *Staphyloccus aureus* (MRSA, strain USA300_TCH1516, NC_010079.1) was purchased from American Type Cell Culture (ATCC). Lyophilized DNA was resuspended in a 50% glycerol stock at 10^7 copies/µL, and its concentration was verified by measuring the OD260 with the NanoDrop ND-3000 (ThermoFisher Scientific). The genomic DNA was then aliquoted to 50 µL volumes and stored at -20 °C. Ten-fold dilutions of the stock DNA were prepared in water for all experiments.

4.2.2 LAMP Primer Design

Targets amplified and quantified in this study are genes associated with the resistance and virulence factors present in the MRSA genome. Genes encoding for *femB* (Genbank: ABX29322.1) and *mecA* (Genbank: ABX28076.1) were chosen as resistant-specific genes, and *spa* (Genbank: ABX28159.1) was chosen as a bacteria-specific control. The four-primer

system targeting *femB* was described previously[200] and the *mecA*, *spa*, and *femB*-2 primer systems were designed using the PrimerExplorer_v5 software (http://primerexplorer.jp/e/, Eiken Chemical Co., Ltd.). All DNA oligonucleotides (listed in Table 4.1) were purchased through Integrated DNA Technologies (IDT). 100 µM working stocks were prepared in 1x Tris-EDTA buffer (provided through IDT) and stored at -20 ºC.

Table 4.1. LAMP primer and probe sequences. * denotes that the 5' end of the sequence was labeled with an Iowa Black FQ or RQ quencher. All probes have the designated fluorophore labeled at the 3' end.

Targeted gene	Primers	Sequence (5' – 3')
femB	FIP*	TACCTTCAAGGTTTAATACGCCCATCATCATGGCTTTACAACTGAG
	BIP	ACACCCGAAACATTGAAAAAGACACTTTAACACCATAGTTTATCGCTT
	F3	TGTTTAAATCACATGGTTACGAG
	B3	TCACGTTCAAGGAATCTGA
	Probe	ATGGGCGTATTAAACCTTGAAGGTA – **FAM**
femB-2	FIP	GCTCGTAACCATGTGATTTAAACAAATATGATAAAGATATCGTGCCAT
	BIP	CAACTGAGTATGATACATCGAGCCTGTTTCGGGTGTTTTACCTT
	F3	AGATCCGTATTGGTTATATCATCT
	B3	TTACGTTGACTATCAAATGTCTT
	LoopF	GCATCATTTTTCTCGCGACCTTCAA
	LoopB	CGATGGATGGGCGTATTAAACCTT
mecA	FIP	ACGTCTATCCATTTATGTATGGCATCAGAGCTTCTTTTTTATCTTCGG
	BIP*	TGAAGGTGTGCTTACAAGTGCCATGAAAAATGATTATGGCTCAG
	F3	TGTAATCTGGAACTTGTTGAG

	B3	TGATGCTAAAGTTCAAAAGAGT
	Probe	GCACTTGTAAGCACACCTTCA – **TAM**
spa	FIP	ATTGCTGCAGATAACAAATTAGCTGGTTGCTTCTTATCAACAACAAGT
	BIP*	AGCAGTAGTGCCGTTTGCTTGGTAACGGAGTACATGTCG
	F3	TTAGCATCTGCATGGTTTG
	B3	GCAAAGAAGATGGCAACAA
	Probe	AAGCAAACGGCACTACTGCT – **Cy5**

4.2.3 Amplification time dependence on primer number or engineered polymerases

To investigate the impact of increasing primer number on Time to Positive (TTPs), two primer sets were designed specific to the *femB* gene. The first primer set, *femB* (Table 4.1), only allowed for design of one loop primer given the constraints of the PrimerExplorer software. The second *femB* primer set (*femB*-2) was redesigned as an AT-rich genome to facilitate design of both a forward and backward loop primer. These experiments did not include the quencher probe duplex. Instead, unlabeled primers were used, with an intercalator as the fluorescent readout.

For these experiments, 20 µL reaction volumes were prepared where the primer concentrations were kept constant: 0.2 µM of F and B outer primers (F3 and B3), 0.8 µM of loop primers (LoopF and LoopB), and 1.6 µM of F and B inner primers (FIP and BIP). Experiments using Bst Large Fragment (Bst LF, New England Biolabs) consisted of 1x ThermoPol buffer (New England

71

Biolabs) supplemented with 0.6 M betaine (Sigma-Aldrich), 8 mM MgSO$_4$ (New England Biolabs), 1.4 mM dNTPs (New England Biolabs), 1 µM SYTO-82 (ThermoFisher Scientific), and 0.32 U/µL of Bst LF. Reactions were then heated to 61 °C for 60 minutes followed by a 2-minute heat kill step at 80 °C using a thermocycler (LightCycler 480 System II). Reaction conditions for Bst 2.0 consisted of 1x Isothermal Amplification Buffer I (New England Biolabs), 0.2 M betaine, 0.64 mM dNTPs, 1 µM SYTO 82, and 0.32 U/µL of Bst 2.0 (New England Biolabs). These reactions followed the same heating protocol as Bst LF. Lastly, Bst 3.0 had the same conditions as Bst 2.0 except that 1x Isothermal Amplification Buffer II (New England Biolabs) was used, and 1 mM MgSO$_4$ was supplemented into the reaction. Bst 3.0 (New England Biolabs) was added to those reactions at the same concentration used for Bst LF and Bst 2.0. Reactions containing Bst 3.0 were heated at 65 °C for 60 minutes where fluorescent readings were taken every 30 seconds. This incubation was followed by a 2-minute 80 °C heat kill step.

4.2.4 Titration of quencher probe duplex into LAMP reactions

As noted by Tanner, et al.,[201] some amount of unlabeled inner primer must be present in the reaction to prevent full inhibition of amplification. The original paper used a 1:1 ratio, where one half was the unlabeled inner primer, and the other have was the quenched inner primer and the labeled probed (quencher probe duplex, QPD). Initial experiments at this ratio inhibited all amplification; thus, we conducted a titration of the QPD, with the *mecA* primer set to determine optimal conditions for the assay. First, quenched inner primer

and labeled probe were hybridized by incubating the sequences at 5 µM at 95 °C for two minutes, and slow cooled to room temperature using a heat block. DARQ LAMP assays using Bst 2.0 (at the conditions describe above with 10^5 copies of MRSA genomes) were then performed using the denoted percentages in relation to the total amount of unlabeled forward inner primer. Similarly, DARQ LAMP reactions for Bst 3.0 were also performed at the conditions described above. For both enzymes, EvaGreen (Biotium) was included in the reactions to confirm amplification had occurred.

4.2.5 DARQ LAMP reactions

Once the optimal amount of QPD was determined from the titration experiments, 10% QPD were incorporated into all LAMP reactions using Bst 3.0. Inner primers labeled with asterisks in Table 1 were reduced to 1.44 µM for these reactions to maintain a 10% ratio of QPD to unlabeled inner primer. All reactions conditions for Bst 3.0 outlined previously were applied to these experiments, without including intercalator. Fluorescent readings were taken every 30 seconds during a 65 °C incubation, followed by a 2-minute heat-kill step at 80 °C. Signals were normalized to maximum fluorescence to account for differences in quantum yield.

4.2.6 Melt curves for quencher probe duplexes

To assess the melt temperature of the hybridized probe and quenched inner primer, reactions consisting of 1x Isothermal Amplification Buffer II, 0.2 M betaine, 1 mM MgSO$_4$, 0.64 mM dNTPs, and 200 nM quencher probe duplex

were prepared. Primers and SYTO 82 were not included as they minimally impact hybridization of the QPD. Reactions then underwent a melt protocol where the temperature was raised from 55 °C to 95 °C at 0.2 °C increments, and were read at each increment using the LightCycler. Melt temperatures were calculated by plotting the derivative of each melt curve and taking the minimum value from the data set.

4.2.7 Calculation of time-to-positive

Given that the thermocycler's included software calculates cycle threshold, the software-provided analysis is not as accurate for LAMP. Using the raw data collected from the thermocycler, data was plotted against time, and the amplification curves were then fitted to a modified generalized logistic curve:

$$F = F_0 + \frac{F_{max} - F_0}{1 + e^{-b(t - t_{half})}} \qquad \text{(Eq. 4.1)}$$

Here, F_{max} is the fluorescence at infinite time, or at saturation, F_0 is the baseline fluorescence (at $t \approx 0$), b is the growth rate, and t_{half} is the time at which the fluorescence is at half maximum. Using the same methodology presented by Subramanian and Gomez,[202] the TTP can then be calculated with Equation 2. All curve fits had a coefficient of determination $R^2 > 0.95$ before TTPs were calculated using the fitted constants.

$$T_p = t_{half} - \frac{2}{b} \qquad \text{(Eq. 4.2)}$$

4.3 Results and Discussion

4.3.1 Higher generations of strand-displacing polymerases provide faster assay times

While the elimination of thermal cycling contributes to a reduction in assay time as compared to PCR, another significant reason for the increased speed of product generation is the processivity of the strand-displacing polymerase, New England Biolabs (NEB) has developed three strand-displacing polymerases that have been consistently used in LAMP assays. The original enzyme employed in LAMP is Bst DNA Polymerase, Large Fragment (Bst LF). With this enzyme, there were reports where times to positive were shown to be as low as 20 minutes.[203] However, given that each LAMP assay must be optimized for each designed primer set, amplification times can vary widely for different assays, and TTPs can be as high as 45 minutes, even for high template concentrations (Figure 4.2A). As a result, quicker and more robust Bst polymerases have been introduced. NEB's Bst 2.0 DNA polymerase (Bst 2.0) was developed not only to achieve faster amplification times, but also to show enhanced activity extending off of RNA targets, thus eliminating the need for an additional reverse transcription step. The next iteration, Bst 3.0 DNA polymerase (Bst 3.0), further builds upon these improvements, providing faster amplifications times and robustness against inhibitors as compared to Bst 2.0. With both of these enzymes, we have observed that amplification times can be achieved in less than 30 minutes with high discrimination between positive and negative samples. Reactions with

Bst 3.0 are 10 minutes faster than those with Bst 2.0 (Figure 4.2B). As a result,

the majority of LAMP publications have moved away from using Bst LF, and

now primarily use Bst 2.0 or Bst 3.0.
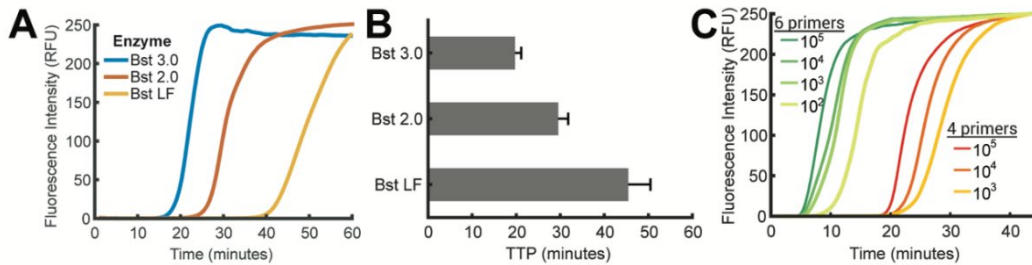
Figure 4.2. Amplification time dependence upon different strand-displacing enzymes and upon the number of primers. (A) Averaged traces (n = 3) of 10^5 copies of MRSA genome using three different strand-displacing enzymes. Reactions run with the latest iteration of Bst DNA polymerase, Bst 3.0, show faster amplification times as compared with Bst polymerase used in the original LAMP publication, Bst DNA polymerase Large Fragment (Bst LF). (B) Amplification of reactions in A show Bst 3.0 has time to positives (TTPs) of roughly 20 minutes, 10-25 minutes faster than Bst 2.0 and Bst LF respectively. Error bars represent the standard deviation across n = 3. (C) Incorporation of loop primers into LAMP reactions leads to assay times reduced by 15 minutes in comparison to assays run with only the four core primers.

4.3.2 Increased primer number enables 15 minute assay times with higher generation polymerases

An additional reason for reduced assay times is the number of primers

present in the assay. The incorporation of four core primers allows for

increased assay times due to their consistent extension when hybridized to the

template, as well as the multitude of downstream amplicons. Since the original

publication, Notomi, et al., developed another method to decrease assay times

with the incorporation of two loop primers that participate downstream of the

initial reaction.[204] Briefly, the starting material produced by LAMP is a

dumbbell-like structure, and as inner primers continue to hybridize and extend

76

of this dumbbell structure, more complex structures consisting of multiple loops are generated. The loop primers hybridize to these secondary loop structures, where inner primers do not anneal, and provide more extension sites to further produce exponential signal generation. From the two loop primers for the *femB*-2 set, amplification times were observed to be 15 minutes less than an assay run with only the core primers (Figure 4.2C). Additionally, the increased extension sites that loop primers offer can provide increased sensitivity.

While these advantages are very attractive for any assay, it is important to note that the design of a six-primer system is not straightforward. Once the core primers have been designed, those primers are input into the software again to design the loop primers. Loop primers will not be designed if there is limited space between the F2 and F1c regions (or B2 and B1c) or the sequence does not have the required GC content to sustain the necessary melt temperatures. In addition, each primer set must be validated, and often times several primer sets must be designed given the complexity. Because of these limitations, designing a six-primer system is often challenging, and, in some cases, is not possible.

4.3.3 Bst 3.0 shows more robustness against QPD's inhibitory effects

Previous DARQ LAMP publications suggest using a 1:1 ratio of QPD to unlabeled inner primer, as the unlabeled primer prevents the reaction from being completely inhibited. However with both Bst 2.0 and Bst 3.0 in reactions with MRSA primer sets, these amounts completely inhibited the reaction (data

not shown). We conclude that this occurs because the LAMP assays have been optimized with 8 mM magnesium (Mg^{2+}), a common concentration for most LAMP assays.[201] This is problematic as the Mg^{2+} content for varying primer sets ranges from 2 mM to 10 mM, and therefore this 1:1 ratio cannot be universally applied to all assays. Because the primer sets in this study require a much lower Mg^{2+} concentration of 3 mM, we can assume that the optimal ratio of QPD to unlabeled inner primer is much lower for these assays.
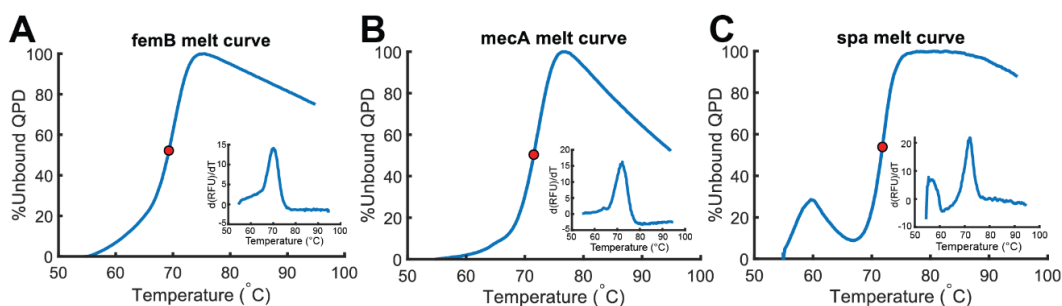
Figure 4.3. Melt curves for QPDs across all primer sets. (A) femB melts show a melt temperature of roughly 70ºC, whereas mecA (B) and spa (C) have melts of roughly 71-72 ºC.

After confirmation that the QPD's melt temperatures were above the operating assay temperature (Figure 4.3), the optimal amount of QPD was determined by titrating QPD in LAMP reactions containing either Bst 2.0 or Bst 3.0 to better discern the inhibitory effects' impact on both enzymes (Figure 4.4). With Bst 2.0, we observe that with lower titrations of QPD, we see no drastic impact on TTPs when compared to reactions with intercalator and no QPD present. However, once we surpass 15% QPD (i.e. 85:15 unlabeled primer to QPD), the TTPs are drastically longer compared to reactions with only 10-15% QPD. In comparison to a primer set optimized for 8 mM Mg^{2+}, the TTP

difference between 10% and 25% QPD is roughly 3 minutes;[199] this suggests that for LAMP reactions that operate at low concentrations of Mg^{2+}, Bst 2.0 has a very narrow range in which DARQ LAMP remains a robust method for detection. In contrast, QPD present in reactions containing Bst 3.0 has a lesser impact on enzyme inhibition. As with Bst 2.0, we observe similar TTPs with 10% QPD when compared to the intercalator-only control. As the amount of QPD increases, we observe a gradual increase in amplification times, however it is not as aggravated as those observed with Bst 2.0.
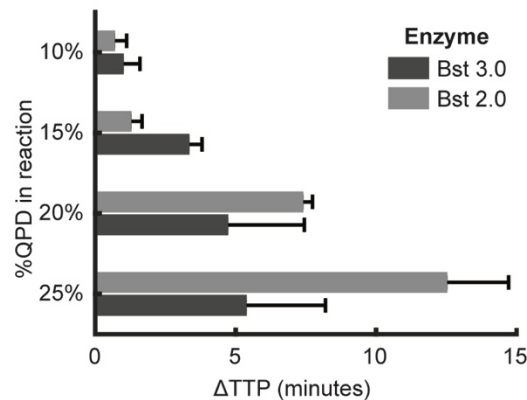
Figure 4.4. Comparison of amplification times with increased QPD concentrations using Bst 2.0 and Bst 3.0 in LAMP reactions. ΔTTPs compare the TTP from the QPD reaction with a LAMP reaction that consists of intercalator only over n = 3. At QPD concentrations higher than 10%, we observe significant amplification delays, suggesting that the polymerase is being inhibited at these concentrations. Overall Bst 2.0 shows amplification times that are harshly aggravated with increasing QPD as compared to Bst 3.0, suggesting that the latter enzyme is more robust against the inhibitory effects of QPD. Error bars represent standard deviations across n = 3 samples.

To further investigate the inhibitory effects on both enzymes, EvaGreen was added to reactions containing QPD to determine whether overall DNA generation was delayed, and more readily observe the kinetic changes occurring the reaction. Overall, the reactions that were supplemented with intercalator showed delayed TTPs that agreed with those that measured the fluorescence from the QPD (Figure 4.5). Reactions with Bst 2.0 showed a delay

in time to positive without any changes to the amplification efficiency, as shown by the minimal change in slope across QPD amounts (Figure 4.5A). Interestingly, while reactions with Bst 3.0 show slight changes in TTPs, we observe decreasing slopes in the amplification curves as we increase the amount of QPD. This seems to suggest that the presence of QPD does inhibit both enzymes, however the mechanisms of inhibition are different. The differences observed between Bst 2.0 and Bst 3.0 are most likely due to design changes made during the directed evolution of the enzyme and therefore, may only be alleviated with changes to assay conditions that further promote polymerase activity such as adding DMSO.[205]
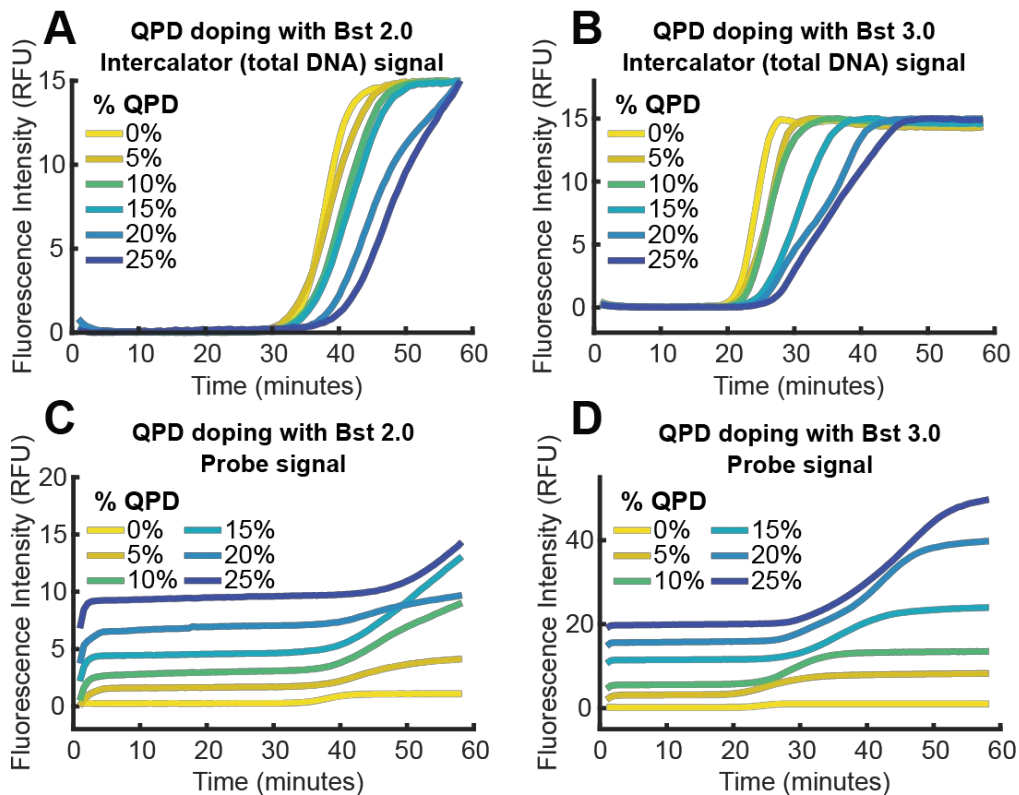
Figure 4.5. Amplification traces from either intercalator or probe in QPD doping reactions. Reactions with either Bst 2.0 or Bst 3.0 were supplemented with intercalator (A and B). Intercalator signals confirm that the presence of QPD delays amplification times that agreed with TTPs calculated from the probe signal alone (C and D).

4.3.4 DARQ LAMP enables singleplex and multiplex detection of MRSA genomes across all three genes

The original DARQ LAMP publication had demonstrated its multiplexing capabilities by assaying different genomes within a single reaction. For applications that require the identification of different genes present within a single genome, it remains unclear how the increasing amount of primers and QPDs impacts the efficiency of DARQ LAMP. One example of such an application is the identification of MRSA, where PCR tests have become a gold standard diagnostic.[10] To investigate this, three primer sets that identify *S. aureus* and genes that encode its methicillin resistance were designed and validated. Two resistance genes, *mecA* and *femB*, are often tested as they encode methicillin resistance and the virulence of this resistance,[206] respectively, whereas *spa* is a known virulence factor[207] associated with *S. aureus* specifically. LAMP reactions were first optimized for the *femB* primer set and were then applied to reactions with *mecA* and *spa* primer sets. Using an intercalator for single gene detection and purified MRSA genomic DNA (MRSA gDNA), the limit of detection for all three primer sets was $10^2 - 10^3$ copies per reaction (Figure 4.6). Given the results shown in Figure 4.3, 10% QPD was chosen to minimize the delay in TTP while maintaining high discrimination between baseline and signal amplitude. Using DARQ LAMP for singleplex detection, we observe that for the *femB* and *spa* primer sets, we can detect 10^3 copies within 30 minutes (Figure 4.7). However, for the mecA primer set, we no longer can reliably quantify 10^3 copies with the QPD. While the

reaction conditions were optimized for *femB* using an intercalator to assess fluorescence, it is apparent that these conditions are suboptimal for DARQ LAMP reactions.
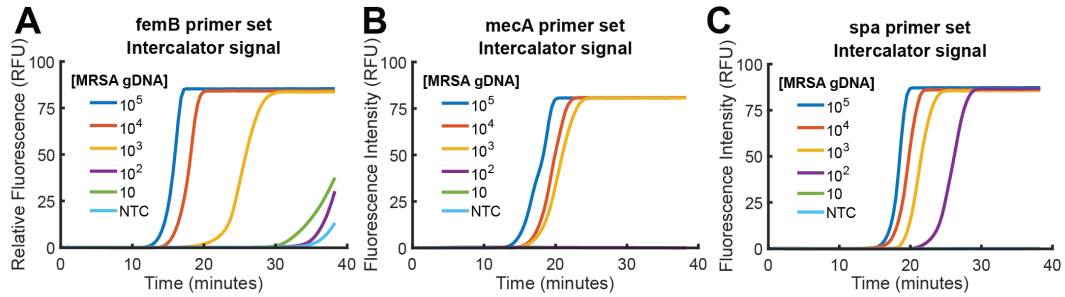
Figure 4.6. Genome dilutions with 1 μM SYTO 82 (intercalator) to assess limits of detection across all three primer sets. (A) femB shows high discrimination between concentrations of 10^3 copies and higher, and 100 copies and lower. (B) mecA show amplification of 10^3 copies and higher, with no amplification at lower concentrations. (C) spa shows amplification at 100 copies and higher.
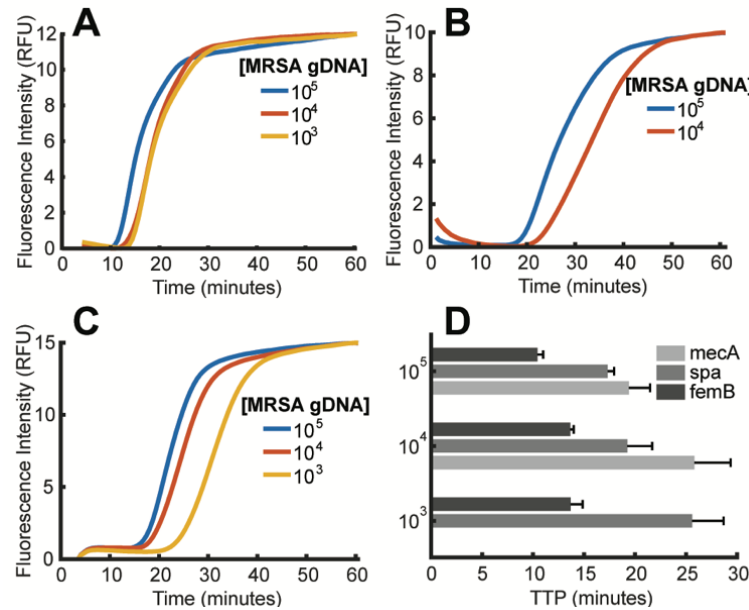
Figure 4.7. Singleplex detection of femB (A), mecA (B), and spa (C). All amplification reactions used 160 nM of QPD in the LAMP reactions. Amplification traces are averaged over n = 3. (D) plots the TTPs for all primer sets across copy number, where error bars represent standard deviation.

Duplex detection of MRSA gDNA was investigated by using the *femB* and *spa* primer sets. Looking at the individual primer sets following

amplification, we observe that while the *spa* primer set maintains strong amplification curves (Figure 4.8B) without significant changes to TTP (Figure 4.8F), detection from the *femB* primer set shows detection of 10^5 and 10^4 copies only (Figure 4.8A), suggesting that the reaction conditions for this primer set become less favorable with the increased number of primers and QPDs present in the reaction. This applies to triplex detection that includes all three primer sets (Figure 4.8D), where 10^4 copies detected with the *femB* primer set amplifies 10 minutes later when compared to TTPs from duplex detection (Figure 4.8F). It appears that the reaction efficiency with the *femB* primer set worsens with additional primer sets, as well. Interestingly, *mecA* and *spa* primer sets show similar delays (approximately 5 minutes) in TTPs for triplex detection in comparison to singleplex detection.
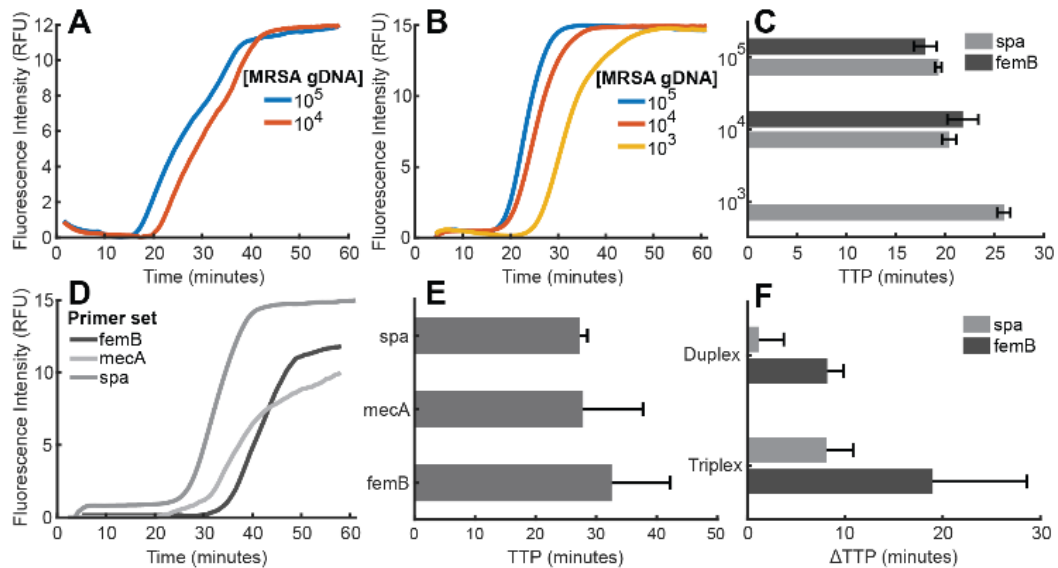
Figure 4.8. Duplex and triplex detection of MRSA genes. Duplex detection of MRSA measured fluorescence of QPDs for the femB (A) and spa (B) primer sets, where TTPs were calculated and plotted in (C). Triplex detection was evaluated using 10^4 copies of MRSA with all three primer sets (D). TTPs were plotted (E) and TTPs for spa and femB primer sets were compared to those from singleplex detection with QPD to assess the impact of increased primer sets present in the reaction (F). All amplification traces are averaged over n = 3, with QPD concentration at 160 nM, and all error bars represent standard deviation.

4.4   Conclusion

Here we have designed and demonstrated a LAMP assay that simultaneously detects three MRSA genes within a single sample. To enable multiplexing, we have utilized the DARQ LAMP paradigm, which we believe to be the most robust and universal approach for multiplexing with LAMP. However, unlike Taqman PCR, DARQ LAMP is highly sensitive to reaction conditions and thus requires additional study to be broadly applied.

Specifically, we have shown that DARQ LAMP is best suited for assays that require a high Mg^{2+} concentration. This provides greater stability for the QPD and provides a greater working range of %QPD when using Bst 2.0. In fact, a narrow range of 10-15% QPD shows similar TTPs to intercalator-only controls when using Bst 2.0 and moderate Mg^{2+} concentration. Given the emergence of Bst 3.0, we studied its use in DARQ LAMP for the first time. We investigated the optimal quencher-probe duplex fraction in the assay for both Bst 2.0 and Bst 3.0 and (i) we determined the optimal ratio, and (ii) we demonstrated that Bst 3.0 is more tolerant to the QPD doping required for DARQ LAMP. We then further optimized the DARQ LAMP assay for triplex detection of MRSA genes. While the performance of DARQ LAMP is hindered when optimizing for three gene targets simultaneously, we were ultimately able to achieve detection of all three MRSA genes in a single sample with a TTP under 30 minutes.

Chapter 5. Transcription Cycling Amplification: a novel isothermal amplification scheme for the direct detection of microRNA

5.1 Introduction

Within the last decade, miRNA have become a focus in biomarker discovery and subsequently disease diagnostics. These nucleic acids are a subclass of noncoding RNAs that are roughly 22 nucleotides in length,[208] and are largely known to regulate the translation of mRNAs by promoting mRNA degradation or inhibiting protein translation.[209] As a result, miRNAs play a large role in various cell processes, such as proliferation,[210–212] differentiation,[213–215] and cell death.[216,217] Because each class of miRNA has a characteristic expression profile, they hold promise as diagnostic biomarkers for tissue-specific or stage-specific diseases. Additionally, miRNA targets have been reported to circulate either freely in bodily fluids[218,219] or within exosomes,[220,221] suggesting great potential towards the development of a liquid biopsy for minimally-invasive diagnostic techniques.

Early miRNA detection techniques were variations of hybridization assays, the most popular of these techniques being the Northern Blot. Similar to the Southern blot, Northern blots rely on electrophoresis for band identification, transfer onto a nitrocellulose membrane, and labeling with fluorescent or radiolabeled complementary probes. This method can take over 24 hours to perform, and is only semi-quantitative.[222] Given the laborious

expertise involved, it also does not facilitate high throughput analyses. As traditional hybridization assays evolved into DNA microarrays to address the need for high throughput analyses, these were quickly adopted towards the detection of various miRNA targets. With the conjugation of various complementary probes, these platforms enable the screening of a large number of miRNA that cannot be achieved with traditional hybridization assays. Detection with DNA microarrays requires multiple steps, starting with the isolation of miRNA targets, which are converted to complementary DNA (cDNA) with use of reverse transcriptase (RT). These cDNA sequences are then labeled and added to a microarray for hybridization. As a result, detection with this method involves various procedures beforehand that not only require technical expertise, but lengthen the amount of time required to run the assay.

With the advent of PCR and its derivative for RNA targets, RT-PCR, this amplification-based detection scheme has become the gold standard for miRNA expression quantification, and is often used to confirmed results obtained for microarray profiling.[223] However, miRNA have presented a very unique problem for traditional RT-PCR methods: first, miRNA are roughly the same size as primers used for both cDNA synthesis and PCR; second, they do not have the poly-A tail that is normally leveraged for cDNA synthesis of mRNA. The most popular alternative method specific for miRNA targets involves the use of a stem-loop primer. This method requires the design of a hairpin primer where the 3' arm is elongated compared to the 5' arm. The longer arm can then hybridize with miRNA in such a way that the reverse transcriptase will template

against the miRNA target and further elongate the 3' arm. As a result of primer elongation, the complementary sequence is embedded into the product, thus creating a longer template that is better suited for PCR. However, traditional RT protocols for RNA targets involve converting all RNA targets in a sample to cDNA, and therefore the specific detection of RNA is still heavily reliant on PCR with the use of target-specific primers. While it would be ideal to perform PCR directly by assaying the RNA targets themselves, RNA is highly sensitive to temperature, where temperatures above 65 °C begin to degrade RNA targets. Therefore, this RT step is crucial for any PCR-based method for RNA quantification.

To address the need for direct RNA detection to shorten assay times, several isothermal amplification schemes have been developed to operate in temperature ranges better suited for RNA targets. The two most popular methods are nucleic acid sequence-based amplification (NASBA)[125] and exponential amplification reaction (EXPAR),[224] where both assays create analogs of the target sequence to enable positive feedback into the reaction, thus facilitating exponential amplification. However, NASBA (described in section 2.3.2.2.4) is better suited for longer RNA targets, such as mRNA.[225] As a result, EXPAR (described in section 2.3.2.2.2) is one of the few amplification schemes that enables direct detection of miRNA[226] by leveraging both a DNA polymerase and a nicking enzyme, along with a symmetric template. However, for low copy number detection, EXPAR often suffers from nonspecific amplification, either from nonspecific DNA polymerase activity,[112,113] which is

further exacerbated by the presence of the nicking enzyme,[114] or nonspecific hybridization of templates and molecular beacons for multiplex detection.[227]

Here, we aim to create a novel amplification scheme that leverages elements from both EXPAR and NASBA. Like EXPAR, we leverage a symmetric template where the generated analogs of miRNA targets feed back into the system to enable rapid, exponential signal generation. Instead of flanking a nicking enzyme recognition sequence like in EXPAR, the symmetric template instead flanks the anti-sense recognition sequence of an RNA polymerase and a user-designed sequence for easy integration of a labeled probe (Figure 5.1A). By leveraging the sequence recognition of RNA polymerases to initiate RNA generation, a RNA transcript is generated that hybridizes to the target binding region, resulting in amplification through this cyclic transcription process (Figure 5.1B); thus we have named this approached Transcription Cycling Amplification (TCA).

In this endeavor, there are several questions that need to be answered towards the design of a multi-enzyme isothermal amplification system. Specifically, we aim to study the following: (i) assessing the impact of various DNA and RNA polymerases, (ii) evaluating template designs to limit nonspecific interactions, and lastly (iii) optimizing buffer conditions to achieve rapid, specific amplification and detection. Each of these studies will provide information regarding nucleic acid and enzyme interactions, and inform key design constraints when expanding this system for multiplex detection. With

the investigation of these three areas, we aim to achieve a direct amplification method specifically for microRNA that enables rapid quantification.
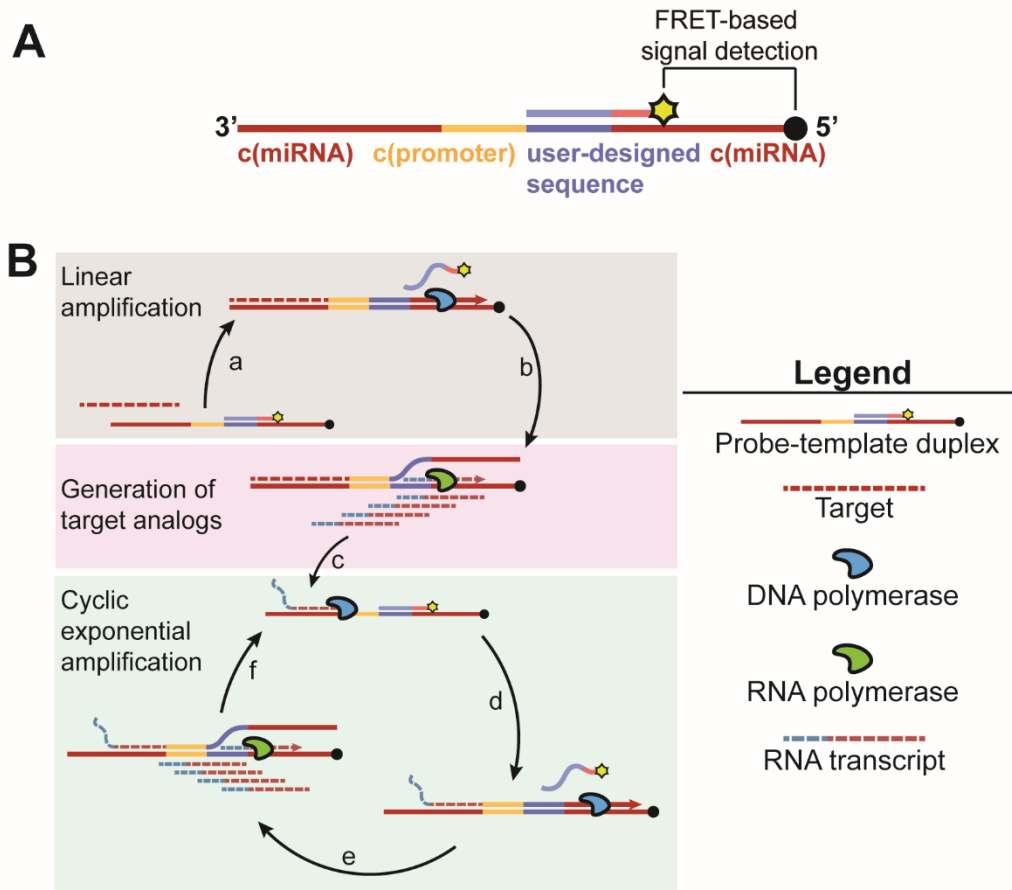
Figure 5.1. Transcription Cycling Amplification (TCA). (A) The starting material in TCA centers around a prehybridized duplex, consisting of a template with 5' quencher and a probe with a 3' fluorophore. The template consists of two regions that are complementary to the target of interest. These two regions flank the anti-sense sequence of an RNA polymerase promoter and a user-designed sequence. This user-designed sequence is then leveraged to design probes that are specific to the target of interest, and therefore its complementary target. Additionally, because the probe partially overlaps the right half of the template, this enables the target to preferentially bind to the left side of the template to begin TCA. (B) TCA begins upon binding of the miRNA target to the left half of the template. A DNA polymerase (blue) then recognizes the target's 3' end to begin extension. (a) Extension of the target forms the double-stranded promoter region, and either displacement (as drawn) or degradation of the probe. Separation of the probe from the template leads to unquenched fluorescence that can be monitored in real-time. (b) With the creation of the double-stranded promoter, the RNA polymerase (green) recognizes the synthesized sense sequence to transcribe everything downstream. As the template is symmetric, the RNA transcripts are analogous to the miRNA targets. (c) These RNA transcripts can then bind to another prehybridized probe-template duplex and continue the same extension (d), transcription (e), and hybridization (f) steps to achieve exponential signal generation.

5.2   Materials and Methods

5.2.1 Synthetic oligonucleotide design and preparation

Let7a, a common miRNA target for cancer expression profiles, was chosen as the target of interest for the work presented here. Templates consist of the reverse complement of the let7a target on both the 3' and 5' ends (Figure 5.2); however, to favor target binding and extension along the template, the reverse complement on the 5' end only contains the last 15 of the 22 nucleotides. To further increase the probability of the target binding to the full complement, a user-designed sequence, different for each assayed target, follows the 13-nucleotide complement. This enables a probe to hybridize at this site and to cover a small portion of the miRNA complement, and therefore act as interfering or blocking DNA to further bias the miRNA binding to the 3' end. The designed probes should have a melt temperature of at least 45 °C to ensure stable binding of the probe and template during the reaction, and secondary structures should be verified to ensure that probes do not bind to any other region of the template. Lastly, the reverse complement of the RNA

Figure 5.2. Sequence design for TCA templates. The reverse complement of the intended target is present on both the 3' and 5' ends of the target. However the sequence on the 3' contains the full complement to bias hybridization to the 3' end. These two reverse complements flank the anti-sense recognition sequence of the RNA polymerase, and a sequence of the user's design to enable probe hybridization with minimal secondary structure.

90

polymerase recognition sequence, known as the promoter, is incorporated between the full complement and the user-designed sequence.

Secondary structures of all template and probe designs were assessed using the web-based software, NuPack. Often, secondary structures arise at the promoter region, or between the designed probe region and the reverse complement. Here, the designed probe can be elongated as necessary to minimize secondary structure, however the probe (including the complementary target region) should not be less than 15 nucleotides, should not contain the full complement of the target, and should have at least 50% GC-content to ensure stable binding onto the template. All nucleotides were purchased through Integrated DNA Technologies (IDT). Table 5.1 lists all the sequences used in this work. All templates were ordered with HPLC purification, and with a 3' phosphate group to prevent extension.

Table 5.1. Oligonucleotide sequences for TCA.

Oligonucleotide	Sequence (5' → 3')
Sequences with T7 RNA polymerase promoter	
Target*	TTT TTT TTT TGA GGT AGT AGG TTG TAT AGT T
Template	AAC TAT ACA ACC TGA CTG CAT GCT ATA GTG AGT CGT ATT AAA CTA TAC AAC CTA CTA CCT CA
Probe[a]	CAT GCA GTC* AGG TTG TAT AGT T
Sequences with T7 RNA polymerase promoter for displacement	
Template[b]	AAC TAT ACA ACC TGA CTG CAT GCT ATA GTG AGT CGT ATT AAA CTA TAC AAC CTA CTA CCT CA
Probe[c]	CAT GCA GTC AGG TT

Sequences comparing SP6 and T7 RNA polymerase activities[d]	
SP6 template	GAT ACA ACC TCA TGG CTC TTC TAT AGT GTC ACC TAA AT
SP6 probe[e]	AAG AGC CAT GAG GTT GTA TC
SP6 promoter	ATT TAG GTG ACA CTA TAG
T7 probe[e]	CAT GCA GTC AGG TTG TAT AGT T
T7 promoter	TAA TAC GAC TCA CTA TAG
SP6 templates with various sequence configurations	
let7a SP6 template[b,f] (probe after promoter)	AAC TAT ACA ACC TGA CTG CAT GCT ATA GTG TCA CCT AAA TAA CTA TAC AAC CTA CTA CCT CA
SP6 template2 (probe before promoter)	AAC TAT ACA ACC TAC TAT AGT GTC ACC TAA ATG GGC TTC TAT TCT ACT TCA ACC TAA CTA TAC AAC CTA CTA CCT C
Probe for template2[e]	GAA GTA GAA TAG AAG C
SP6 hairpin template	AAC TAT ACA ACC TAC GCT GCT ATA GTG TCA CCT AAA TGC AGC GTA GGT TGT ATA GTT AAT GGA ACT ATA CAA CCT ACT ACC TC

(a) FRET probe labeled with a 5' fluorophore, and 3' quencher. The asterisk denotes the location of an internal quencher (b) Oligonucleotide labeled with a 5' quencher (c) Oligonucleotide modified with a 3' fluorophore (d) T7 templates used for these experiments are uses the unlabeled template under "Seqences with T7 RNA Polymerase promoter" (e) Oligonucleotide modified with a 3' phosphate group (f) Template uses the same probe used for T7 displacement experiments. *Target includes a 5' poly-T tail to differentiate target extended by DNA polymerase from the template in gel analyses for assay characterization.

FRET probes and unlabeled templates, or labeled probes and quenched templates are prehybridized at 2 μM in nuclease-free water (NEB), where sequences are incubated at 95 °C for two minutes on a heat block and left to cool until the temperature reaches room temperature.

5.2.2 TCA reactions

TCA reactions were conducted in buffer conditions that favor RNA polymerase, given its sensitivity to monovalent salts. Therefore, all reactions

consisted of 1× optimized transcription buffer (Promega, consisting of 10 mM Tris-HCl, 6 mM MgCl$_2$, 10 mM NaCl and 1 mM spermidine), 10 mM DTT (Promega), 500 µM dNTPs (NEB), 500 µM NTPs (NEB), 20 U of human placenta-derived RNase inhibitor (NEB), nuclease-free water, and 200 nM prehybridized probe-template duplex in 20 µL reactions, unless otherwise noted. The impact of various buffer components such as NaCl (JT Baker) and KCl (JT Baker) were investigated with relevant concentration information included in the figure captions. For experiments where various DNA polymerases were tested, 1 U of the designated DNA polymerase was used for each reaction. All DNA polymerases were purchased from NEB. The RNA polymerases in this study, T7 and SP6 RNA Polymerases, were purchased from Promega. 10 U of T7 RNA polymerase or 10 U of SP6 RNA polymerase were used for each reaction, unless otherwise noted. All assays were incubated at 37 °C for 30 – 60 minutes, followed by a 2-minute 80 °C enzyme-kill step. Reactions incubated at 42 °C are noted in the figure captions.

5.2.3 Real-time fluorescent measurements

All fluorescence values reported here were measured using a BioRad MJ MiniOpticon thermocycler, with software supplied by the manufacturer. The real-time measurements on this instrument were made using an isothermal protocol with plate reads every 20 seconds.

5.2.4 Product verification with gel electrophoresis

All amplification products were run on a 15% denaturing gel (29:1 acrylamide:bis-acrylamide), with 8 M urea (Sigma Aldrich). Samples were denatured in a 1x RNA loading buffer consisting of 47.5% formamide (Sigma Aldrich) and 0.5 mM EDTA (Sigma Aldrich). Gels were run for 20 minutes at 500 V in 0.5x TBE buffer, and were then stained using 0.5x SYBR Gold. Experiments that assessed nonspecific degradation with labeled probes were imaged first without staining under UV excitation, and were then stained with 0.5x SYBR gold.

5.3 Results and Discussion

5.3.1 The impact of various polymerases on TCA

Overall, the crux of this assay is the sequence-dependent initiation of RNA polymerase to produce target analogs. To achieve this goal, the first study aims to determine which DNA polymerase enables robust extension to produce the double-stranded promoter region. Because the assay conditions favor the activity of the RNA polymerase, the DNA polymerase must be able to extend the target efficiently in these sub-optimal conditions. Additionally, the extension of the target must enable probe degradation or displacement such that real-time fluorescent signals are robust enough to differentiate positive and negative samples. This section evaluates several different DNA polymerases for optimal TCA performance.

5.3.1.1 Investigating the impact of DNA polymerases with exonuclease activities

When considering which of the abundant DNA polymerases to use for this assay, we first investigated the impact of both 5' $\rightarrow$ 3' and 3' $\rightarrow$ 5' exonuclease domains. The 5' $\rightarrow$ 3' domain is known as the nuclease portion of the enzyme, and is primarily used in Taqman PCR applications. Here, as the the Taq polymerase extends the primer, the 5' $\rightarrow$ 3' domain is responsible for the degradation of the Taqman probe downstream for signal generation. The 3' $\rightarrow$ 5' exonuclease domain is responsible for proof-reading activity, and is primarily responsible for excising mismatched nucleotides during the polymerization process. It has been previously suggested that the activity of these 2 – 3 domains (including the polymerase domain) involves competition between the active sites as a primer is shuttled between them.[228] Therefore, it is crucial to evaluate how the presence of these exonuclease domains interact with both the target and the probe, and subsequently, impact target extension and probe degradation or displacement.

5.3.1.1.1 Bst DNA Polymerase, Full Length

Our first design of TCA used a linear template, with a prehybridized FRET probe with a 5' label and 3' quencher, instead of a quenched template and labeled probe as drawn in Figure 5.1A. By isolating the FRET signal to a single sequence, it was assumed that this would greatly simplify the system. We first assessed TCA using two standard DNA and RNA polymerases. For

DNA extension, Bst DNA polymerase, Full Length (Bst Full) was chosen for two main reasons. First, it is a DNA polymerase that also has 5' to 3' exonuclease activity, similar to Taq Polymerase. This would enable the degradation of any nucleic acid it encounters as it is extending the target sequence, and can facilitate probe degradation for signal generation. Second, this DNA polymerase recognizes both DNA and RNA primers. This is especially important because in order to achieve both the linear amplification via the extension of the miRNA target, and exponential feedback using the downstream RNA transcripts, the DNA polymerase must be able to extend an RNA sequence. For the RNA polymerase, T7 RNA polymerase (T7) was chosen, as it is a widely-used polymerase for cloning and RNA synthesis applications given its strong promoter activity.[229–231] Because TCA is heavily reliant on the generation of RNA for feedback, having an RNA polymerase that robustly transcribes a template is essential.

Using these two enzymes with this initial design, we first demonstrated in a piece-wise fashion the feasibility of TCA. In Figure 5.3A, we confirm that linear amplification and the generation of target analogs occur as we expect. In lanes 1 and 2, Bst Full is added to a reaction with target and template, and we observe in lane 2 the disappearance of the target band (roughly 30 nucleotides in length) from lane 1 and the emergence of a band longer than the template. This demonstrates we have efficient and complete conversion with Bst Full. Lanes 3 and 4 assess the exonuclease activity of Bst Full by including the probe in the reaction. With the addition of Bst Full (lane 4), we observe both

incomplete conversion of the target, seen by the faint target band still present in comparison to lane 3, and incomplete conversion of the probe, suggesting that when both polymerase and exonuclease functions are engaged, this enzyme loses some efficiency in comparison to having polymerase activity alone. Lastly we verify that the synthesis of a double-stranded promoter leads to the generation of RNA. By including T7 in the reaction (lane 5), we observe a new band that is present beneath target band that matches the expected length of the RNA transcripts. RNA transcripts were confirmed with a post—amplification treatment of DNase I to remove the probe, templates, and targets from the reaction (data not shown). This isolated DNA was then used to confirm that the exponential feedback occurs as expected. Reactions consisting of isolated RNA, template alone, and Bst Full demonstrated that RNA can be extended (lane 6), and with the addition of RNA polymerase, the
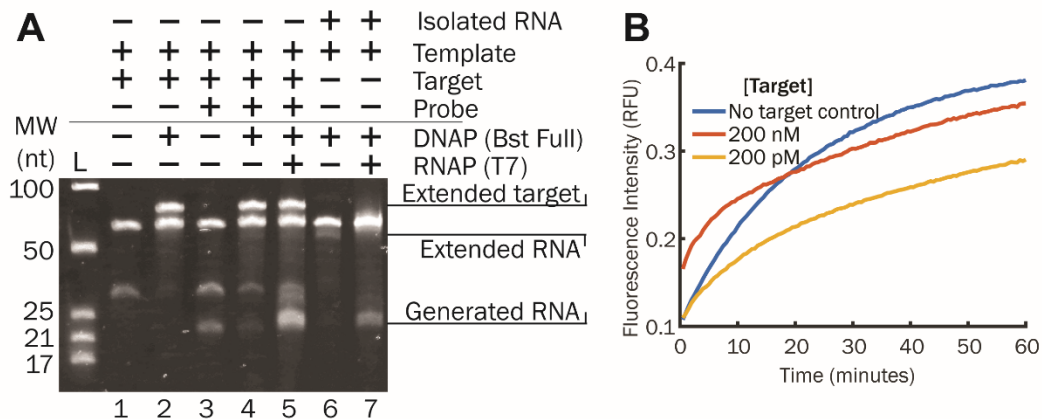
Figure 5.3. Piecewise demonstration of TCA. (A) Lanes 1 and 2 verify that the target is extended when bound to the template. Lanes 3 – 5 confirm that alongside Bst Full's polymerase activity, the exonuclease activity leads to the degradation of the probe. Addition of the RNA polymerase leads to transcription due to the presence of the double-stranded promoter. Lanes 6 and 7 confirm positive feedback where isolated RNA is extended along the template in the presence of the Bst Full, and alongside the T7, it will further propagate transcription that is observed in the initial linear amplification phase. (B) Real-time signals of TCA using T7 RNA polymerase and Bst Full for 200 nM, 200 pM and 0 target concentrations.

97

double-stranded promoter will lead to transcription (lane 7), increasing the potential for positive feedback in the reaction.

Thus far, we have demonstrated that upon binding to the template, a target can be extended by Bst Full, leading to probe degradation and formation of the double-stranded promoter. Only in the presence of this double-stranded promoter does the RNA polymerase begin transcription, where the generated RNA can bind to template to repeat the steps of extension and probe degradation. However, when we assess the full system with two different target concentrations and a no target control (NTC), the result does not distinguish the two concentrations, and more concerning, there is a signal in the absence of target (Figure 5.3B). The only way for signal generation to occur with a dual-labeled probe is if the fluorophore was separated from the oligonucleotide by nonspecific activity of Bst Full. However, given that the probe is also labeled with a quencher, visualization of a clipped or degraded probe compared to the intact probe with traditional staining methods is difficult. Therefore, we looked at reactions with only the DNA polymerase and either one of two probes: one being the original FRET probe, and the other being that same probe with only a 5' fluorophore.

In Figure 5.4, when looking at the reactions with the FRET probe (bands in blue), reactions with just probe and template show significant clipping of fluorophore (lane 1 vs lane 5), even in comparison to the clipping that is observed in the presence of the target (lane 6). This observed activity was also seen in reactions using the 5' labeled probe (bands in pink). Both in the

98

presence and absence of target, the clipped fluorophore can be visualized, and therefore indicates that Bst Full can nonspecifically act on a labeled probe, and is thus not the appropriate enzyme for this assay.
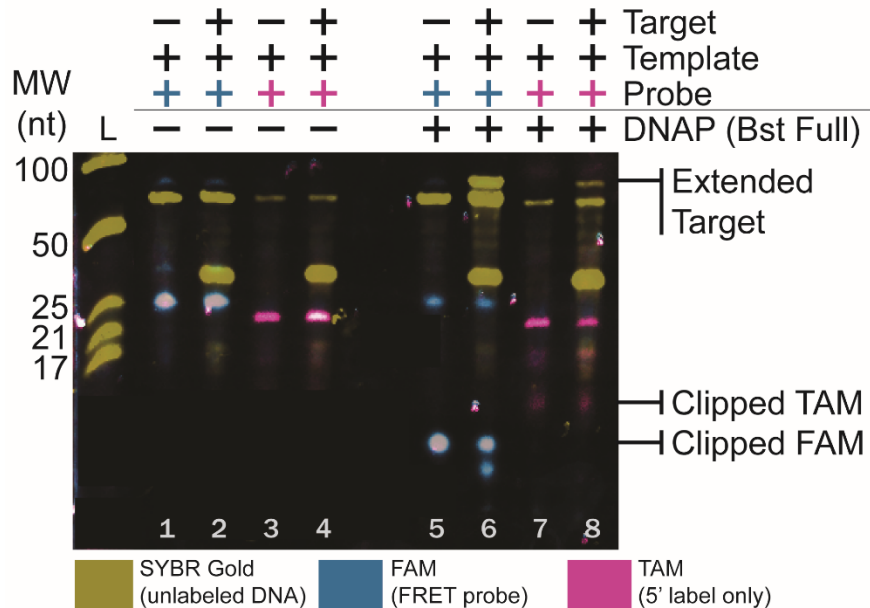
Figure 5.4. Bst Full nonspecifically degrades oligonucletides in the absence of target extension. Lanes 1 and 2 show the three sequences involved in the reaction, and serve as length reference. Lanes 3 through 6 show the probe and template with and without target for both the FRET and 5' labeled probe. Lanes 7 through 10 are analagous to lanes 3 through 6, but with the DNA polymerase present. Across the four lanes, we observe incomplete degradation of probe, with a significant portion of fluorophore clipped off the probe, shown with the bands towards the bottom of the gel.

5.3.1.1.2   DNA Polymerase I

When considering other polymerases with the required exonuclease activity, DNA Polymerase I presents an advantage in that it is optimal at the same temperature as RNA polymerases. While Bst Full is active at these lower operating temperatures, its optimal temperature ranges between 50 – 72 °C. Given that its overall activity is at roughly 10-15% as noted by the vendor information, we hypothesize that this decreased activity may result in the exonuclease being more active than the polymerase function at this suboptimal

condition. Despite DNA Polymerase I having both 5' → 3' exonuclease activity and 3' → 5' exonuclease activity, we hypothesized that the polymerase activity would overwhelm both of these exonucleases if the assay temperature and the enzyme's optimal temperature are the same.

We tested this hypothesis using both a high and low concentration of target, alongside an NTC, using the full TCA system. Figure 5.5A shows a concentration dependence where the highest target concentration shows a higher end-point fluorescence than the lower concentration, suggesting that this may be a viable option for the assay. However, when confirming the assay products with gel electrophoresis, we observe either smears within a lane or shorter bands than expected. Smears are often indicative of degradation products, and the short bands of interest (lanes 2 and 3, beneath the template and) are potential degradation products of the template. A possible explanation
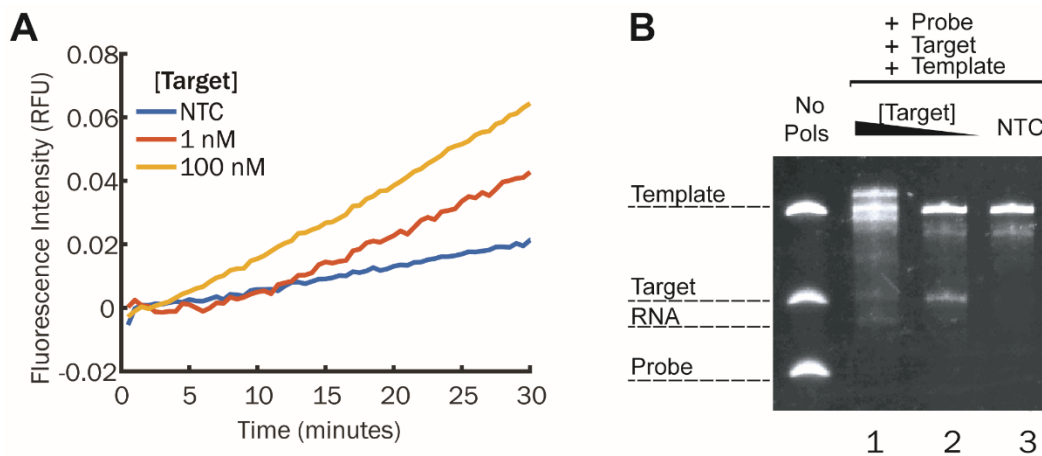
Figure 5.5. Impact of DNA Polymerase I for TCA. (A) Real-time curves resulting from probe-degradataion during TCA of 100 nM and 1 nM target, alongside a no target control (NTC). (B) Confirmation of products with gel electrophoresis. Lane 1 are the products from the 100 nM target reaction, and shows significant degradation products. Lane 2 shows the products from the 1 nM reaction, with some degradation products present beneath the template. Lastly lane 3 shows the products from the NTC, exhibiting very similar results to the 1 nM reaction.

for this behavior is that once templates have been saturated with extension products, the DNA Polymerase I recognizes 3' ends, and instead of extending, the exonuclease becomes active, resulting in the degradation products seen in the gel. While there are strategies to avoid degradation of the designed template and probe (incorporation of inverted dT bonds, carbon spacers at either end of oligonucleotides, etc.), it is difficult to include protection strategies for oligonucleotides that are synthesized *in vitro* by either the DNA or RNA polymerases. Additionally, incorporation of these modifications increases the cost of the assay and increases the complexity of assay design.

5.3.1.1.3   phi29 DNA Polymerase

The last study involving polymerases with exonuclease domains was to evaluate a polymerase with an optimal temperature lower than the operating temperature of the assay. Unlike the previous two polymerases, this polymerase, phi29 DNA polymerase (phi29), does not have a 5' → 3' exonuclease activity, but instead has a 3' → 5' exonuclease. As a result, as phi29 encounters a DNA strand as it is extending a primer, this DNA would simply be pushed off the template instead of degraded. For these experiments, a single-labeled probe at the 3' end and a quenched template were used to monitor the real-time fluorescence (as depicted in Figure 5.1A). Initial experiments with a high target concentration and an NTC show signal generation with significant end-point values for both reactions (Figure 5.6A). Gels revealed that (i) there was inefficient extension of target given the intensity of the target band and (ii) transcription occurred in the NTC (Figure 5.6B,

lane 1). It is likely that the efficiency of phi29 dramatically decreases at temperatures above its optimal temperature, which would result in less extension of the target as what has been observed with DNA Polymerase I, and Bst Full. With this displacement model, any nonspecific transcription can lead to the probe being pushed off of the template, separating the fluorophore on the probe from the quencher on the template and thus generating a fluorescent signal. We hypothesize that there may be unintended synergy between the DNA and RNA polymerases that leads to nonspecific T7 RNA polymerase activity, and is further elaborated in section 5.3.1.3. Given the nonspecific transcription that we observe in lane 1, this is likely to be the cause of the fluorescent signal observed in Figure 5.5A.

Given the previous experimental results involving a 3' → 5' exonuclease, we expect to see the same nonspecific degradation for low target concentrations and NTCs. Evidence of this was observed previously with DNA Polymerase I, with high target concentrations. In this strand-displacing model,
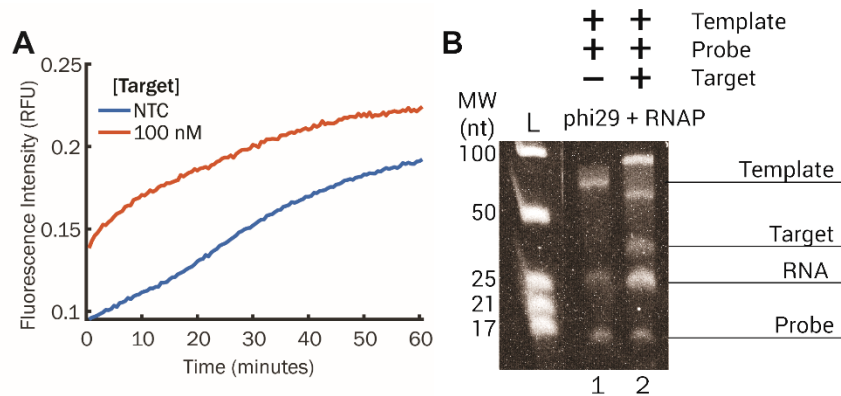
Figure 5.6. Impact of phi29 DNA polymerase on TCA. (A) Real-time fluorescence of reactions with either 100 nM target or the absence of target (NTC). (B) Denaturing gel shows that there is nonspecific transcription present in the NTC, which most likely is what is causing the observed fluorescence in A.

it would be difficult to discern in a gel whether there are degradation products from the template due to the presence of the quencher, and troubleshooting would become cumbersome with the use of hybridized probes or labeling. Therefore, we decided to continue with the strand-displacing model of TCA, with a DNA polymerase that has no exonuclease activities, also known as strand-displacing polymerases.

5.3.1.1.4 Summary of findings

Thus far, we have shown that polymerases with exonuclease domains are poorly suited for TCA. While each step of the assay generates the expected products, these polymerases lead to nonspecific degradation of the oligonucleotides. Consequently, the observed degradation further impacts fluorescent measurements, or the stability of the oligonucleotides in the assay. The table below further details the activities that have been observed in this study.

Table 5.2. Summary of polymerases with various exonuclease domains' impact on TCA

Enzyme	Exonuclease domains	Findings
Bst Full	5' → 3'	• Clipping of 5' fluorophore on probes in the absence of target • For FRET probes, nonspecific degradation of entire probe is apparent • For 5' labeled probes, only clipping of the fluorophore with inefficient probe degradation
DNA polymerase I	5' → 3' 3' → 5'	• Degradation of the template is observed in the presence and absence of target
Phi29	3' → 5'	• Inefficient extension of targets

103

		• Poor discrimination between positive and negative samples

5.3.1.2 Investigating the impact of strand-displacing DNA polymerases

The next study evaluates polymerases that do not have exonuclease domains. Due to the unexpected degradation that was observed across polymerases with exonuclease domains, we expect that strand-displacing polymerases will offer higher extension efficiencies given the absence of other active sites, and minimize downstream troubleshooting given its singular function. The two strand-displacing polymerases studied below were selected for investigation because of their prevalence in existing isothermal amplification schemes.

5.3.1.2.1 Bst 2.0

Bst 2.0 is a derivative of Bst Full that has the exonuclease portion removed, and has been modified for improved processivity and robustness against inhibitors that are common in crude samples (further discussed in Chapter 4). However, Bst 2.0 has the same optimal temperature range as Bst Full (50 – 72 °C), and therefore its efficiency must be determined for the lower operating temperature of TCA.

Bst 2.0 was evaluated with reactions of the probe and template with either only Bst 2.0 present (DNAP only) or both Bst 2.0 and T7 (DNAP and RNAP) in either absence or presence of target. Figure 5.7A shows the real-time amplification curves for these reactions. For reactions with only DNA polymerase, there is not a significant change in fluorescent signal in the presence or absence of target. This is surprising for reactions containing target, as it is expected that extension of the target would lead to the displacement of the probe, and generate a fluorescent signal. However, when looking at reactions with both polymerases, there is a significant change in signal only in NTCs. Products separated by gel electrophoresis show that despite the nonspecific transcription we observe in the NTC, the products in all other reactions are indicative of a successful amplification reaction (Figure 5.7B). It is unclear how or why Bst 2.0 is interacting with the oligonucleotides to produce such a low signal in comparison to the NTC, and requires further studies to understand the mechanism of the observed behavior.
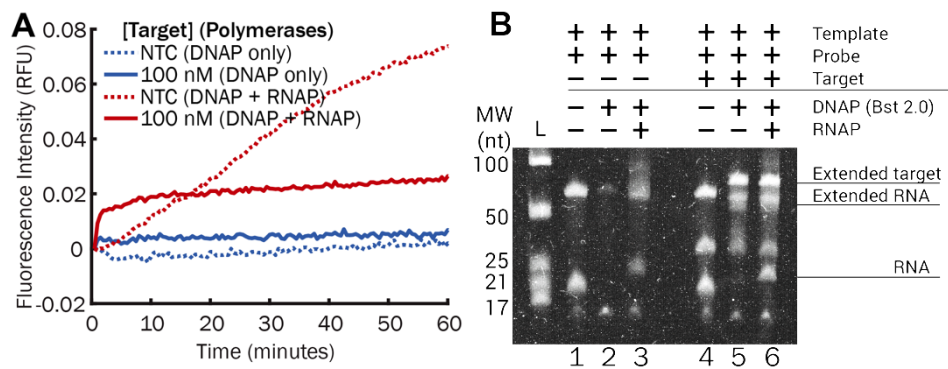
Figure 5.7. Impact of Bst 2.0 on TCA. (A) Real-time amplification curves show a high fluorescent signal for NTC reactions with both enzymes, in comparison to reactions with target or with DNA polymerase enough. (B) Products separated by gel electrophoresis show nonspecific transcription in NTC reactions, but reactions with target present show products indicative of successful amplification.

5.3.1.2.2   Klenow exo-

Klenow exo- (referred to as Klenow in this chapter) is a derivative of DNA Polymerase I with both exonuclease domains removed. Klenow therefore has the same optimal temperature as TCA's operating temperature of 37 °C, and has been previously used for amplification schemes like RCA (described in section 2.3.2.2.3). We assessed these two enzymes for TCA by evaluating the real-time amplification curves, and assessing the degree of nonspecific transcription occurring in the reaction.

From previous experiments using Bst 2.0 and phi29, nonspecific transcription activity of T7 is present in all NTC reactions, and therefore when assessing Klenow as a DNA polymerase candidate, it was expected that NTC reactions would still show RNA transcripts. Therefore, preliminary studies with Klenow only evaluated target dilutions in TCA reactions and their fluorescent signals. The expected signal for these reactions should appear as a sigmoidal curve, instead of the relatively flat signals observed with Bst 2.0. The sigmoidal curve would indicate that RNA has been robustly generated, and the RNA has bound onto the template for extension and probe displacement for exponential signal generation.

Fluorescent signals from reactions with Klenow have drastically different signals, compared to those using Bst 2.0. Signal gains of roughly 0.1 RFU (typical of PCR reactions run on this instrument) are observed across all target concentrations (Figure 5.8A), and we observe RNA production and extension

of RNA across all lanes in the gels (Figure 5.8B). Additionally, the sigmoidal

curves that are characteristic of exponential amplification reactions is now more
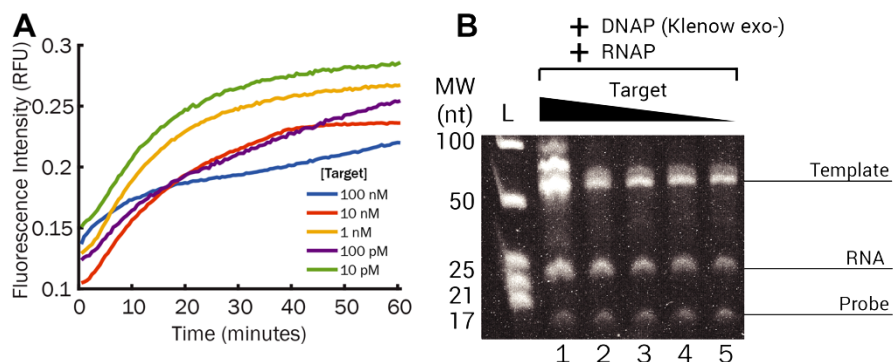
Figure 5.8. Investigating the impact of Klenow on TCA. (A) Real-time amplification curves of reactions with varying concentrations of target show a sigmoidal amplification curve, characteristic of exponential amplification reactions. (B) Products separated by gel electrophoresis show robust RNA production and RNA extension across all target-containing reactions.

apparent. It is important to note that there is no concentration-dependent

amplification that is normally observed, and this is most likely due to the

nonspecific transcription activity of the RNA polymerase. However, this

behavior can be addressed with investigating other RNA polymerases besides

T7, and also optimizing buffer conditions to promote and inhibit the activity of

either polymerase as needed.

5.3.1.2.3   Summary of findings

Unlike polymerases with exonuclease domains, strand-displacing

polymerases are better suited for TCA given their singular function of DNA

extension. However, it is important to note that across the strand-displacing

polymerases, we now observe nonspecific transcription, where in the presence

of a single-stranded promoter, T7 RNA polymerase still initiates transcription,

and thus limits the sensitivity of our assay. The table below summarizes the phenomena observed in this study.

Table 5.3. Summary of observed findings using strand-displacing polymerases for TCA.

Enzyme	Findings
Bst 2.0	• Inefficient extension of target • No change in real-time signals in the presence of target • Sharp change in real-time signals in the absence of target
Klenow	• Real-time fluorescence shows sigmoidal amplification curves, indicative of exponential amplification • High efficiency of target extension • Poor discrimination between positive and negative samples

5.3.1.3   Investigating various RNA polymerases to limit nonspecific transcription

Thus far, TCA is shown to suffer greatly from nonspecific transcription. While there is consensus in the nucleic acids field that transcription only occurs when the promoter is double-stranded, the work presented here has shown that the presence of a single-stranded promoter, specifically the anti-sense sequence, is still recognized by the T7. When reviewing possible causes for this behavior, it is important to note that transcription in the presence of a single-stranded promoter is often not considered in assessing the specificity of the enzyme. Because RNA polymerases are often used for *in vitro* cloning, groups have leveraged the sequence-specific nature to ensure strong transcription, with little regard to whether transcription occurs in the presence of single-stranded or double-stranded promoter. A few groups have noted that

T7 does not require a double-stranded promoter for transcription,[232] however most groups that have researched the impact of duplexed promoter regions have used purified RNA polymerases isolated from bacteria.[233,234] While the observed behavior may stem from domains present in T7 RNA polymerases in vivo, it is unclear if directed evolution methods normally employed by commercial vendors have addressed these phenomena. A more recent paper has shown that this observed behavior negatively impacts amplification schemes, like RCA (described in section 2.3.2.2.3) for RNA detection described by Li, et al.,[235] where nonspecific activity of the T7 leads to very high limits of detection and negatively impacts binding and melting of DNA nanostructures leveraged for biosensing.[236] This suggests that activity with a single-stranded promoter is more common with commercial RNA polymerases than those purified from *in vitro* cloning.

Another aspect to note is that traditional transcription reactions are normally done only in the presence of an RNA polymerase, whereas our system involves both DNA and RNA polymerases. While Li, et al., has shown that T7 alone leads to false positives, preliminary tests with our sequences show that NTC reactions with T7 alone does not lead to any transcription (data not shown). Nonspecific transcription only occurs when both T7 and a DNA polymerase are present, supporting the hypothesis that the enzymes may be working in tandem during the reaction, inadvertently enabling transcription. Recently, Emery, et al., published a paper where both Bsu DNA polymerase, another strand-displacing polymerase, and T7 together produce the same

nonspecific transcription observed in TCA,[237] and claimed this behavior can generally occur with a wide variety of DNA polymerases. However, strategies to mitigate this activity are not discussed given the challenges in investigating the different mechanisms at play.

While it is unlikely that nonspecific transcription can be totally eliminated with the use of other common bacteriophage RNA polymerases, such as SP6 and T3, we hypothesize that SP6 RNA Polymerase (SP6) may be a more suitable enzyme for TCA. A previous report investigated the impact of transcript length and sequence on transcription yield using SP6, as previous groups have shown that T7 transcription is significantly impacted by these factors.[229,230] Stump and Hall have shown specifically for short RNA transcripts that SP6 RNA polymerase is very efficient,[238] producing a high yield of products. In addition, studies were conducted to compare the yields of full duplexed promoters and partially duplexed promoters using SP6 and T7 RNA polymerases. While the partial duplex showed 5% relative yield in comparison to the full duplex with SP6, the partial duplex with T7 RNA polymerase produced roughly a third of yield to the full duplex control. This specificity of SP6 is promising for TCA applications, where the observed minimal SP6 transcription with a partial duplex promoter may lead to further diminished activity with a single-stranded promoter. Additionally, because the transcripts produced in TCA are roughly 23 nucleotides, using SP6 we expect to still observe high yields with a full duplex promoter.

Preliminary studies were conducted using our TCA system, redesigned with templates containing the anti-sense promoter of either SP6 or T7, where transcription yields were qualitatively assessed. These conditions involved assessing transcription with a single-stranded promoter, a partial duplex (where only the promoter region is double-stranded, and the transcribed region is single-stranded), and a full duplex (both the promoter and transcription regions are double-stranded).
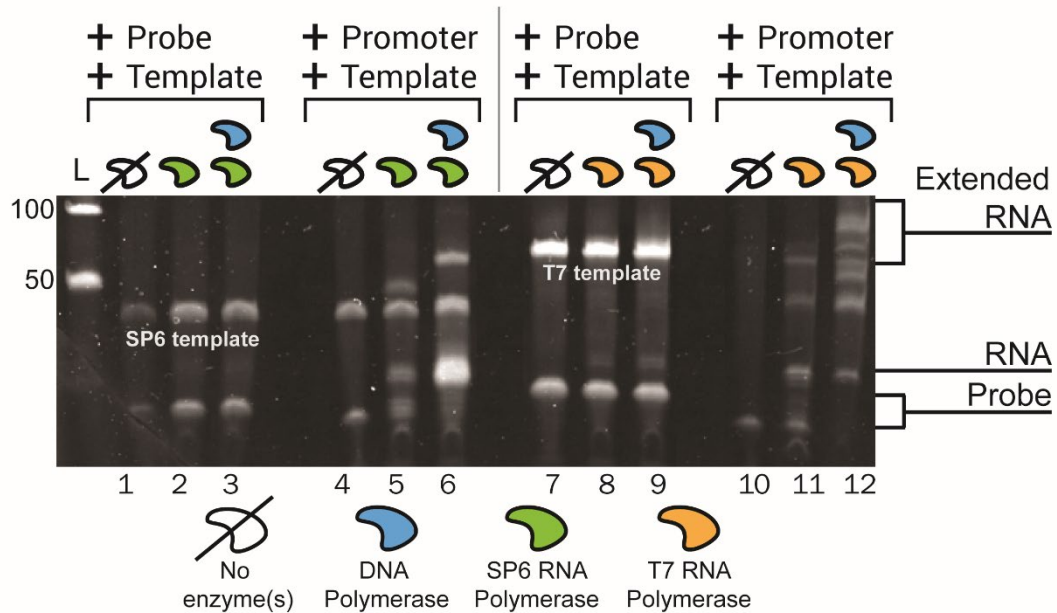
Figure 5.9. Assessing the activity of SP6 and T7 RNA polymerases with single-stranded, partial duplex, or full duplex promoters. Lanes 1-3 and 7-9 evaluate nonspecific transcription of the RNA polymerase alone or in tandem with a DNA polymerase with a single-stranded promoter. Lanes 4-6 and 10-12 evaluate specific transcription with partial (lanes 5 and 11) and full duplex (lanes 6 and 12) promoters. SP6 shows more specific and robust activity in comparison to T7. All probe-template and promoter-template duplexes were prehybridized before addition into the reaction, as outlined in the methods section, at 2 µM stock concentrations.

In Figure 5.9, lanes 1 – 3 assess the activity of SP6 against a single-stranded promoter. In instances of only SP6 or both a DNA polymerase and

111

SP6 present, little to no transcription can be observed between the probe and template bands. Lanes 4 – 6 assess the activity of SP6 with either a partial duplex or a full duplex promoter and transcription region. The partial duplex in lane 5 leads to transcription, however the yield is distinctly less than the transcription observed with the full duplex in lane 6. This suggest that once target extension has occurred in TCA, robust transcription should be apparent and enable positive feedback into the reaction. Lanes 7-12 assess the same conditions with T7. Interestingly, for reactions with only probe and template (single-stranded promoter only), transcription is observed only when both DNA and RNA polymerases are present (lane 9), similar to what has been observed previously. The amount of transcription is comparable to the observed band with a partial duplex (lane 11). Because the template used for these T7 experiments is the symmetric template for TCA, a brighter RNA band is not observed in lane 12 for the full duplex, however multiple higher molecular weight products are observed instead. This indicates that the transcripts have fed back into the system and have been extended by the DNA polymerase. From these results, SP6 appears to be a more specific and robust enzyme, when compared to T7, and in turn, may be better suited for TCA.

5.3.1.3.1   Summary of findings

From these preliminary studies, we have found that T7 is a very robust RNA polymerase, capable of transcription of both a double- and single-stranded purposes. Because TCA is dependent on transcription only in the presence of a double-stranded promoter, SP6 was evaluated as a RNA

polymerase candidate that may offer more specificity than T7. SP6 was shown to be more robust in the presence of the double-stranded promoter when compared to T7, and shows no observed transcription with a single-stranded promoter. The table below further summarizes the other results of these preliminary studies.

Table 5.4. Summary of findings investigating RNA polymerases for TCA.

Enzyme	Findings
SP6	Probe and template (single-stranded promoter) • No observed transcription alone or in the presence of DNA polymerase Promoter and template • In the presence of SP6 alone (partial duplex), observe low transcription activity • In the presence of SP6 and DNA polymerase (full duplex), observe high transcription activity
T7	Probe and template (single-stranded promoter) • Observe minimal transcription alone or in the presence of DNA polymerase Promoter and template • In the presence of SP6 alone (partial duplex), observe stronger transcription activity • In the presence of SP6 and DNA polymerase (full duplex), observe higher molecular weight products that would arise from extensions of RNA products, suggesting there is high transcription activity

5.3.2 Assay performance with Klenow and SP6

Now that both Klenow and SP6 polymerases have been selected as the optimal enzymes for TCA, experiments were performed to evaluate the limit of detection and to assess whether further optimizations were required to achieve lower sensitivities. Initial experiments show that across all target concentrations, increasing fluorescence is observed for the three highest

concentrations of 100 nM, 10 nM, and 1 nM (Figure 5.10). However the NTC amplifies similarly to the 1 nM target concentrations, and all lower target concentrations, indicating that the low amount of nonspecific transcription is possibly doing one of two things.
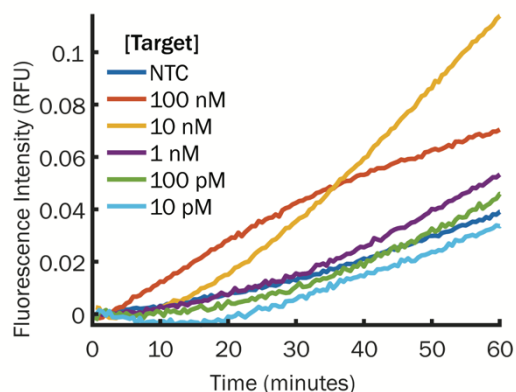
Figure 5.10. Amplification curves for various concentrations of target with Klenow and SP6 polymerases. Given the early amplification in the NTC, the limit of detection with the current iteration of TCA is 10 nM.

The first possibility is that the generated transcript in the NTC simply displaces the probe, but remains hybridized to the template. In such an instance, the amplification curves that are observed would be linear, with trace amounts of transcripts visible in the gels. The second possibility is that the transcripts produced nonspecifically continue to be displaced with constant activity of RNA polymerase, and would in turn lead to exponential amplification. Here, a bright band of RNA transcripts would be observed, comparable to that belonging to a reaction with target, due to the stronger activity of RNA polymerase in the presence of a full duplex promoter and transcription region. These two possibilities are further explored in the next section.

5.3.3 Alternative template designs

As mentioned previously, there are two possibilities that could be contributing to the signal observed in NTC reactions. One instance would lead to linear amplification, and the second would lead to exponential amplification. To determine which of these phenomena is occurring, a second linear template was designed such that the sequence locations of the promoter and the user-designed sequence for probe hybridization were switched. With this template, in the presence of the target, the probe would get displaced immediately, followed by the formation of the promoter and transcription duplex. Transcription would then lead to RNA products feeding back into the system. However, if nonspecific transcription were to occur in NTC reactions, the probe should not be displaced unless the transcripts bind to the 3' end of the template and begin extension.

Figure 5.11A shows the products separated with gel electrophoresis with the second template, assessing the specific versus nonspecific activity in the presence and absence of target, respectively. As noted earlier, should exponential amplification occur, the band intensity of RNA should be equal in comparable between the two reactions. Lanes 1 and 2 do show comparable intensity of RNA transcripts. As a result, alternative strategies were investigated to inhibit this nonspecific activity, without compromising the overall activity of the enzyme.
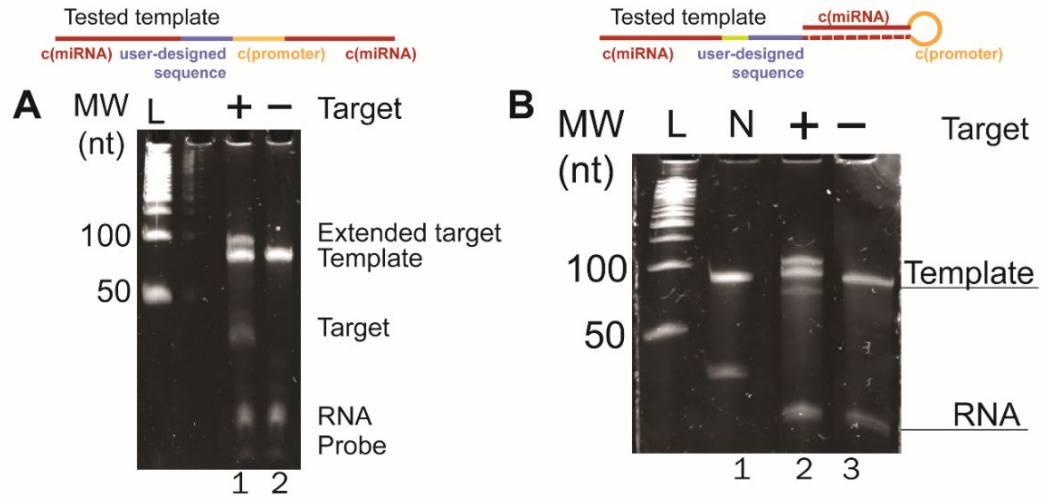
Figure 5.11. Investigation of alternative templates to minimize nonspecific transcription. (A) By switching the promoter and probe hybridization regions, the generated transcripts are indicative of their participation into the assay's positive feedback. (B) Redesign of template involved obscuring the promoter with the loop of a hairpin structure, to obstruct the RNA polymerase's ability of reading and binding onto the promoter sequence. While there is a subtle decrease in transcription observed in NTC reactions (lane 2), it is still comparable to levels observed with target present in the reaction (lane 1). All reactions for these experiments contained 3 U of Klenow and 5 U of SP6, to further minimize the occurrence of nonspecific SP6 activity.

Throughout this work, a linear template has been used to simplify the design in a cost-effective manner. However, given the persistence of T7 and SP6 activity for the various templates and enzymes tested, a concern is that the linear nature of the template facilitates quicker binding of both the DNA and RNA polymerases, especially in instances of low target concentrations or absence of target entirely. We thus hypothesized that if the promoter region is obscured with the introduction of secondary structures within the template, this would decrease the accessibility of the promoter region to the RNA polymerase and in turn decrease the nonspecific RNA polymerase activity. To test this hypothesis, the template was redesigned such that while it was still symmetric to allow transcription to create target analogs, the 5' half of the template would be folded into a hairpin configuration, where the loop portion would contain the

promoter sequence (Figure 5.11B). Reactions with the addition or absence of target showed that a lesser amount of transcription occurred in the NTC (lane 3) as compared to the target-containing reaction (lane 2); however, the transcripts are of sufficient quantity to negatively impact the limit of detection for the assay.

The results from these studies show that templates that are either linear or contain some secondary structure to obscure the single-stranded promoter, RNA polymerase is still able to recognize the promoter sequence and initiate transcription. When assessing what is mechanistically occurring with the hairpin template, it is unclear whether the RNA polymerase reads in the 3' → 5' direction and displaces the hairpin to initiate transcription, or if the loop of the hairpin does not change the interactions between the RNA polymerase and the promoter region of the template. Further studies are required to better evaluate the feasibility of the template for alternative iterations of TCA.

5.3.4 Optimizing buffer conditions

Thus far, the optimizations we have considered towards limiting that amount of nonspecific activity involve enzyme and template design considerations. However, a key component towards any successful amplification reaction are the buffer components. Often, the buffer components of an assay largely promote activity of an enzyme, and for systems that leverage multiple enzymes, these buffer conditions can bias the activity of one over another. As mentioned previously, commercial vendors always note that

RNA polymerases are highly sensitive to monovalent cations, and thus all transcription reactions normally use 10 mM of monovalent cations. However, NASBA, a popular isothermal method developed for the direct detection of mRNA and large RNA targets, leverages T7 to produce transcripts in the presence of 70 mM monovalent cations. Therefore, the last strategy we employed was investigating if monovalent cations can be used to selectively promote the activity of SP6, while concurrently inhibiting the nonspecific activity that has been observed throughout this work.

Traditionally, amplification reactions have used monovalent cations such as sodium and potassium in reaction buffers. Therefore, various amounts of either sodium chloride or potassium chloride were used to investigate the impact of these cations on both the specific and nonspecific activities of SP6 with the presence and absence of target, respectively. Since NASBA generally uses a concentration of 70 mM monovalent cations, this was chosen as the highest assayed concentration.

For reactions with NaCl addition (Figure 5.12A), as the NaCl concentration increases there is an observed decrease in the amount of transcription occurring in the NTCs, indicative of less nonspecific SP6 activity. However, the specific activity of the enzyme is compromised given the reduced band intensities of reactions with target. Reactions with KCl addition (Figure 5.12B) show a similar trend to NaCl, however reactions containing 40 mM KCl and higher reveal a distinct difference in transcription in the presence and absence of target (lanes 7-10). NTC reactions show a decrease in the RNA

band intensity as compared to reactions with target, suggesting that higher KCl concentrations can be leveraged to favor specific activity of the RNA polymerase. However, it is important to note that the reactions with target, namely lanes 7 and 9, have a decreased band intensity compared to the reactions with no supplemented KCl (lane 1). While the KCl allows for transcription selectively with a double-stranded promoter, the activity of the polymerase is overall reduced, and potentially increased assay times may be required.

Figure 5.12. Impact of monovalent salts on specific and nonspecific RNA polymerase activity. (A) Varying amounts of sodium chloride were added to reactions with and without target. Overall there is diminished SP6 activity given the decreased RNA band intensities with increasing sodium content. Additionally there is no distinct difference in the transcription yields when comparing reactions with and without target for each concentration. These experiments used the template tested in Figure 5.11A, where the template is unlabeled and thus stains strongly in the gel. (B) Varying amounts of potassium chloride were added to reactions with and without target. While transcription yields overall decreased with increasing potassium content, with 40 mM and 60 mM there is more intense RNA band in reactions with target compared to those without. This suggest that nonspecific SP6 activity may be inhibited without totally inhibiting its specific activity. The original quenched template was used in these experiments, and consequently the template does not appear strongly in this gel. (C) To recover the specific SP6 activity, reactions were incubated at 42 °C and 37 °C to determine if improved activity could be visualized with real-time fluorescence. While reactions with and without target cannot be differentiated at 37 °C, a concentration-dependent fluorescence can be observed when incubated at 42 °C. All reactions here contain 3 U Klenow and 5 U SP6.

While RNA polymerases maintain strong activity at 37 °C, their optimal temperature is normally at 40 – 42 °C.[239] The experiments that have been presented throughout this work have been incubated at 37 °C to ensure activity of both enzymes. Since Klenow is robust against the higher concentrations of

119

monovalent cations presented, it is critical to also ensure that the specific activity of SP6 is also maintained for robust exponential feedback. To evaluate whether an increased assay temperature would improve fluorescent signals, the labeled probe and quenched template were incubated with and without target in parallel reaction at either 37 °C or 42 °C using the BioRad thermocyler's gradient protocol (Figure 5.12C). Reactions incubated at 37 °C saw minimal signal differences between 10 nM and 1 nM target in the reaction compared to the NTC, however reactions incubated at 42 °C saw more drastic differences that would increase the dynamic range of the assay and potentially lower the previously observed sensitivity and limit of detection.

While the inclusion of monovalent salts can inhibit the overall efficiency of the RNA polymerases, we have shown that raising the operating temperature of the assay helps recover some of the activity. Future work to further discriminate the dynamic range and achieve higher quality sigmoidal amplification curves will involve the addition of BSA and DMSO, two known chemical agents that promote polymerase activities. These studies will first involve optimizing these agents to better characterize their individual and collective impact on target extension and transcription yield. With these additive, we hope that rapid and sensitive quantification can be achieved.

5.4   Conclusion

miRNA detection platforms currently are time-consuming due to the time-consuming two-step process of RT-PCR, and prevent rapid quantification of these targets. To this end, we seek to develop a direct detection method that

enables isothermal exponential amplification that can be further expanded to include multiplex detection. However, before this assay can be implemented for miRNA detection, there are several questions that need to be addressed to better inform design constraints of the assay.

We first investigated the impact of DNA polymerases for this assay. In these studies, we found that DNA polymerases with exonucleases domain negatively impact the assay, where nonspecific degradation of sequences either led to false positives, or the instability of oligonucleotides. Strand-displacing polymerases addressed this issues as they do not have exonuclease domains, however depending on the enzyme, fluorescent signals were not generated as expected despite generating the products that indicate successful amplification. However, with these experiments, we found that Klenow was the strongest candidate for the DNA polymerase in this system.

Second, we looked to optimize the RNA polymerase activity by assessing the transcription yield of SP6 and T7 polymerase. Overall, we have observed nonspecific transcription with a single-stranded promoter with the use of T7, and thus we investigated the performance of SP6 with a single-stranded promoter, and varying degrees of duplex promoters, in comparison of T7. We found that there was no observed transcription in the presence of a single-stranded promoter with both SP6 and a DNA polymerase, however with T7 and a DNA polymerase, we observed low transcription yield. More importantly, we observed robust transcription with SP6 with a double-stranded promoter, when compared to T7. Given the increased yield and observed

specificity of SP6, we found that SP6 was the strongest candidate for the RNA polymerase in this system.

We sought to eliminate the reduced nonspecific transcription activity with various template designs, and introducing monovalent cations into our system. Unfortunately, transcription was observed with the different linear designs and the hairpin template format, however further studies need to be conducted to better understand how SP6 interacts with the template to initiate transcription with a single-stranded promoter. Drawing on NASBA buffer conditions, we investigated the inhibitory impact of monovalent cations to bias the specific activity of SP6 and eliminate the nonspecific activity. While NaCl did not show promise towards biasing this behavior, KCl showed no transcription in the absence of target and a moderate amount of transcription in the presence of target, suggesting that KCl along with other chemical agents may improve the dynamic range of TCA.

Future work of TCA will involve optimization of KCl concentrations, investigating whether polymerase promoters such as DMSO and BSA will need to be integrated into the assay to recover any diminished activity at higher KCl concentrations, and evaluation of the dynamic range, sensitivity and limit of detection of TCA. Once an initial formulation for TCA mastermix has been devised, the amplification of other miRNA targets with varying degrees of secondary structures will need to be validated. We expect that with these miRNA targets, such as mi-R21 and mi-R16, we will observe a decrease in amplification efficiency if toe-hold exchange alone does not facilitate binding

onto the template. In such cases, chemical agents that weaken the stability of secondary structures (i.e. betaine) will be investigated, and we will assess if these chemical agents can be applied universally to all miRNA targets or only those with secondary structures.

The culmination of this work will ultimately lead to a platform suitable for both commercial and research applications that aims to quantify multiple miRNA targets. The work presented here further informs the diagnostic and biochemistry communities about the interactions of nucleic acids alongside DNA and RNA polymerases working in tandem, towards multi-enzyme systems.

Chapter 6. Conclusion

6.1 Overview

This work details the development of technologies and assays to simplify the traditional approaches to sample preparation and nucleic acid amplification for near-patient settings. First, this work aims to invent a novel sample preparation method that moves away from the cumbersome reagent exchange approach and accomplishes the three time consuming tasks of cell lysis, DNA extraction, and DNA purification in a single-step. Second, we address the limitations of PCR (complex instrumentation due to thermocycling) by either leveraging or designing novel isothermal amplification schemes that enable multiplex detection in a single reaction. Simplifying these modules to enable a single-step or single-tube format not only minimizes the technical burden associated with these protocols, but enables a streamlined method towards cheap, rapid, and comprehensive diagnostic tests.

6.2 Chapter 3: Simplifying nucleic acid amplification from whole blood blood with direct PCR on chitosan microparticles

While there is consensus that the laborious nature of sample preparation is a bottleneck towards an integrated device for NAATs, there has been little direction for strategies to approach this challenge. While previous solutions have either miniaturized these steps, or have leveraged capture probes conjugated to the microparticles to enable DNA isolation with standard cell lysis techniques, these methods are often difficult to integrate within a device for near-patient settings. Chapter 3 details the development of a microparticle-

based platform that simultaneously accomplishes cell lysis, DNA extraction, and DNA purification from complex matrices. Because bound genomes are difficult to elute off the chitosan layer, we have leveraged this to enable direct amplification on the solid phase.

6.2.1 Scientific contributions

While the application of chitosan-coated microparticles addresses the challenges of sample-preparation, the underlying aspects of the platform generally advance both research and commercial endeavors.

- A novel DNA extraction method that leverages classic bead-beating techniques that isolates DNA from cells within 10 minutes amenable to a variety of cell suspensions (buffer, cell media, and whole blood).

- A solid phase extraction technique to enable stable, direct amplification on the solid phase. These microparticles provide a robust amplification platform for protocols that require high temperatures of 95 °C.

- An isolation method for a variety of targets that range from small DNA plasmids to large genomes.

- A platform that enables multi-stage PCR reactions, where products from the first reaction can serve as templates for a second PCR reaction downstream.

125

- A streamlined method where sample preparation steps are achieved in 2 manual steps within 10 minutes, where traditional methods require roughly 5 manual steps within 30 minutes.
  - The two manual steps involve first adding the cell suspension to the chitosan-coated microparticles and second, aspirating out the lysate and adding the amplification mastermix.

6.2.2 Limitations and future work

The work presented in this chapter only investigated the extraction of genomic DNA and plasmids that would mimic viral genomes. However it is unclear how efficient this platform would be for smaller nucleic acid targets, such as mRNAs and miRNAs for expression profiles. Our hypothesis assumes that a portion of genomic DNA is embedded within the chitosan matrix, and thus limits the accessibility of the polymerase to replicate these regions. While the embedded portion of DNA only leads to a 3 – 5 Ct delay when compared to a typical solution-based PCR reaction, it is unclear whether this observed Ct delay would translate to smaller nucleic acids. In lieu of PCR, NASBA and EXPAR would be better amplification systems to assess this as they enable direct detection of these sensitive targets.

I have shown that chitosan-coated microparticles can reduce the hands-on steps as well as the time needed to isolate DNA from a complex sample. Since chitosan-coated microparticles offer a simplified approach

towards sample preparation, it would be interesting to assess the efficiency of direct amplification with popular isothermal amplification schemes. Demonstration of efficient amplification with methods such as LAMP or RCA would drive this platform's potential towards a device that is significantly less resource-intensive compared to PCR-based POC NAATs, specifically for resource-limited settings.

Considering future applications of this platform, chitosan-coated microparticles can be integrated within a NAAT by using its magnetic core. Actuating the magnetic core of the particle would enable simple transport into different NAAT modules, and eliminate the need for user intervention for sample transfer. Previously, groups have actuated magnetic particles with an external magnet to demonstrate a simple system for reagent handling.[240,241] A similar approach could be applied to enable sample transfer of the chitosan-coated microparticles from sample preparation reagents to an amplification reaction. The more challenging aspect of the platform would be demonstrating efficient lysis using a bead-beating approach. While using a vortexer provides a simple method of lysis on the bench-top, miniaturizing this effect is not straightforward, and is often why chemical and thermal agents are integrated into POC devices instead. Mixing has been demonstrated within microdevices with magnetic particles, but often these applications are looking to enhance binding events without cell damage.[242–244] It is unclear if these systems could be further developed to enable cell lysis. However if this challenge could be addressed without further complicating the instrumentation,

the development of an automated system would offer a novel approach towards integrated sample preparation and DNA amplification platforms.

6.3   Chapter 4: Demonstration of a quantitative triplex LAMP assay with an improved probe-based readout for the detection of MRSA

As novel assays are leveraging isothermal amplification schemes towards the development of POC NAATs, LAMP is the method at the forefront of these endeavors. Its increased specificity and speed in comparison to PCR offer attractive features for these tests. However, as the iterations of LAMP have improved the robustness and processivity of these enzymes for amplification, there is little direction to inform assay design. Chapter 4 details the development of a triplex assay towards the identification of MRSA genomes, and outlines the factors to consider when designing a multiplex assay for rapid detection. This chapter also re-evaluates a probe-based detection method for assaying multiple genes within a single genome.

6.3.1   Scientific contributions

The work presented in this chapter aimed to inform diagnostic developers of factors to consider when designing LAMP assays. The information presented was used towards the identification of MRSA by testing for the *femB*, *mecA*, and *spa* genes.

- A single-tube triplex platform that specifically detects the presence of three genes with TTPs of less than 30 minutes.

- A clear demonstration of TTP comparison with various strand-displacing polymerases that have been developed specifically for LAMP applications.

- Insight regarding primer number (four versus six) when using the latest iteration of Bst on TTPs, and the resulting sensitivities and limits of detection that can be achieved.

- Evaluation of how DARQ LAMP impacts assays that require low magnesium content for two commonly-used strand-displacing polymerases.

6.3.2 Limitations and future work

Throughout chapter four, we observed inhibition when the QPD was in excess, or when the number of primer sets and QPDs increased in the system. A significant limitation of this method remains that the exact mechanism of the observed inhibition when using FRET probes with LAMP is unclear, especially when evaluating each iteration of a strand-displacing enzymes used in this work. Without this knowledge, devising strategies to overcome inhibition will be challenging. However, traditional means of alleviating delays in amplification with chemical agents can be investigated. Specifically, using chemical agents to either enhance binding of the probe-quencher duplex (TMAC, ammonium sulfate), or enhance the activity of polymerase (DMSO, BSA) can be assessed towards stabilizing the probe-quencher duplex for improved signal gains.

We observed the trend of later amplification with increasing primer sets in the reaction. It is very likely that the high concentration of primers (roughly 9.5 µM) may negatively impact the assay. Further optimizations to determine whether high oligonucleotide concentrations should be assessed to elucidate the impact of these primers towards TTPs.

6.4 Chapter 5: Transcription Cycling Amplification: a novel isothermal amplification scheme for the direct detection of microRNA

Robust solutions towards the direct detection of miRNA are lacking given the instability of RNA targets. To this end, TCA aims to address this need with the use of both DNA and RNA polymerases to create a system with positive feedback and achieve exponential signal generation. In this chapter, several design considerations were outlined when devising a multi-enzyme system, namely the choice of enzymes, template designs, and buffer components.

6.4.1 Scientific contributions

Chapter 5 details the development and evaluations of design constraints towards the development of a novel amplification reactions. While this platform was used towards the detection of a single biomarker, the design of a probe that participates with the template to achieve FRET can be leveraged for multiplex detection. The following observations can inform future development of isothermal amplification that leverages multiple polymerases.

- Insight towards the interactions between DNA polymerase and RNA polymerase towards nonspecific activity.

- Strategies to minimize nonspecific activity of both polymerases.

- Insight regarding using a combination of inhibitors and promoters of polymerase activity to selectively reduce nonspecific transcription, without compromising specific activity.

- A novel amplification scheme that can enables sensitive and multiplex detection.

6.4.2 Limitations and future work

The observed transcription behavior with the single-stranded anti-sense promoter has not been previously discussed with RNA polymerases that were isolated from bacteria. To better understand this behavior, a study between commercial and isolated polymerases can be conducted to ascertain whether the directed evolution of the enzyme leads to this behavior, or whether addressing nonspecific transcription will remain to be a challenge regardless of the enzyme source.

The work presented in this chapter used the miRNA target let7a, which has minimal secondary structures. Most miRNA targets present in a variety of secondary structures to promote their stability. Binding of these types of miRNA to templates should be evaluated across varying secondary structures. Toe-hold exchange can be leveraged if the miRNA have overhangs to leverage,

and chemical agents like betaine can be used to promote the instability of the miRNA; however this may impact the probe and template as well.

6.5   Afterword

I have described several technologies and techniques to address the challenges of integration of sample preparation and DNA amplification for POC NAATS. The contributions outlined here aim to inform considerations towards shifting the molecular diagnostic field's approach from these traditional but cumbersome methods. These advances contribute to the goal of developing a diagnostic for nucleic acid targets that are low-cost, rapid, and comparable in performance to molecular diagnostics performed in the central laboratories.

References

1.   Palamountain, K. M., Baker, J., Cowan, E. P., Essajee, S., Mazzola, L. T., Metzler, M., Schito, M., Stevens, W. S., Young, G. J. & Domingo, G. J. Perspectives on Introduction and Implementation of New Point-of-Care Diagnostic Tests. *J Infect Dis* **205**, S181–S190 (2012).

2.   Trevino, E. A. & Weissfeld, A. S. The Case for Point-of-Care Testing in Infectious-Disease Diagnosis. *Clin Microbiol Newsl* **29**, 177–179 (2007).

3.   Bissonnette, L. & Bergeron, M. G. Diagnosing infections—current and anticipated technologies for point-of-care diagnostics and home-based testing. *Clin Microbiol Infect* **16**, 1044–1053 (2010).

4.   Raja, S., Ching, J., Xi, L., Hughes, S. J., Chang, R., Wong, W., Mcmillan, W., Gooding, W. E., Mccarty, K. S., Chestney, M., Luketich, J. D. & Godfrey, T. E. Technology for Automated, Rapid, and Quantitative PCR or Reverse Transcription-PCR Clinical Testing. *Clin Chem* **51**, 882–890 (2005).

5.   Ulrich, M. P., Christensen, D. R., Coyne, S. R., Craw, P. D., Henchal, E. A., Sakai, S. H., Swenson, D., Tholath, J., Tsai, J., Weir, A. F. & Norwood, D. A. Evaluation of the Cepheid GeneXpertR system for detecting *Bacillus anthracis*. *J Appl Microbiol* **100**, 1011–1016 (2006).

6.   Jaroenram, W., Kiatpathomchai, W. & Flegel, T. W. Rapid and sensitive detection of white spot syndrome virus by loop-mediated isothermal amplification combined with a lateral flow dipstick. *Mol Cell Probes* **23**, 65–70 (2009).

7.   Prompamorn, P., Sithigorngul, P., Rukpratanporn, S., Longyant, S., Sridulyakul, P. & Chaivisuthangkura, P. The development of loop-mediated isothermal amplification combined with lateral flow dipstick for detection of *Vibrio parahaemolyticus*. *Lett Appl Microbiol* **52**, 344–351 (2011).

8.   Roskos, K., Hickerson, A. I., Lu, H.-W., Ferguson, T. M., Shinde, D. N., Klaue, Y. & Niemz, A. Simple system for isothermal DNA amplification coupled to lateral flow detection. *PLoS One* **8**, e69355 (2013).

9.   Giljohann, D. A. & Mirkin, C. A. Drivers of biodiagnostic development. *Nature* **462**, 461–464 (2009).

10.   te Witt, R., van Belkum, A. & van Leeuwen, W. B.. Molecular diagnostics and genotyping of MRSA: an update. *Expert Rev Mol Diagn* **10**, 375–380 (2010).

11.   Dineva, M. A., Mahilum-Tapay, L. & Lee, H. Sample preparation: a challenge in the development of point-of-care nucleic acid-based assays for resource-limited settings. *Analyst* **132**, 1193 (2007).

12.   Niemz, A., Ferguson, T. M. & Boyle, D. S. Point-of-care nucleic acid testing for infectious diseases. *Trends biotechnol* **29**, 240–50 (2011).

13.   Demeke, T. & Jenkins, G. R. Influence of DNA extraction methods, PCR inhibitors and quantification methods on real-time PCR assay of biotechnology-derived traits. *Anal Bioanal Chem* **396**, 1977–1990 (2010).

14.   Berensmeier, S. Magnetic particles for the separation and purification of nucleic acids. *Appl Microbiol Biotechnol* **73**, 495–504 (2006).

15.   McCormick, R. M. A solid-phase extraction procedure for DNA purification. *Anal Biochem* **181**, 66–74 (1989).

16.   Sia, S. K. *et al.* Microfluidics and point-of-care testing. *Lab Chip* **8**, 1982 (2008).

17.   Sorger, P. K. Microfluidics closes in on point-of-care assays. *Nature Biotechnol* **26**, 1345–1346 (2008).

18.   Linder, V. Microfluidics at the crossroad with point-of-care diagnostics. *Analyst* **132**, 1186 (2007).

19.   Mahalanabis, M., Al-Muayad, H., Dominika Kulinski, M., Altman, D. & Klapperich, C. M. Cell lysis and DNA extraction of gram-positive and gram-negative bacteria from whole blood in a disposable microfluidic chip. *Lab Chip* **9**, 2811–2817 (2009).

20.   Carlo, D. D., Jeong, K.-H. & Lee, L. P. Reagentless mechanical cell lysis by nanoscale barbs in microchannels for sample preparation. *Lab Chip* **3**, 287–291 (2003).

21.   Kido, H., Micic, M., Smith, D., Zoval, J., Norton, J. & Madou, M. A novel, compact disk-like centrifugal microfluidics system for cell lysis and sample homogenization. *Colloids Surf B Biointerfaces* **58**, 44–51 (2007).

22.   Yun, S.-S., Yoon, S. Y., Song, M.-K., Im, S.-H., Kim, S., Lee, J.-H. & Yang, S. Handheld mechanical cell lysis chip with ultra-sharp silicon nano-blade arrays for rapid intracellular protein extraction. *Lab Chip* **10**, 1442–1446 (2010).

23.   Privorotskaya, N., Liu, Y.-S., Lee, J., Zeng, H., Carlisle, J. A., Radadia, A., Millet, L., Bashir, R. & King, W. P. Rapid thermal lysis of cells using silicon–diamond microcantilever heaters. *Lab Chip* **10**, 1135–1141 (2010).

24.   Cheong, K. H., Yi, D. K., Lee, J.-G., Park, J.-M., Kim, M. J., Edel, J. B. & Ko, C. Gold nanoparticles for one step DNA extraction and real-time PCR of pathogens in a single chamber. *Lab Chip* **8**, 810–813 (2008).

25.   Lee, C.-Y., Lee, G.-B., Lin, J.-L., Huang, F.-C. & Liao, C.-S. Integrated microfluidic systems for cell lysis, mixing/pumping and DNA amplification. *J Micromech Microeng* **15**, 1215–1223 (2005).

26.   Baek, S., Min, J. & Park, J.-H. Wireless induction heating in a microfluidic device for cell lysis. *Lab Chip* **10**, 909–917 (2010).

27.   Sethu, P., Anahtar, M., Moldawer, L. L., Tompkins, R. G. & Toner, M. Continuous Flow Microfluidic Device for Rapid Erythrocyte Lysis. *Anal Chem* **76**, 6247–6253 (2004).

28.   Irimia, D., Tompkins, R. G. & Toner, M. Single-Cell Chemical Lysis in Picoliter-Scale Closed Volumes Using a Microfabricated Device. *Anal Chem* **76**, 6137–6143 (2004).

29.   Santillo, M. F., Heien, M. L. & Ewing, A. G. Temporal analysis of protozoan lysis in a microfluidic device. *Lab Chip* **9**, 2796–2802 (2009).

30.   Yeates, C., Gillings, M. R., Davison, A. D., Altavilla, N. & Veal, D. A. Methods for microbial DNA extraction from soil for PCR amplification. *Biol Proced Online* **1**, (1998).

31.   Legendre, L. A., Bienvenue, J. M., Roper, M. G., Ferrance, J. P. & Landers, J. P. A Simple, Valveless Microfluidic Sample Preparation Device for Extraction and Amplification of DNA from Nanoliter-Volume Samples. *Anal Chem* **78**, 1444-1451 (2006).

32.   Reedy, C. R., Price, C. W., Sniegowski, J., Ferrance, J. P., Begley, M. & Landers, J. P. Solid phase extraction of DNA from biological samples in a post-based, high surface area poly(methyl methacrylate) (PMMA) microdevice. *Lab Chip* **11**, 1603–11 (2011).

33.   Tian, H., Hühmer, A. F. R. & Landers, J. P. Evaluation of Silica Resins for Direct and Efficient Extraction of DNA from Complex Biological Matrices in a Miniaturized Format. *Anal Biochem* **283**, 175–191 (2000).

34.   Nakagawa, T., Hashimoto, R., Maruyama, K., Tanaka, T., Takeyama, H. & Matsunaga, T. Capture and release of DNA using aminosilane-modified bacterial magnetic particles for automated detection system of single nucleotide polymorphisms. *Biotechnol Bioeng* **94**, 862–868 (2006).

35.   Deggerdal, A. & Larsen, F. Rapid Isolation of PCR-Ready DNA from Blood, Bone Marrow and Cultured Cells, Based on Paramagnetic Beads. *BioTechniques* **22**, 554–557 (1997).

36.   Hu, J., Wang, S., Wang, L., Li, F., Pingguan-Murphy, B., Lu, T. J. & Xu, F. Advances in paper-based point-of-care diagnostics. *Biosens Bioelectron* **54**, 585–597 (2014).

37.   Lisowski, P. & Zarzycki, P. K. Microfluidic Paper-Based Analytical Devices (μPADs) and Micro Total Analysis Systems (μTAS): Development, Applications and Future Trends. *Chromatographia* **76**, 1201–1214 (2013).

38.   Tang, R. H., Yang, H., Choi, J. R., Gong, Y., Feng, S. S., Pingguan-Murphy, B., Huang, Q. S., Shi, J. L., Mei, Q. B. & Xu, F. Advances in paper-based sample pretreatment for point-of-care testing. *Crit Rev Biotechnol* **37**, 411–428 (2017).

39.   Rodriguez, N. M., Wong, W. S., Liu, L., Dewar, R. & Klapperich, C. M. A fully integrated paperfluidic molecular diagnostic chip for the extraction, amplification, and detection of nucleic acids from clinical samples. *Lab Chip* **16**, 753–763 (2016).

40.   Linnes, J. C. *et al.* Paper-based molecular diagnostic for *Chlamydia trachomatis*. *RSC Adv.* **4**, 42245–42251 (2014).

41.   Byrnes, S. A., Bishop, J. D., Lafleur, L., Buser, J. R., Lutz, B. & Yager, P. One-step purification and concentration of DNA in porous membranes for point-of-care applications. *Lab Chip* **15**, 2647–2659 (2015).

42.   Agirre, M., Zarate, J., Ojeda, E., Puras, G., Desbrieres, J. & Pedraz, J. Low Molecular Weight Chitosan (LMWC)-based Polyplexes for pDNA Delivery: From Bench to Bedside. *Polymers* **6**, 1727–1755 (2014).

43.   Buschmann, M. D., Merzouki, A., Lavertu, M., Thibault, M., Jean, M. & Darras, V. Chitosans for delivery of nucleic acids. *Adv Drug Deliv Rev* **65**, 1234–1270 (2013).

44.   Huang, M., Fong, C.-W., Khor, E. & Lim, L.-Y. Transfection efficiency of chitosan vectors: Effect of polymer molecular weight and degree of deacetylation. *J Control Release* **106**, 391–406 (2005).

45.   Domard, A. pH and c.d. measurements on a fully deacetylated chitosan: application to CuII—polymer interactions. *Int J Biol Macromol* **9**, 98–104 (1987).

46.   Cao, W., Easley, C. J., Ferrance, J. P. & Landers, J. P. Chitosan as a Polymer for pH-Induced DNA Capture in a Totally Aqueous System. *Anal Chem* **78**, 7222-7228 (2006).

47.   Kendall, E. L., Wienhold, E. & DeVoe, D. L. A chitosan coated monolith for nucleic acid capture in a thermoplastic microfluidic chip. *Biomicrofluidics* **8**, 044109 (2014).

48.   Pandit, K. R., Nanayakkara, I. A., Cao, W., Raghavan, S. R. & White, I. M. Capture and Direct Amplification of DNA on Chitosan Microparticles in a Single PCR-Optimal Solution. *Anal Chem* **87**, 11022–11029 (2015).

49.   Kricka, L. J. Nucleic Acid Detection Technologies — Labels, Strategies, and Formats. *Clin Chem* 6 (1999).

50.   Southern, E. M. Detection of Specific Sequences Among DNA Fragments Separated by Gel Electrophoresis. *J Mol Biol* **98**, 503–517 (1975).

51.   Kafatos, F. C., Jones, C. W. & Efstratiadis, A. Determination of nucleic acid sequence homologies and relative concentrations by a dot hybridization procedure. *Nucleic Acids Res* **7**, 1541–1552 (1979).

52.   Ehrenreich, A. DNA microarray technology for the microbiologist: an overview. *Appl Microbiol Biotechnol* **73**, 255–273 (2006).

53.   Trayhurn, P. Northern blotting. *Proc Nut Soc* **55**, 583–589 (1996).

54.   Uhl, G. R. In situ hybridization: Quantitation using radiolabeled hybridization probes. in *Methods in Enzymology* **168**, 741–752 (Academic Press, 1989).

55.   Hauber, R. & Geiger, R. A sensitive, bioluminescent-enhanced detection method for DNA dot-hybridization. *Nucleic Acids Res* **16**, 1213 (1988).

56.   Leong, M. M., Milstein, C. & Pannell, R. Luminescent detection method for immunodot, Western, and Southern blots. *J Histochem Cytochem* **34**, 1645–1650 (1986).

57.   Musiani, M., Pasini, P., Zerbini, M., Roda, A., Gentilomi, G., Gallinella, G., Venturoli, S. & Manaresi, E. Chemiluminescence: a sensitive detection system in in situ hybridization. *Histol Histopathol* **13**, 243–248 (1998).

58.   Burg, J. L., Cahill, P. B., Kutter, M., Stefano, J. E. & Mahan, D. E. Real-Time Fluorescence Detection of RNA Amplified by Qβ Replicase. *Anal Biochem* **230**, 263–272 (1995).

59.   Nederlof, P. M., Robinson, D., Abuknesha, R., Wiegant, J., Hopman, A. H. N., Tanke, H. J. & Raap, A. K. Three-color fluorescence in situ hybridization for the simultaneous detection of multiple nucleic acid sequences. *Cytometry* **10**, 20–27 (1989).

60.   Saiki, R. K., Scharf, S., Faloona, F., Mullis, K. B., Horn, G. T., Erlich, H. A. & Arnheim, N. Enzymatic amplification of beta-globin genomic sequences and restriction site analysis for diagnosis of sickle cell anemia. *Science* **230**, 1350–1354 (1985).

61.   Saiki, R. K., Gelfand, D. H., Stoffel, S., Scharf, S., Mullis, K. B. & Erlich, H. A. Primer-Directed Enzymatic Amplification of DNA with a Thermostable DNA Polymerase. *Science* **239**, 487-491 (1988).

62.   Sorenson, G. D., Pribish, D. M., Valone, F. H., Memoli, V. A., Bzik, D. J. & Yao, S. L. Soluble normal and mutated DNA sequences from single-copy genes in human blood. *Cancer Epidemiol Biomarkers Prev* **3**, 67–71 (1994).

63.   Patterson, B. K., Till, M., Otto, P., Goolsby, C., Furtado, M. R., McBride, L. J. & Wolinsky, S. M. Detection of HIV-1 DNA and messenger RNA in individual cells. *Science* **260**, 976 (1993).

64.   Baltimore, D. Viral RNA-dependent DNA Polymerase: RNA-dependent DNA Polymerase in Virions of RNA Tumour Viruses. *Nature* **226**, 1209 (1970).

65.   Temin, H. M. & Mizutani, S. Viral RNA-dependent DNA Polymerase: RNA-dependent DNA Polymerase in Virions of Rous Sarcoma Virus. *Nature* **226**, 1211 (1970).

66.   El-Hefnawy, T., Raja, S., Kelly, L., Bigbee, W. L., Kirkwood, J. M., Luketich, J. D. & Godfrey, T. E. Characterization of Amplifiable, Circulating RNA in Plasma and Its Potential as a Tool for Cancer Diagnostics. *Clin Chem* **50**, 564–573 (2004).

67.   Kopreski, M. S., Benko, F. A. & Gocke, C. D. Circulating RNA as a Tumor Marker: Detection of 5T4 mRNA in Breast and Lung Cancer Patient Serum. *Ann N Y Acad Sci* **945**, 172–178 (2006).

68.   Poon, L. L. M., Leung, T. N., Lau, T. K. & Lo, Y. M. D. Presence of Fetal RNA in Maternal Plasma. *Clin Chem* **46**, 1832–1834 (2000).

69.   Bellau-Pujol, S., Vabret, A., Legrand, L., Dina, J., Gouarin, S., Petitjean-Lecherbonnier, J., Pozzetto, B., Ginevra, C. & Freymuth, F. Development of three multiplex RT-PCR assays for the detection of 12 respiratory RNA viruses. *J Virol Methods* **126**, 53–63 (2005).

70.   Bertolini, E., Olmos, A., Martínez, M. C., Gorris, M. T. & Cambra, M. Single-step multiplex RT-PCR for simultaneous and colourimetric detection of six RNA viruses in olive trees. *J Virol Methods* **96**, 33–41 (2001).

71.   Lanford, R. E., Sureau, C., Jacob, J. R., White, R. & Fuerst, T. R. Demonstration of in Vitro Infection of Chimpanzee Hepatocytes with Hepatitis C Virus Using Strand-Specific RT/PCR. *Virology* **202**, 606–614 (1994).

72.   Mitchell, P. S. *et al.* Circulating microRNAs as stable blood-based markers for cancer detection. *Proc Natl Acad Sci USA* **105**, 10513–10518 (2008).

73.   Chen, C., Ridzon, D. A., Broomer, A. J., Zhou, Z., Lee, D. H., Nguyen, J. T., Barbisin, M., Xu, N. L., Mahuvakar, V. R., Andersen, M. R., Lao, K. Q., Livak, K. J. & Guegler, K. J. Real-time quantification of microRNAs by stem–loop RT–PCR. *Nucleic Acids Res* **33**, e179 (2005).

74.   Lao, K., Xu, N. L., Yeung, V., Chen, C., Livak, K. J. & Straus, N. A. Multiplexing RT-PCR for the detection of multiple miRNA species in small samples. *Biochem Biophys Res Comm* **343**, 85–89 (2006).

75.   Peters, I. R., Helps, C. R., Hall, E. J. & Day, M. J. Real-time RT-PCR: considerations for efficient and sensitive assay design. *J Immunol Methods* **286**, 203–217 (2004).

76.   Higuchi, R., Fockler, C., Dollinger, G. & Watson, R. Kinetic PCR Analysis: Real-time Monitoring of DNA Amplification Reactions. *Nat Biotechnol* **11**, 1026–1030 (1993).

77.   Wittwer, C. T., Herrmann, M. G., Moss, A. A. & Rasmussen, R. P. Continuous Fluorescence Monitoring of Rapid Cycle DNA Amplification. *BioTechniques* **54**, (2013).

78.   Wittwer, C. T., Ririe, K. M., Andrew, R. V., David, D. A., Gundry, R. A. & Balis, U. J. The LightCyclerTM: A Microvolume Multisample Fluorimeter with Rapid Temperature Control. *BioTechniques* **22**, 176–181 (1997).

79.   Eischeid, A. C. SYTO dyes and EvaGreen outperform SYBR Green in real-time PCR. *BMC Res Notes* **4**, 263 (2011).

80.   Gudnason, H., Dufva, M., Bang, D. D. & Wolff, A. Comparison of multiple DNA dyes for real-time PCR: effects of dye concentration and sequence composition on DNA amplification and melting temperature. *Nucleic Acids Res* **35**, e127 (2007).

81.   Heid, C. A., Stevens, J., Livak, K. J. & Williams, P. M. Real time quantitative PCR. *Genome Res.* **6**, 986–994 (1996).

82.   Lo, Y. M. D., Tein, M. S. C., Lau, T. K., Haines, C. J., Leung, T. N., Poon, P. M. K., Wainscoat, J. S., Johnson, P. J., Chang, A. M. Z. & Hjelm, N. M.

Quantitative Analysis of Fetal DNA in Maternal Plasma and Serum: Implications for Noninvasive Prenatal Diagnosis. *Am J Hum Genet* **62**, 768–775 (1998).

83.   van Vuren, P. J., Grobbelaar, A., Storm, N., Conteh, O., Konneh, K., Kamara, A., Sanne, I. & Paweska, J. T. Comparative Evaluation of the Diagnostic Performance of the Prototype Cepheid GeneXpert Ebola Assay. *J Clin Microbiol* **54**, 359–367 (2016).

84.   Dheda, K., Ruhwald, M., Theron, G., Peter, J. & Yam, W. C. Point-of-care diagnosis of tuberculosis: Past, present and future. *Respirol* **18**, 217–232 (2013).

85.   Paul, N., Shum, J. & Le, T. Hot Start PCR. in *RT-PCR Protocols: Second Edition* (ed. King, N.) 301–318 (Humana Press, 2010).

86.   Dang, C. & Jayasena, S. D. Oligonucleotide Inhibitors of TaqDNA Polymerase Facilitate Detection of Low Copy Number Targets by PCR. *J Mol Biol* **264**, 268–278 (1996).

87.   Mizuguchi, H., Nakatsuji, M., Fujiwara, S., Takagi, M. & Imanaka, T. Characterization and Application to Hot Start PCR of Neutralizing Monoclonal Antibodies against KOD DNA Polymerase. *J Biochem* **126**, 762–768 (1999).

88.   Tanzer, L. R., Hu, Y., Cripe, L. & Moore, R. E. A Hot-Start Reverse Transcription–Polymerase Chain Reaction Protocol That Initiates Multiple Analyses Simultaneously. *Anal Biochem* **273**, 307–310 (1999).

89.   Akane, A., Matsubara, K., Nakamura, H., Takahashi, S. & Kimura, K. Identification of the Heme Compound Copurified with Deoxyribonucleic Acid (DNA) from Bloodstains, a Major Inhibitor of Polymerase Chain Reaction (PCR) Amplification. *J Forensic Sci* **39**, 362–372 (1994).

90.   Wilson, I. G. Inhibition and Facilitation of Nucleic Acid Amplification. *Appl Environ Microbiol* **63**, 11 (1997).

91.   Dirks, R. M. & Pierce, N. A. Triggered amplification by hybridization chain reaction. *Proc Natl Acad Sci USA* **101**, 15275–15278 (2004).

92.   Xuan, F. & Hsing, I.-M. Triggering Hairpin-Free Chain-Branching Growth of Fluorescent DNA Dendrimers for Nonlinear Hybridization Chain Reaction. *J Am Chem Soc* **136**, 9810–9813 (2014).

93.   Bi, S., Chen, M., Jia, X., Dong, Y. & Wang, Z. Hyperbranched Hybridization Chain Reaction for Triggered Signal Amplification and Concatenated Logic Circuits. *Angew Chem Int Ed Engl* **54**, 8144–8148 (2015).

94.   Bi, S., Yue, S. & Zhang, S. Hybridization chain reaction: a versatile molecular tool for biosensing, bioimaging, and biomedicine. *Chem Soc Rev* **46**, 4281–4298 (2017).

95.   Wang, X., Lau, C., Kai, M. & Lu, J. Hybridization chain reaction-based instantaneous derivatization technology for chemiluminescence detection of specific DNA sequences. *Analyst* **138**, 2691–2697 (2013).

96.   Niu, S., Jiang, Y. & Zhang, S. Fluorescence detection for DNA using hybridization chain reaction with enzyme-amplification. *Chem Comm* **46**, 3089–3091 (2010).

97.   Notomi, T., Okayama, H., Masubuchi, H., Yonekawa, T., Watanabe, K., Amino, N. & Hase, T. Loop-mediated isothermal amplification of DNA. *Nucleic Acids Res* **28**, e63–e63 (2000).

98.   Mahony, J., Chong, S., Bulir, D., Ruyter, A., Mwawasi, K. & Waltho, D. Multiplex loop-mediated isothermal amplification (M-LAMP) assay for the detection of influenza A/H1, A/H3 and influenza B can provide a specimen-to-result diagnosis in 40min with single genome copy sensitivity. *J Clin Virol* **58**, 127–131 (2013).

99.   Martin, A., Grant, K. B., Stressmann, F., Ghigo, J.-M., Marchal, D. & Limoges, B. Ultimate Single-Copy DNA Detection Using Real-Time Electrochemical LAMP. *ACS Sens* **1**, 904–912 (2016).

100.   Gong, P., Zhang, T., Chen, F., Wang, L., Jin, S. & Bai, X. Advances in loop-mediated isothermal amplification: integrated with several point-of-care diagnostic methods. *Anal Methods* **6**, 7585–7589 (2014).

101.   Liu, C., Geva, E., Mauk, M., Qiu, X., Abrams, W. R., Malamud, D., Curtis, K., Owen, S. M. & Bau, H. H. An isothermal amplification reactor with an integrated isolation membrane for point-of-care detection of infectious diseases. *Analyst* **136**, 2069 (2011).

102.   LaBarre, P., Gerlach, J., Wilmoth, J., Beddoe, A., Singleton, J. & Weigl, B. Non-instrumented nucleic acid amplification (NINA): Instrument-free molecular malaria diagnostics for low-resource settings. in *2010 Annual International Conference of the IEEE Engineering in Medicine and Biology* 1097–1099 (2010).

103.   LaBarre, P., Hawkins, K. R., Gerlach, J., Wilmoth, J., Beddoe, A., Singleton, J., Boyle, D. & Weigl, B. A Simple, Inexpensive Device for Nucleic Acid Amplification without Electricity—Toward Instrument-Free Molecular Diagnostics in Low-Resource Settings. *PLoS One* **6**, e19738 (2011).

104.   Liu, C., G. Mauk, M., Hart, R., Qiu, X. & H. Bau, H. A self-heating cartridge for molecular diagnostics. *Lab Chip* **11**, 2686–2692 (2011).

105.   Li, J. & Macdonald, J. Advances in isothermal amplification: novel strategies inspired by biological processes. *Biosens Bioelectron* **64**, 196–211 (2015).

106.   Ball, C. S., Light, Y. K., Koh, C.-Y., Wheeler, S. S., Coffey, L. L. & Meagher, R. J. Quenching of Unincorporated Amplification Signal Reporters in Reverse-Transcription Loop-Mediated Isothermal Amplification Enabling Bright, Single-Step, Closed-Tube, and Multiplexed Detection of RNA Viruses. *Anal Chem* **88**, 3562–3568 (2016).

107.   Ness, J. V., Ness, L. K. V. & Galas, D. J. Isothermal reactions for the amplification of oligonucleotides. *Proc Natl Acad Sci USA* **100**, 4504–4509 (2003).

108.   Jia, H., Li, Z., Liu, C. & Cheng, Y. Ultrasensitive Detection of microRNAs by Exponential Isothermal Amplification. *Angew Chem Int Ed Engl* **49**, 5498–5501 (2010).

109.   Zhang, Y. & Zhang, C. Sensitive Detection of microRNA with Isothermal Amplification and a Single-Quantum-Dot-Based Nanosensor. *Anal Chem* **84**, 224–231 (2012).

110.   Ye, L.-P., Hu, J., Liang, L. & Zhang, C. Surface-enhanced Raman spectroscopy for simultaneous sensitive detection of multiple microRNAs in lung cancer cells. *Chem Comm* **50**, 11883–11886 (2014).

111.   Reid, M. S., Le, X. C. & Zhang, H. Exponential Isothermal Amplification of Nucleic Acids and Assays for Proteins, Cells, Small Molecules, and Enzyme Activities: An EXPAR Example. *Angew Chem Int Ed Engl* **57**, 11856–11866 (2018).

112.   Hanaki, K., Odawara, T., Nakajima, N., Shimizu, Y. K., Nozaki, C., Mizuno, K., Muramatsu, T., Kuchino, Y. & Yoshikura, H. Two Different Reactions Involved in the Primer/Template-Independent Polymerization of dATP and dTTP byTaqDNA Polymerase. *Biochem Biophys Res Comm* **244**, 210–219 (1998).

113.   Hanaki, K., Odawara, T., Muramatsu, T., Kuchino, Y., Masuda, M., Yamamoto, K., Nozaki, C., Mizuno, K. & Yoshikura, H. Primer/Template-Independent Synthesis of Poly d(A-T) by Taq Polymerase. *Biochem Biophy Res Comm* **238**, 113–118 (1997).

114.   Zyrina, N. V., Zheleznaya, L. A., Dvoretsky, E. V., Vasiliev, V. D., Chernov, A. & Matvienko, N. I. N.BspD6I DNA nickase strongly stimulates

template-independent synthesis of non-palindromic repetitive DNA by Bst DNA polymerase. *Biol Chem* **388**, (2007).

115. Tan, E., Erwin, B., Dames, S., Ferguson, T., Buechel, M., Irvine, B., Voelkerding, K. & Niemz, A. Specific versus Nonspecific Isothermal DNA Amplification through Thermophilic Polymerase and Nicking Enzyme Activities. *Biochemistry* **47**, 9987–9999 (2008).

116. Qian, J., Ferguson, T. M., Shinde, D. N., Ramírez-Borrero, A. J., Hintze, A., Adami, C. & Niemz, A. Sequence dependence of isothermal DNA amplification via EXPAR. *Nucleic Acids Res* **40**, e87–e87 (2012).

117. Mok, E., Wee, E., Wang, Y. & Trau, M. Comprehensive evaluation of molecular enhancers of the isothermal exponential amplification reaction. *Sci Rep* **6**, 37837 (2016).

118. Nilsson, M., Malmgren, H., Samiotaki, M., Kwiatkowski, M., Chowdhary, B. P. & Landegren, U. Padlock Probes: Circularizing Oligonucleotides for Localized DNA Detection. *Science* **265**, 2085–2088 (1994).

119. Fire, A. & Xu, S. Q. Rolling replication of short DNA circles. *Proc Natl Acad Sci USA* **92**, 4641–4645 (1995).

120. Jonstrup, S. P., Koch, J. & Kjems, J. A microRNA detection system based on padlock probes and rolling circle amplification. *RNA* **12**, 1747–1752 (2006).

121. Cheng, Y., Zhang, X., Li, Z., Jiao, X., Wang, Y. & Zhang, Y. Highly Sensitive Determination of microRNA Using Target-Primed and Branched Rolling-Circle Amplification. *Angew Chem Int Ed Engl* **121**, 3318–3322 (2009).

122. Ali, M. M., Li, F., Zhang, Z., Zhang, K., Kang, D.-K., A. Ankrum, J., Chris Le, X. & Zhao, W. Rolling circle amplification: a versatile tool for chemical biology, materials science and medicine. *Chem Soc Rev* **43**, 3324–3341 (2014).

123. Deng, R., Tang, L., Tian, Q., Wang, Y., Lin, L. & Li, J. Toehold-initiated Rolling Circle Amplification for Visualizing Individual MicroRNAs In Situ in Single Cells. *Angew Chem Int Ed Engl* **53**, 2389–2393 (2014).

124. Zhou, Y., Huang, Q., Gao, J., Lu, J., Shen, X. & Fan, C. A dumbbell probe-mediated rolling circle amplification strategy for highly sensitive microRNA detection. *Nucleic Acids Res* **38**, e156 (2010).

125. Compton, J. Nucleic acid sequence-based amplification. *Nature* **350**, 91 (1991).

126.   Leone, G., van Gemen, B., Schoen, C. D., van Schijndel, H. & Kramer, F. R. Molecular beacon probes combined with amplification by NASBA enable homogeneous, real-time detection of RNA. *Nucleic Acids Res* **26**, 2150–2155 (1998).

127.   Van Gemen, B., Kievits, T., Schukkink, R., Van Strijp, D., Malek, L. T., Sooknanan, R., Huisman, H. G. & Lens, P. Quantification of HIV-1 RNA in plasma using NASBA™ during HIV-1 primary infection. *J Virol Methods* **43**, 177–187 (1993).

128.   van Gemen, B., van Beuningen, R., Nabbe, A., van Strijp, D., Jurriaans, S., Lens, P. & Kievits, T. A one-tube quantitative HIV-1 RNA NASBA nucleic acid amplification assay using electrochemiluminescent (ECL) labelled probes. *J Virol Methods* **49**, 157–167 (1994).

129.   Hollingsworth, R. C., Sillekens, P., van Deursen, P., Neal, K. R. & Irving, W. L. Serum HCV RNA levels assessed by quantitative NASBA®: stability of viral load over time, and lack of correlation with liver disease. *J Hepatol* **25**, 301–306 (1996).

130.   Damen, M., Sillekens, P., Sjerps, M., Melsert, R., Frantzen, I., Reesink, H. W., Lelie, P. N. & Cuypers, H. T. M. Stability of hepatitis C virus RNA during specimen handling and storage prior to NASBA amplification. *J Virol Methods* **72**, 175–184 (1998).

131.   Gemen, B. V., Kievits, T. & Romano, J. Transcription based nucleic acid amplification methods like NASBA and 3SR applied to viral diagnosis. *Rev Med Virol* **5**, 205–211 (1995).

132.   Gabrielle, M. E., van der, V., Schukkink, R. A. F., van Gemen, B., Schepers, y & Klatser, y. Nucleic acid sequence-based amplification (NASBA) for the identification of mycobacteria. *Microbiology* **139**, 2423–2429 (1993).

133.   Blais, B. W., Turner, G., Sooknanan, R., Malek, L. T. & Phillippe, L. M. A nucleic acid sequence-based amplification (NASBA) system for *Listeria monocytogenes* and simple method for detection of amplimers. *Biotechnol Tech* **10**, 189–194 (1996).

134.   Morré, S. A., Sillekens, P., Jacobs, M. V., Aarle, P. van, Blok, S. de, Gemen, B. van, Walboomers, J. M., Meijer, C. J. & Brule, A. J. van den. RNA amplification by nucleic acid sequence-based amplification with an internal standard enables reliable detection of *Chlamydia trachomatis* in cervical scrapings and urine samples. *J Clin Microbiol* **34**, 3108–3114 (1996).

135.   Deiman, B., van Aarle, P. & Sillekens, P. Characteristics and applications of nucleic acid sequence-based amplification (NASBA). *Mol Biotechnol* **20**, 163–179 (2002).

136. van Zyl, G. U., Korsman, S. N. J., Maree, L. & Preiser, W. NucliSens EasyQ® HIV-1 V1.2 system: Detection of human plasma-derived background signal. *J Virol Methods* **165**, 318–319 (2010).

137. Jeantet, D., Schwarzmann, F., Tromp, J., Melchers, W. J. G., van der Wurff, A. A. M., Oosterlaken, T., Jacobs, M. & Troesch, A. NucliSENS® EasyQ® HPV v1 test – Testing for oncogenic activity of human papillomaviruses. *J Clin Virol* **45**, S29–S37 (2009).

138. Muenchhoff, M., Madurai, S., Hempenstall, A. J., Adland, E., Carlqvist, A., Moonsamy, A., Jaggernath, M., Mlotshwa, B., Siboto, E., Ndung'u, T. & Goulder, P. J. R. Evaluation of the NucliSens EasyQ v2.0 Assay in Comparison with the Roche Amplicor v1.5 and the Roche CAP/CTM HIV-1 Test v2.0 in Quantification of C-Clade HIV-1 in Plasma. *PLoS One* **9**, e103983 (2014).

139. Craw, P. & Balachandran, W. Isothermal nucleic acid amplification technologies for point-of-care diagnostics: a critical review. *Lab Chip* **12**, 2469–2486 (2012).

140. Mugasa, C. M., Adams, E. R., Boer, K. R., Dyserinck, H. C., Büscher, P., Schallig, H. D. H. F. & Leeflang, M. M. G. Diagnostic Accuracy of Molecular Amplification Tests for Human African Trypanosomiasis—Systematic Review. *PLoS Negl Trop Dis* **6**, e1438 (2012).

141. Morabito, K., Wiske, C. & Tripathi, A. Engineering Insights for Multiplexed Real-Time Nucleic Acid Sequence-Based Amplification (NASBA): Implications for Design of Point-of-Care Diagnostics. *Mol Diagn Ther* **17**, 185–192 (2013).

142. Northrup, M. A., Ching, M. T., White, R. M. & Watson, R. T. DNA amplification with a microfabricated reaction chamber. in *Technical Digest of 7th Intl. Conf. on Solid-State Sensors and Actuators* 924–926 (1993).

143. Wilding, P., Shoffner, M. A. & Kricka, L. J. PCR in a silicon microstructure. *Clin Chem* **40**, 1815–1818 (1994).

144. Auroux, P.-A., Koc, Y., deMello, A., Manz, A. & Day, P. J. R. Miniaturised nucleic acid analysis. *Lab Chip* **4**, 534–546 (2004).

145. Zhang, Y. & Ozdemir, P. Microfluidic DNA amplification—A review. *Anal Chim Acta* **638**, 115–125 (2009).

146. Asiello, P. J. & Baeumner, A. J. Miniaturized isothermal nucleic acid amplification, a review. *Lab Chip* **11**, 1420–1430 (2011).

147. Boom, R., Sol, C. J., Salimans, M. M., Jansen, C. L., Dillen, P. M. W. & Noordaa, J. van der. Rapid and simple method for purification of nucleic acids. *J Clin Microbiol* **28**, 495–503 (1990).

148. Easley, C. J., Karlinsey, J. M., Bienvenue, J. M., Legendre, L. A., Roper, M. G., Feldman, S. H., Hughes, M. A., Hewlett, E. L., Merkel, T. J., Ferrance, J. P. & Landers, J. P. A fully integrated microfluidic genetic analysis system with sample-in–answer-out capability. *Proc Natl Acad Sci USA* **103**, 19272–19277 (2006).

149. Legendre, L. A., Bienvenue, J. M., Roper, M. G., Ferrance, J. P. & Landers, J. P. A Simple, Valveless Microfluidic Sample Preparation Device for Extraction and Amplification of DNA from Nanoliter-Volume Samples. *Anal Chem* **78**, 1444–1451 (2006).

150. Dimov, I. K., Garcia-Cordero, J. L., O'Grady, J., Poulsen, C. R., Viguier, C., Kent, L., Daly, P., Lincoln, B., Maher, M., O'Kennedy, R., Smith, T. J., Ricco, A. J. & Lee, L. P. Integrated microfluidic tmRNA purification and real-time NASBA device for molecular diagnostics. *Lab Chip* **8**, 2071–2078 (2008).

151. Sauer-Budge, A. F., Mirer, P., Chatterjee, A., Klapperich, C. M., Chargin, D. & Sharon, A. Low cost and manufacturable complete microTAS for detecting bacteria. *Lab Chip* **9**, 2803–2810 (2009).

152. Kim, Y. T., Lee, D., Heo, H. Y., Kim, D. H. & Seo, T. S. An integrated slidable and valveless microdevice with solid phase extraction, polymerase chain reaction, and immunochromatographic strip parts for multiplex colorimetric pathogen detection. *Lab Chip* **15**, 4148–4155 (2015).

153. Lim, G. S., Chang, J. S., Lei, Z., Wu, R., Wang, Z., Cui, K. & Wong, S. A lab-on-a-chip system integrating tissue sample preparation and multiplex RT-qPCR for gene expression analysis in point-of-care hepatotoxicity assessment. *Lab Chip* **15**, 4032–4043 (2015).

154. Roy, E., Stewart, G., Mounier, M., Malic, L., Peytavi, R., Clime, L., Madou, M., Bossinot, M., Bergeron, M. G. & Veres, T. From cellular lysis to microarray detection, an integrated thermoplastic elastomer (TPE) point of care Lab on a Disc. *Lab Chip* **15**, 406–416 (2014).

155. Sun, Y., Quyen, T. L., Hung, T. Q., Chin, W. H., Wolff, A. & Bang, D. D. A lab-on-a-chip system with integrated sample preparation and loop-mediated isothermal amplification for rapid and quantitative detection of *Salmonella spp.* in food samples. *Lab Chip* **15**, 1898–1904 (2015).

156. Stumpf, F., Schwemmer, F., Hutzenlaub, T., Baumann, D., Strohmeier, O., Dingemanns, G., Simons, G., Sager, C., Plobner, L., Stetten, F. von, Zengerle, R. & Mark, D. LabDisk with complete reagent prestorage for sample-

to-answer nucleic acid based detection of respiratory pathogens verified with influenza A H3N2 virus. *Lab Chip* **16**, 199–207 (2015).

157.   Chen, L., Tian, Y., Chen, S. & Liesenfeld, O. Performance of the Cobas® Influenza A/B Assay for Rapid PCR-Based Detection of Influenza Compared to Prodesse ProFlu+ and Viral Culture. *Eur J Microbiol Immunol (Bp)* **5**, 236–245 (2015).

158.   Tanriverdi, S., Chen, L. & Chen, S. A rapid and automated sample-to-result HIV load test for near-patient application. *J Infect Dis* **201**, S52–S58 (2010).

159.   Edwards, T. R. K., Mullarkey, T. C. E., Neale, K. D., Taylor, J. K. & Arlett, B. Fluidic cartridge for nucleic acid amplification and detection. (2017).

160.   Lawn, S. D. & Nicol, M. P. Xpert® MTB/RIF assay: development, evaluation and implementation of a new rapid molecular diagnostic for tuberculosis and rifampicin resistance. *Future Microbiol* **6**, 1067–1082 (2011).

161.   Pourahmadi, F., McMillan, W. A., Ching, J., Chang, R., Lee, C. A., Kovacs, G. T. A., Allen, N. M. & Kurt, P. E. Device for lysing cells, spores, or microorganisms. (2005).

162.   Cao, W., Easley, C. J., Ferrance, J. P. & Landers, J. P. Chitosan as a Polymer for pH-Induced DNA Capture in a Totally Aqueous System. *Anal Chem* **78**, 7222–7228 (2006).

163.   Ma, P. L., Lavertu, M., Winnik, F. M. & Buschmann, M. D. New Insights into Chitosan−DNA Interactions Using Isothermal Titration Microcalorimetry. *Biomacromolecules* **10**, 1490–1499 (2009).

164.   Ma, P. L., Buschmann, M. D. & Winnik, F. M. Complete Physicochemical Characterization of DNA/Chitosan Complexes by Multiple Detection Using Asymmetrical Flow Field-Flow Fractionation. *Anal Chem* **82**, 9636–9643 (2010).

165.   Burke, S. E. & Barrett, C. J. Acid−Base Equilibria of Weak Polyelectrolytes in Multilayer Thin Films. *Langmuir* **19**, 3297–3303 (2003).

166.   Zhuang, B., Gan, W., Wang, S., Han, J., Xiang, G., Li, C.-X., Sun, J. & Liu, P. Fully automated sample preparation microsystem for genetic testing of hereditary hearing loss using two-color multiplex allele-specific PCR. *Anal Chem* **87**, 1202–1209 (2015).

167.   Ahrberg, C. D., Ilic, B. R., Manz, A. & Neužil, P. Handheld real-time PCR device. *Lab Chip* **16**, 586–592 (2016).

168.   Myers, F. B., Henrikson, R. H., Bone, J. & Lee, L. P. A Handheld Point-of-Care Genomic Diagnostic System. *PLoS One* **8**, (2013).

169.   Higgins, J. A., Nasarabadi, S., Karns, J. S., Shelton, D. R., Cooper, M., Gbakima, A. & Koopman, R. P. A handheld real time thermal cycler for bacterial pathogen detection. *Biosens Bioelectron* **18**, 1115–1123 (2003).

170.   Hwang, K.-Y., Kwon, S. H., Jung, S.-O., Lim, H.-K., Jung, W.-J., Park, C.-S., Kim, J.-H., Suh, K.-Y. & Huh, N. Miniaturized bead-beating device to automate full DNA sample preparation processes for Gram-positive bacteria. *Lab Chip* **11**, 3649–3655 (2011).

171.   Chung, S. H., Baek, C., Cong, V. T. & Min, J. The microfluidic chip module for the detection of murine norovirus in oysters using charge switchable micro-bead beating. *Biosens Bioelectron* **67**, 625–633 (2015).

172.   Lee, S. H., Noort, D. van, Lee, J. Y., Zhang, B.-T. & Park, T. H. Effective mixing in a microfluidic chip using magnetic particles. *Lab Chip* **9**, 479–482 (2009).

173.   Wang, Y., Zhe, J., Chung, B. T. F. & Dutta, P. A rapid magnetic particle driven micromixer. *Microfluid Nanofluid* **4**, 375–389 (2008).

174.   Petkovic, K., Metcalfe, G., Chen, H., Gao, Y., Best, M., Lester, D. & Zhu, Y. Rapid detection of Hendra virus antibodies: an integrated device with nanoparticle assay and chaotic micromixing. *Lab Chip* **17**, 169–177 (2016).

175.   Liu, W., Huang, S., Liu, N., Dong, D., Yang, Z., Tang, Y., Ma, W., He, X., Ao, D., Xu, Y., Zou, D. & Huang, L. Establishment of an accurate and fast detection method using molecular beacons in loop-mediated isothermal amplification assay. *Sci Rep* **7**, 40125 (2017).

176.   Notomi, T., Mori, Y., Tomita, N. & Kanda, H. Loop-mediated isothermal amplification (LAMP): principle, features, and future prospects. *J Microbiol* **53**, 1–5 (2015).

177.   Safavieh, M., Kanakasabapathy, M. K., Tarlan, F., Ahmed, M. U., Zourob, M., Asghar, W. & Shafiee, H. Emerging Loop-Mediated Isothermal Amplification-Based Microchip and Microdevice Technologies for Nucleic Acid Detection. *ACS Biomater Sci Eng* **2**, 278–294 (2016).

178.   Du, W., Lv, M., Li, J., Yu, R. & Jiang, J. A ligation-based loop-mediated isothermal amplification (ligation-LAMP) strategy for highly selective microRNA detection. *Chem Comm* **52**, 12721–12724 (2016).

179.   Sun, Y., Tian, H., Liu, C., Sun, Y. & Li, Z. One-step detection of microRNA with high sensitivity and specificity via target-triggered loop-

mediated isothermal amplification (TT-LAMP). *Chem Comm* **53**, 11040–11043 (2017).

180.   Li, C., Li, Z., Jia, H. & Yan, J. One-step ultrasensitive detection of microRNAs with loop-mediated isothermal amplification (LAMP). *Chem Comm* **47**, 2595–2597 (2011).

181.   Okafuji, T., Yoshida, N., Fujino, M., Motegi, Y., Ihara, T., Ota, Y., Notomi, T. & Nakayama, T. Rapid Diagnostic Method for Detection of Mumps Virus Genome by Loop-Mediated Isothermal Amplification. *J Clin Microbiol* **43**, 1625–1631 (2005).

182.   Parida, M., Posadas, G., Inoue, S., Hasebe, F. & Morita, K. Real-Time Reverse Transcription Loop-Mediated Isothermal Amplification for Rapid Detection of West Nile Virus. *J Clin Microbiol* **42**, 257–263 (2004).

183.   Ushio, M., Yui, I., Yoshida, N., Fujino, M., Yonekawa, T., Ota, Y., Notomi, T. & Nakayama, T. Detection of respiratory syncytial virus genome by subgroups-A, B specific reverse transcription loop-mediated isothermal amplification (RT-LAMP). *J Med Virol* **77**, 121–127 (2005).

184.   Imai, M., Ninomiya, A., Minekawa, H., Notomi, T., Ishizaki, T., Tashiro, M. & Odagiri, T. Development of H5-RT-LAMP (loop-mediated isothermal amplification) system for rapid diagnosis of H5 avian influenza virus infection. *Vaccine* **24**, 6679–6682 (2006).

185.   Kaneko, H., Kawana, T., Fukushima, E. & Suzutani, T. Tolerance of loop-mediated isothermal amplification to a culture medium and biological substances. *J Biochem Biophys Methods* **70**, 499–501 (2007).

186.   Curtis, K. A., Rudolph, D. L. & Owen, S. M. Rapid detection of HIV-1 by reverse-transcription, loop-mediated isothermal amplification (RT-LAMP). *J Virol Methods* **151**, 264–270 (2008).

187.   Edwards, T., Burke, P. A., Smalley, H. B., Gillies, L. & Hobbs, G. Loop-Mediated Isothermal Amplification Test for Detection of Neisseria gonorrhoeae in Urine Samples and Tolerance of the Assay to the Presence of Urea. *J Clin Microbiol* **52**, 2163–2165 (2014).

188.   Zhu, Q., Gao, Y., Yu, B., Ren, H., Qiu, L., Han, S., Jin, W., Jin, Q. & Mu, Y. Self-priming compartmentalization digital LAMP for point-of-care. *Lab Chip* **12**, 4755–4763 (2012).

189.   Fang, X., Liu, Y., Kong, J. & Jiang, X. Loop-Mediated Isothermal Amplification Integrated on Microfluidic Chips for Point-of-Care Quantitative Detection of Pathogens. *Anal Chem* **82**, 3002–3006 (2010).

190. Safavieh, M., Ahmed, M. U., Tolba, M. & Zourob, M. Microfluidic electrochemical assay for rapid detection and quantification of Escherichia coli. *Biosens Bioelectron* **31**, 523–528 (2012).

191. Goto, M., Honda, E., Ogura, A., Nomoto, A. & Hanaki, K.-I. Colorimetric detection of loop-mediated isothermal amplification reaction by using hydroxy naphthol blue. *BioTechniques* **46**, 167–172 (2009).

192. Tomita, N., Mori, Y., Kanda, H. & Notomi, T. Loop-mediated isothermal amplification (LAMP) of gene sequences and simple visual detection of products. *Nat Protoc* **3**, 877–882 (2008).

193. Linnes, J. C., Rodriguez, N. M., Liu, L. & Klapperich, C. M. Polyethersulfone improves isothermal nucleic acid amplification compared to current paper-based diagnostics. *Biomed Microdevices* **18**, 30 (2016).

194. Park, B. H., Oh, S. J., Jung, J. H., Choi, G., Seo, J. H., Kim, D. H., Lee, E. Y. & Seo, T. S. An integrated rotary microfluidic system with DNA extraction, loop-mediated isothermal amplification, and lateral flow strip based detection for point-of-care pathogen diagnostics. *Biosens Bioelectron* **91**, 334–340 (2017).

195. Ding, X., Wang, G., Sun, J., Zhang, T. & Mu, Y. Fluorogenic bidirectional displacement probe-based real-time isothermal DNA amplification and specific visual detection of products. *Chem Comm* **52**, 11438–11441 (2016).

196. R. Kubota, A. M. Alvarez, W.W. Su & D. M. Jenkins. FRET-Based Assimilating Probe for Sequence-Specific Real-Time Monitoring of Loop-Mediated Isothermal Amplification (LAMP). *Biol Eng Trans* **4**, 81–100 (2011).

197. Jenkins, D. M., Kubota, R., Dong, J., Li, Y. & Higashiguchi, D. Handheld device for real-time, quantitative, LAMP-based detection of Salmonella enterica using assimilating probes. *Biosens Bioelectron* **30**, 255–260 (2011).

198. Kubota, R. & Jenkins, D. M. Real-Time Duplex Applications of Loop-Mediated AMPlification (LAMP) by Assimilating Probes. *Int J Mol Sci* **16**, 4786–4799 (2015).

199. Tanner, N. A., Zhang, Y. & Evans Jr., T. C. Simultaneous multiple target detection in real-time loop-mediated isothermal amplification. *BioTechniques* **53**, 81–89 (2012).

200. Chen, C., Zhao, Q., Guo, J., Li, Y. & Chen, Q. Identification of Methicillin-Resistant Staphylococcus aureus (MRSA) Using Simultaneous Detection of mecA, nuc, and femB by Loop-Mediated Isothermal Amplification (LAMP). *Curr Microbiol* **74**, 965–971 (2017).

201. Tanner, N. A. & Evans Jr., T. C. Loop-Mediated Isothermal Amplification for Detection of Nucleic Acids. *Curr Protoc Mol Biol* **105**, 15.14.1-15.14.14 (2014).

202. Subramanian, S. & Gomez, R. D. An Empirical Approach for Quantifying Loop-Mediated Isothermal Amplification (LAMP) Using Escherichia coli as a Model System. *PLoS One* **9**, e100596 (2014).

203. Fang, X., Liu, Y., Kong, J. & Jiang, X. Loop-Mediated Isothermal Amplification Integrated on Microfluidic Chips for Point-of-Care Quantitative Detection of Pathogens. *Anal Chem* **82**, 3002–3006 (2010).

204. Nagamine, K., Hase, T. & Notomi, T. Accelerated reaction by loop-mediated isothermal amplification using loop primers. *Mol Cell Probes* **16**, 223–229 (2002).

205. Wang, D.-G., Brewster, J. D., Paul, M. & Tomasula, P. M. Two Methods for Increased Specificity and Sensitivity in Loop-Mediated Isothermal Amplification. *Molecules* **20**, 6048–6059 (2015).

206. Kobayashi, N., Wu, H., Kojima, K., Taniguchi, K., Urasawa, S., Uehara, N., Omizu, Y., Kishi, Y., Yagihashi, A. & Kurokawa, I. Detection of mecA, femA, and femB genes in clinical strains of staphylococci using polymerase chain reaction. *Epidemiol Infect* **113**, 259–266 (1994).

207. Votintseva, A. A., Fung, R., Miller, R. R., Knox, K., Godwin, H., Wyllie, D. H., Bowden, R., Crook, D. W. & Walker, A. S. Prevalence of *Staphylococcus aureus* protein A (spa) mutants in the community and hospitals in Oxfordshire. *BMC Microbiol* **14**, 63 (2014).

208. Wang, J., Chen, J. & Sen, S. MicroRNA as Biomarkers and Diagnostics. *J Cell Physiol* **231**, 25–30 (2016).

209. Etheridge, A., Lee, I., Hood, L., Galas, D. & Wang, K. Extracellular microRNA: A new source of biomarkers. *Mut Res* **717**, 85–90 (2011).

210. Johnnidis, J. B., Harris, M. H., Wheeler, R. T., Stehling-Sun, S., Lam, M. H., Kirak, O., Brummelkamp, T. R., Fleming, M. D. & Camargo, F. D. Regulation of progenitor cell proliferation and granulocyte function by microRNA-223. *Nature* **451**, 1125–1129 (2008).

211. Johnson, C. D., Esquela-Kerscher, A., Stefani, G., Byrom, M., Kelnar, K., Ovcharenko, D., Wilson, M., Wang, X., Shelton, J., Shingara, J., Chin, L., Brown, D. & Slack, F. J. The let-7 MicroRNA Represses Cell Proliferation Pathways in Human Cells. *Cancer Res* **67**, 7713–7722 (2007).

212. Liu, N., Bezprozvannaya, S., Williams, A. H., Qi, X., Richardson, J. A., Bassel-Duby, R. & Olson, E. N. microRNA-133a regulates cardiomyocyte proliferation and suppresses smooth muscle gene expression in the heart. *Genes Dev* **22**, 3242–3254 (2008).

213. Chen, J.-F., Mandel, E. M., Thomson, J. M., Wu, Q., Callis, T. E., Hammond, S. M., Conlon, F. L. & Wang, D.-Z. The role of microRNA-1 and microRNA-133 in skeletal muscle proliferation and differentiation. *Nat Genet* **38**, 228–233 (2006).

214. Esau, C. *et al.* MicroRNA-143 Regulates Adipocyte Differentiation. *J Biol Chem* **279**, 52361–52365 (2004).

215. Makeyev, E. V., Zhang, J., Carrasco, M. A. & Maniatis, T. The MicroRNA miR-124 Promotes Neuronal Differentiation by Triggering Brain-Specific Alternative Pre-mRNA Splicing. *Mol Cell* **27**, 435–448 (2007).

216. Lizé, M., Pilarski, S. & Dobbelstein, M. E2F1-inducible microRNA 449a/b suppresses cell proliferation and promotes apoptosis. *Cell Death Differ* **17**, 452–458 (2010).

217. Welch, C., Chen, Y. & Stallings, R. L. MicroRNA-34a functions as a potential tumor suppressor by inducing apoptosis in neuroblastoma cells. *Oncogene* **26**, 5017–5022 (2007).

218. Masotti, A., Baldassarre, A., Guzzo, M. P., Iannuccelli, C., Barbato, C. & Di Franco, M. Circulating microRNA Profiles as Liquid Biopsies for the Characterization and Diagnosis of Fibromyalgia Syndrome. *Mol Neurobiol* **54**, 7129–7136 (2017).

219. Sestini, S., Boeri, M., Marchiano, A., Pelosi, G., Galeone, C., Verri, C., Suatoni, P., Sverzellati, N., La Vecchia, C., Sozzi, G. & Pastorino, U. Circulating microRNA signature as liquid-biopsy to monitor lung cancer in low-dose computed tomography screening. *Oncotarget* **6**, 32868–32877 (2015).

220. Yoshioka, Y. *et al.* Ultra-sensitive liquid biopsy of circulating extracellular vesicles using ExoScreen. *Nat Comm* **5**, 3591 (2014).

221. Valentino, A., Reclusa, P., Sirera, R., Giallombardo, M., Camps, C., Pauwels, P., Crispi, S. & Rolfo, C. Exosomal microRNAs in liquid biopsies: future biomarkers for prostate cancer. *Clin Transl Oncol* **19**, 651–657 (2017).

222. Cissell, K. A. & Deo, S. K. Trends in microRNA detection. *Anal Bioanal Chem* **394**, 1109–1116 (2009).

223. Murphy, J. & Bustin, S. A. Reliability of real-time reverse-transcription PCR in clinical diagnostics: gold standard or substandard? *Exp Rev Mol Diagn* **9**, 187–197 (2009).

224. Ness, J. V., Ness, L. K. V. & Galas, D. J. Isothermal reactions for the amplification of oligonucleotides. *Proc Natl Acad Sci USA* **100**, 4504–4509 (2003).

225. Deiman, B., van Aarle, P. & Sillekens, P. Characteristics and Applications of Nucleic Acid Sequence-Based Amplification (NASBA). *Mol Biotechnol* **20**, 163–180 (2002).

226. Jia, H., Li, Z., Liu, C. & Cheng, Y. Ultrasensitive Detection of microRNAs by Exponential Isothermal Amplification. *Angew Chem Int Ed Engl* **49**, 5498–5501 (2010).

227. Reid, M. S., Le, X. C. & Zhang, H. Exponential Isothermal Amplification of Nucleic Acids and Assays for Proteins, Cells, Small Molecules, and Enzyme Activities: An EXPAR Example. *Angew Chem Int Ed Engl* **57**, 11856–11866 (2018).

228. Steitz, T. A. DNA Polymerases: Structural Diversity and Common Mechanisms. *J Biol Chem* **274**, 17395–17398 (1999).

229. Arnaud-Barbe, N., Cheynet-Sauvion, V., Oriol, G., Mandrand, B. & Mallet, F. Transcription of RNA templates by T7 RNA polymerase. *Nucleic Acids Res* **26**, 3550–3554 (1998).

230. Milligan, J. F., Groebe, D. R., Witherell, G. W. & Uhlenbeck, O. C. Oligoribonucleotide synthesis using T7 RNA polymerase and synthetic DNA templates. *Nucleic Acids Res* **15**, 8783–8798 (1987).

231. Milligan, J. F. & Uhlenbeck, O. C. [5] Synthesis of small RNAs using T7 RNA polymerase. in *Methods in Enzymology* **180**, 51–62 (Academic Press, 1989).

232. Krupp, G. Unusual promoter-independent transcription reactions with bacteriophage RNA polymerases. *Nucleic Acids Res* **17**, 3023–3036 (1989).

233. Rong, M., Durbin, R. K. & McAllister, W. T. Template Strand Switching by T7 RNA Polymerase. *J Biol Chem* **273**, 10253–10260 (1998).

234. Maslak, M. & Martin, C. T. Kinetic analysis of T7 RNA polymerase transcription initiation from promoters containing single-stranded regions. *Biochemistry* **32**, 4281–4285 (1993).

235. Li, Z., Lau, C. & Lu, J. Effect of the Concentration Difference between Magnesium Ions and Total Ribonucleotide Triphosphates in Governing the

Specificity of T7 RNA Polymerase-Based Rolling Circle Transcription for Quantitative Detection. *Anal Chem* **88**, 6078–6083 (2016).

236.   Schaffter, S. W., Green, L. N., Schneider, J., Subramanian, H. K. K., Schulman, R. & Franco, E. T7 RNA polymerase non-specifically transcribes and induces disassembly of DNA nanostructures. *Nucleic Acids Res* **46**, 5332–5343 (2018).

237.   Emery, N. J., Majumder, S. & Liu, A. P. Synergistic and non-specific nucleic acid production by T7 RNA polymerase and Bsu DNA polymerase catalyzed by single-stranded polynucleotides. *Synth Syst Biotechnol* **3**, 130–134 (2018).

238.   Stump, W. T. & Hall, K. B. SP6 RNA polymerase efficiently synthesizes RNA from short double-stranded DNA templates. *Nucleic Acids Res* **21**, 5480–5484 (1993).

239.   Eun, H.-M. 7 - RNA Polymerases. in *Enzymology Primer for Recombinant DNA Technology* (ed. Eun, H.-M.) 491–565 (Academic Press, 1996).

240.   Tsuchiya, H., Okochi, M., Nagao, N., Shikida, M. & Honda, H. On-chip polymerase chain reaction microdevice employing a magnetic droplet-manipulation system. *Sens Actuators B Chem* **130**, 583–588 (2008).

241.   Kühnemund, M., Witters, D., Nilsson, M. & Lammertyn, J. Circle-to-circle amplification on a digital microfluidic chip for amplified single molecule detection. *Lab Chip* **14**, 2983–2992 (2014).

242.   Ebrahimi Warkiani, M., Guan, G., Bee Luan, K., Cheng Lee, W., S. Bhagat, A. A., Chaudhuri, P. K., Shao-Weng Tan, D., Teck Lim, W., Chin Lee, S., Y. Chen, P. C., Teck Lim, C. & Han, J. Slanted spiral microfluidics for the ultra-fast, label-free isolation of circulating tumor cells. *Lab Chip* **14**, 128–137 (2014).

243.   Rida, A. & Gijs, M. A. M. Manipulation of Self-Assembled Structures of Magnetic Beads for Microfluidic Mixing and Assaying. *Anal Chem* **76**, 6239–6246 (2004).

244.   Lee, T. Y., Hyun, K.-A., Kim, S.-I. & Jung, H.-I. An integrated microfluidic chip for one-step isolation of circulating tumor cells. *Sens Actuators B Chem* **238**, 1144–1150 (2017).